UNIVERSIDADE ESTADUAL PAULISTA - UNESP
CÂMPUS DE JABOTICABAL

GENOMIC IDENTIFICATION OF MATE, ABC, AND MFS TRANSPORTERS IN *Citrus sinensis* AND EXPRESSION ANALYSIS OF CITRUS SPECIES INTERACTING WITH *Xanthomonas citri* subsp. *citri*

Maria Heloisa Moreno Julião
Biotecnologista

2020

UNIVERSIDADE ESTADUAL PAULISTA - UNESP

CÂMPUS DE JABOTICABAL

GENOMIC IDENTIFICATION OF MATE, ABC, AND MFS TRANSPORTERS IN *Citrus sinensis* AND EXPRESSION ANALYSIS OF CITRUS SPECIES INTERACTING WITH *Xanthomonas citri* subsp. *citri*

Discente: Maria Heloisa Moreno Julião

Orientador: Prof. Dr. Alessandro de Mello Varani

Coorientador: Prof. Dr. Jesus Aparecido Ferro

Dissertação apresentada à Faculdade de Ciências Agrárias e Veterinárias – Unesp, Campus de Jaboticabal, como parte das exigências para a obtenção do título de Mestre em Agronomia (Genética e Melhoramento de Plantas).

2020

J94g

Julião, Maria Heloisa Moreno

Genomic identification of MATE, ABC, and MFS Transporters in Citrus sinensis and expression analysis of Citrus species interacting with Xanthomonas citri subsp. citri / Maria Heloisa Moreno Julião. -- Jaboticabal, 2020

84 p. : il., tabs.

Dissertação (mestrado) - Universidade Estadual Paulista (Unesp), Faculdade de Ciências Agrárias e Veterinárias, Jaboticabal

Orientador: Alessandro de Mello Varani

Coorientador: Jesus Aparecido Ferro

1. Genômica Vegetal. 2. Proteínas Transportadoras. 3. Transcriptoma. I. Título.

Sistema de geração automática de fichas catalográficas da Unesp. Biblioteca da Faculdade de Ciências Agrárias e Veterinárias, Jaboticabal. Dados fornecidos pelo autor(a).

UNIVERSIDADE ESTADUAL PAULISTA

Câmpus de Jaboticabal

CERTIFICADO DE APROVAÇÃO

TÍTULO DA DISSERTAÇÃO: GENOMIC IDENTIFICATION OF MATE, ABC, AND MFS TRANSPORTERS IN *Citrus sinensis* AND EXPRESSION ANALYSIS OF CITRUS SPECIES INTERACTING WITH *Xanthomonas citri* subsp. *citri*

AUTORA: MARIA HELOISA MORENO JULIÃO
ORIENTADOR: ALESSANDRO DE MELLO VARANI
COORIENTADOR: JESUS APARECIDO FERRO

Aprovada como parte das exigências para obtenção do Título de Mestra em AGRONOMIA (GENÉTICA E MELHORAMENTO DE PLANTAS), pela Comissão Examinadora:

Prof. Dr. ALESSANDRO DE MELLO VARANI
Departamento de Tecnologia / UNESP/Câmpus de Jaboticabal

Dra. SAURA RODRIGUES DA SILVA
Pós Doutoranda do Departamento de Biologia Aplicada à Agropecuária / Faculdade de Ciências Agrárias e Veterinárias
(VIDEOCONFERÊNCIA)

Profa. Dra. CLAUDIA BARROS MONTEIRO VITORELLO
Departamento de Genética-ESALQ/USP / Piracicaba/SP
(VIDEOCONFERÊNCIA)

Jaboticabal, 08 de maio de 2020

CURRICULAR DATA OF THE AUTHOR

Maria Heloisa Moreno Julião – born on January 29, 1997, in Nova Andradina – MS, Brazil. She has a bachelor's degree in Biotechnology from the Federal University of Grande Dourados - UFGD (2014 - 2017). She was a member of the Research Group on Plant Breeding and Biotechnology, participating as a collaborator in research projects. Developed the course conclusion work entitled “Floral biology and in vitro germination of nasturtium pollen grains (*Tropaeolum majus* L.) in cultivation with chicken litter.” under the guidance of Drª. Lívia Maria Chamma Davide. In the same period, she participated in the coordination of the extension project “Biotechnology for All” under the guidance of Drª. Liliam Silvia Candido. She completed a mandatory internship in 2017 at Fundação MS - Pesquisa e Difusão de Tecnologias Agropecuárias, located in Maracajú - MS. In 2018, he joined the Graduate Program in Agronomy (Genetics and Plant Breeding), Faculty of Agricultural and Veterinary Sciences - Unesp/FCAV, Jaboticabal Campus, at the Laboratory of Biochemistry and Molecular Biology under the guidance of the professors Dr. Alessandro de Mello Varani and Dr. Jesus Aparecido Ferro. The dissertation project was developed as a fellow at the Coordination for the Improvement of Higher Education Personnel (CAPES).

“The task is not so much to see what no one has seen yet, but to think what nobody has thought yet, about what everybody sees.” (Arthur Schopenhauer)

THANKS

To my family, for the love and support in all my choices. For teaching me to believe in my potential, to have faith and perseverance. For being my eternal safe harbor.

To my advisors, for the opportunity, confidence, patience and support in the years of work. Thank you for providing such an expressive personal and professional development, you are my examples of successful professionals.

To the professors of the Graduate Program in Agronomy (Genetics and Plant Breeding), other Unesp/FCAV programs, and my English teacher, for their willingness to help with whatever was possible. For all the knowledge, advice and criticism.

To all Unesp/FCAV employees, for allowing the university to function properly and to execute my project.

To the friends of the Laboratory of Biochemistry and Molecular Biology and the Department of Technology, for the joy in daily living, the spirit at coffee time and the outburst and consolation in difficult times. To all the colleagues at Unesp/FCAV that I met, for teaching me with their experiences, for making my days happier and for encouraging me to continue fighting for my dreams.

To the Unesp University Prayer Group, for filling me with the faith and hope I needed. To the Rotaract Club of Jaboticabal, for the opportunity to contribute to humanitarian projects and complete me personally. To the friends I met in the city of Jaboticabal and became true brothers. Thank you for so many good moments.

To all who contributed directly or indirectly to the execution of this work. My most sincere Thank you.

This study was financed in part by the Coordenação de Aperfeiçoamento de Pessoal de Nível Superior - Brasil (CAPES) - Finance Code 001

SUMMARY

GENOMIC IDENTIFICATION OF MATE, ABC, AND MFS TRANSPORTERS IN *Citrus sinensis* AND EXPRESSION ANALYSIS OF CITRUS SPECIES INTERACTING WITH *Xanthomonas citri* subsp. *citri*

ABSTRACT

Plants as sessile organisms require the synthesis and accumulation of a large array of molecules involved in growth, development, and defense-related processes. The Multi-Antimicrobial Extrusion Protein (MATE), ATP-Binding Cassette (ABC) and Major Facilitator Superfamily (MFS) transporters are the largest families of membrane transporters in plants, playing a central role in the defense-related processes in plant-pathogen interactions. For instance, protecting Citrus species cells under the infection of *Xanthomonas citri* subsp. *citri* (Xac), the etiologic agent of the Citrus Canker type A, one of the most devastating Citrus diseases involved with serious economic and environmental impacts. Herein, we identified genes and transcripts from MATE, ABC, and MFS families using the available *Citrus sinensis* genome (v2.0 HZAU) and the re-annotated Citrus Reference Transcriptome (CRT) from CitrusKB Knowledge Base (http://bioinfo.deinfo.uepg.br). We identified 67 MATE, 91 MFS, and 143 ABC genes in the *C. sinensis* genome and 82 MATE, 139 MFS, and 226 ABC transcripts in the CRT. The transcripts were mapped in the *C. sinensis* genome revealing a high rate of paralogs genes and probably alternative splicing (AS) events, whose expression profiles and potential roles in the Citrus-Xac interaction were proposed. The tandem and dispersed copies along with genes that underwent AS events represents sources of transporters' genes diversity and complexity. Moreover, we also highlighted potential biotechnological targets, which seemed to contribute with the defense responses in the Citrus plants. The seventeen genes belong to MATE I, ABC C and G, and STP subfamilies, potentially involved in the transport of secondary metabolites and xenobiotics, may acts as negative regulators of the disease and can limit the release of sugar from plant cells to apoplast. Overall, this work provides the first MATE, ABC, and MFS transporters' genomic data in *C. sinensis* and their transcriptome-wide characterization in Citrus species infected by Xac, providing fundamental information for studies concerning plant membrane transporters and their role in plant-pathogen interactions.

KEYWORDS: Comparative genomics, membrane transporters, differentially expressed genes, plant-pathogen interactions.

IDENTIFICAÇÃO GENÔMICA DE TRANSPORTADORES MATE, ABC E MFS EM *Citrus sinensis* E ANÁLISE DE EXPRESSÃO EM ESPÉCIES DE CITROS EM INTERAÇÃO COM *Xanthomonas citri* subsp. *citri*

RESUMO

As plantas como organismos sésseis requerem a síntese e o acúmulo de uma ampla variedade de moléculas envolvidas no crescimento, desenvolvimento e processos relacionados à defesa. Os transportadores Proteínas de Extrusão Multi-Antimicrobianas (MATE), Cassette de Ligação de ATP (ABC) e Superfamília dos Facilitadores Maioritários (MFS) são as principais famílias de transportadores de membrana em plantas, desempenhando um papel central nos processos relacionados à defesa nas interações planta-patógenos. Por exemplo, protegem as células das espécies de Citros sob a infecção de *Xanthomonas citri* subsp. *citri* (Xac), o agente etiológico do Cancro Cítrico tipo A, uma das doenças de Citros mais devastadoras envolvidas em sérios impactos econômicos e ambientais. Aqui, identificamos genes e transcritos das famílias MATE, ABC e MFS usando o genoma disponível de *Citrus sinensis* (v2.0 HZAU) e o Transcriptoma Referência de Citros (CRT) re-anotado da base de dados CitrusKB (http://bioinfo.deinfo.uepg.br). Foram identificados 67 genes MATE, 91 MFS e 143 ABC no genoma de *C. sinensis* e 82 transcritos MATE, 139 MFS e 226 ABC no CRT. Os transcritos foram mapeados no genoma de *C. sinensis*, revelando uma alta taxa de genes parálogos e putativos eventos de splicing alternativo (AS), cujos perfis de expressão gênica e potenciais papéis na interação Citros-Xac foram propostos. As cópias de genes em tandem e cópias dispersas juntamente com genes que possivelmente sofreram eventos de AS representam fontes de diversidade e complexidade dos genes transportadores. Além disso, nós destacamos potenciais alvos biotecnológicos que parecem contribuir com as respostas de defesa das plantas cítricas. Os dezessete genes pertencem às subfamílias MATE I, ABC C e G e STP, potencialmente involvidas no transporte de metabólitos secundários e xenobióticos, podem atuar como reguladores negativos da doença e limitar liberação de açúcar das células das plantas para o apoplasto. No geral, este trabalho fornece os primeiros dados genômicos de transportadores

MATE, ABC e MFS em *C. sinensis* e sua caracterização no transcriptoma de espécies de Citros infectadas por Xac, fornecendo informações fundamentais para estudos sobre transportadores de membrana em plantas e seu papel nas interações planta-patógeno.

PALAVRAS-CHAVE: Genômica comparativa, Transportadores de Membrana, Genes Diferencialmente Expressos, Interações Planta-Patógeno.

LIST OF ABBREVIATIONS

ABC	ATP-Binding Cassette
AIC	Akaike Information Criteria
AS	Alternative Splicing
CRT	Citrus Reference Transcriptome
CC	Citrus Canker type A
CitrusKB	A Knowledge Base for Transcriptome of Citrus species and *Xanthomonas citri* subsp. *citri* Interactome
Chr	Chromosome
CsMATE	MATE genomic sequences from the *Citrus sinensis* genome
CsABC	ABC genomic sequences from the *Citrus sinensis* genome
CsMFS	MFS genomic sequences from the *Citrus sinensis* genome
CstMATE	potential MATE sequences expressed by Citrus species
CstABC	potential ABC sequences expressed by Citrus species
CstMFS	potential MFS sequences expressed by Citrus species
DE	Differentially Expressed
DTX	Detoxification Proteins
FBT	Folate-Biopterin Transporter
MATE	Multi-Antimicrobial Extrusion Protein
MFS	Major Facilitator Superfamily
MW	Molecular Weight
pI	Isoelectric point
PHT	Phosphate Transporter
STP	Sugar Transporter Protein
WGD	Whole-genome/segmental duplication
Xac	*Xanthomonas citri* subsp. *citri*

LIST OF TABLES

LIST OF FIGURES

APPENDIX

1. INTRODUCTION

Plant-pathogen interactions result in macro and microscopic changes in the host plant, involving a wide range of morphological, biochemical, genetic, and molecular processes (Schenk et al., 2000; Melotto et al., 2006; Uchida and Tasaka, 2010; Cheval and Faulkner, 2018). The defense-related processes triggered by plants during the interaction are fast and targeted to counter-attack the pathogen to maintain the cellular homeostasis (Jones and Dangl, 2006). One of the most studied and devastating plant diseases affecting all commercial citrus varieties in production areas around the world is the Citrus Canker type A (CC), caused by the Gram-negative bacterium *Xanthomonas citri* subsp. *citri* (Xac) (Behlau et al., 2010).

The Xac infects the citrus tissues through the penetration in stomatal pores or wounds made by thorns and insects. The symptoms of infection start like high injuries soaked with water and evolve until it forms the cankers, reaching plant defoliation and premature fall of fruits (Gottwald et al., 2002). Moreover, distinct susceptibility levels to Citrus Canker across Citrus species (de Carvalho et al., 2015) were observed, reflecting in a complex array of plant-pathogen interaction and defense-response mechanisms.

Among the mechanisms conducted during the defense responses, plants developed and expanded transport mechanisms to excrete or sequester a broad range of synthesized molecules and xenobiotics to provide an efficient immune response (Tegos et al., 2002; Wang et al., 2016b). A large number of primary and secondary active transporter genes found in plants improve the plant competition and adaptation to stress conditions (Hwang et al., 2016), such as under the Citrus Canker disease. The major transporters families Multi-Antimicrobial Extrusion Protein (MATE), ATP-Binding Cassette transporters (ABC), and Major Facilitator Superfamily (MFS) play an essential role in the plants' membrane trafficking network (Shoji, 2014), are ubiquitously present in prokaryotic and eukaryotes organisms, and present distinct protein structures and source of energy used to execute the transport of molecules (Fath and Kolter, 1993; Takanashi et al., 2014a).

Identifying and understanding the features and roles of membrane transporter proteins in plant species, as the MATE, ABC, and MFS transporters in Citrus species has only been possible due to the growing number of genomic and transcriptomic data available in the public databases. Despite that, information concerning membrane transporters in Citrus species is still patchy. Thus, the importance of citriculture along with

the constant threating to citrus cultivation and the posing substantial economic impacts of the citrus canker, and also the possibility of adding scientific advance to the knowledge on membrane transport proteins prompted us to characterize and investigate the role and impact of these important gene families into the Citrus-Xac interaction.

As part of our efforts to understand the Citrus-Xac interaction, we recently build a knowledge base for transcriptome of Citrus and Xac interactome (CitrusKB, http://bioinfo.deinfo.uepg.br/citrus), providing data from Citrus species of divergent Citrus Canker susceptibility levels (e.g. from the less susceptible cultivars: 'Kumquat' *Fortunella* spp., Tangerine mandarin 'Satsuma' *C. unshiu*, and Tangerine mandarin 'Ponkan' *C. reticulata*, to the intermediate susceptible as Sweet oranges 'Pera Rio' and 'Valencia' *C. sinensis*, and highly susceptible as Sweet oranges 'Hamlin' and 'Bahia' *C. sinensis*, and Mexican lime 'Galego' *C. aurantifolia*) (Ferrasa et al., 2020). Using the CitrusKB database along with publicly available *Citrus sinensis* genome (v2.0 HZAU), we identified, classified, and compared the MATE, ABC, and MFS families in the *C. sinensis* genome and in the Citrus Reference Transcriptome (CRT).

We identified the genomic context in which the membrane transporters genes exist to understand how duplicate genes have contributed to their expansion and function and highlighted promising candidates for further exploitation from subfamilies MATE I, ABC C, ABC G, and STP based on their potential role in the Citrus-Xac interaction. Taken together, our results are not only providing novel insights about the main membrane transporters families in Citrus defense-related processes but also revealing a complex layer of the history of these gene families expansions and the transcriptional regulation under a plant-pathogen interaction.

2. LITERATURE REVIEW

2.1. The Citriculture and the Citrus Canker disease

The citrus plants belong to the Rutaceae family, Aurantoideae subfamily, and to the genus *Citrus* and related genera (*Poncirus, Fortunella, Eremocitrus, and Microcitrus*), whose taxonomy and evolutionary processes are complex. Phylogenetic relationships were reconstructed using 54 citrus and related chloroplast genomes accessions (Carbonell-Caballero et al., 2015) and 60 whole-genome (Wu et al., 2018). Both analyses agree with the relatedness of *Fortunella* to *Citrus,* which is nested within the citrus clade

(Wu et al., 2018) and took place in a succession of speciation events (Carbonell-Caballero et al., 2015). Moreover, Poncirus may be more distantly related to *Citrus* than *Fortunella,* which is a distinct clade (Carbonell-Caballero et al., 2015), separate from Citrus based on sequence divergence and whole-genome phylogeny (Wu et al., 2018).

The Brazil's environmental conditions supported the expansion of Citrus species, becoming the Citriculture an important sector of brazilian agribusiness. Brazil is the principal producer of sweet orange in the world, responsible for 37,2% of the total production. Also, it is the largest orange juice exporter in the world, producing 75% of the total juice exported (United States Department of Agriculture; and Foreign Agricultural Service, 2018). The production estimate for the 2019/20 orange crop of the citrus belt of São Paulo and Triângulo Mineiro is 36% higher than the previous crop (2018/19) and 21% the average for the last ten years (Fundecitrus, 2019), which demonstrates the development of the sector and the economy relevance.

However, the phytosanitary challenges of the citricultue make it difficult to maintain the productivity and competitiveness of the national citrus industry (Bassanezi et al., 2011). Citrus cultivated species are severely affected by diseases and vectors, which account for about 60% of total costs in Brazil Citrus production, composing a major challenge in breeding resistant plants. Four main diseases affect citrus groves: Citrus Canker, Citrus Variegated Chlorosis, and Huanglongbing (both caused by bacteria), and Sudden Citrus Death (the exact cause is non-determined). Also, other diseases affect orchards, some of them may be a limiting factor for fruit exports (Mendonça, Zambolim, and Badel, 2017). Of all the diseases mentioned that affect Citrus species, Citrus Canker is one of the most severe diseases as it causes significant losses in fruit quality and production (Gottwald et al., 2002; Mendonça, Zambolim, and Badel, 2017). In the Northwest sector of São Paulo State, the disease is present in about half of the orchards and 40% of the trees (Fundecitrus, 2019).

Citrus canker is caused by the Gram-negative bacterium *Xanthomonas citri* subsp. *citri* (Xac), firstly described in 1915 and classified as *Pseudomonas citri* (Hasse, 1915). The disease causes severe damage to commercial citrus crops in diverse production areas of the world (Behlau et al., 2010). In the infected leaves, the symptoms appear like high injuries, soaked with water which evolves to form the cankers. In advanced stages of the disease, the fruits and leaves fall off, resulting in production losses and a decline of fruits commercial price (Gottwald et al., 2002). Citrus canker disease reaches all commercial citrus varieties, whose severity and incidence of symptoms vary between

species and hybrids from the Citrus genus (Table 1; de Carvalho et al., 2015).The number of lesions on a sample of 10 symptomatic leaves sampled randomly from each plant assess the severity, while the proportion of leaves with lesions in the canopy estimate the incidence (de Carvalho et al., 2015).

The current control measures of citrus canker disease depend on the phytosanitary status of the area (MAPA, 2018). The most common control measures are the elimination of contaminated trees and applications of cupric compounds, which are costly and provide health and environmental risks. Moreover, the extensive use of cupric compounds resulted in the acquisition of resistance to copper in Xac and other phytopathogens, which highlights the need to search for new approaches to control the disease (Behlau et al., 2010).

The genetic breeding of Citrus species aimed to reduce the incidence of diseases but the methods are expensive and laborious since the species are polygenic, highly heterozygous and have a long juvenile period (Peña et al., 2008). Then, the understanding of plant defense mechanisms can overcome such barriers and allow new strategies for controlling the disease (Omura and Shimada, 2016). The growing publication of Citrus genomics data (Table 2) makes it possible to carry out molecular studies so that solutions and alternatives for the treatment of citrus can be identified.

Table 1. Susceptibility level of major Citrus commercially important culivars and Fotunella species to *Xanthomonas citri* subsp. *citri.*

Susceptibility level	Commom name	Specie
Less Susceptible	‘Kumquat’	*Fortunella* spp.
	‘Calamondin’	*C. madurensis*
	Lemon ‘Siciliano’	*C. limon*
	Mandarin ‘Ponkan’	*C. reticulata*
	Mandarin ‘Satsuma’	*C. unshiu*
Intermediate Susceptible	Mandarin ‘Darcy’	*C. reticulata*
	Mandarin ‘Cravo’	*C. reticulata*
	Sweet orange ‘Natal’	*C. sinensis*
Susceptible	Sweet orange ‘Pera Rio’	*C. sinensis*
	Sweet orange ‘Hamlin’	*C. sinensis*
	Sweet orange ‘Bahia’	*C. sinensis*
	Sweet orange ‘Valencia’	*C. sinensis*
Highly Susceptible	Pomelos	*C. paradisi*
	Mandarin ‘Clementine’	*C. clementina*
	Acid Lime ‘Galego’	*C. aurantifolia*

Adapted from de Carvalho et al. (2015) and Kishun e Chand (1987).

Table 2. Genomic data on Citrus species until 2020.

Species / Genome version	Commom name	Assembly size (Mb)	Assembly level	N50	Reference
Citrus sinensis genome v2.0 (HZAU)	Sweet orange 'Valencia'	328	Chromosomes	1,778,813	Xu et al. 2013
Citrus clementina genome v1.0 (JGI)	Clementine	301.4	Scaffolds	31,410,901	Wu et al. 2014
Citrus maxima (*C. grandis*) genome v1.0	Pomelo	302	Chromosomes	4,210,623	Wang, X. et al. 2017
Citrus ichangensis (*C. cavaleriei*) genome v1.0	Papeda	357.2	Scaffolds	501,435	Wang, X. et al. 2017
Citrus medica genome v1.0	Cider	406	Scaffolds	369,527	Wang, X. et al. 2017
*Citrus reticulat*a genome v1.0	Mandarin 'Ponkan'	344.3	Scaffolds	1,288,159	Wang, L. et al. 2018
Citrus unshiu Marc.	Mikan	359.7	Scaffolds	386,404	Shimizu et al. 2017
Citrus paradisi x *Citrus trifoliata*	Citrumelo	265.5	Contigs	2,091	Zhang et al. 2016

2.2 Membrane Transporter Proteins in Plants

In a cell, the control of molecules trafficking depends on the transporters embedded within the lipidic bilayer and organelles. Membrane transporters systems are involved in the maintenance of cellular homeostasis by the excretion and sequestration of molecules into the vacuole, playing a vital role in most of the cellular functions (Shitan and Yazaki, 2013; Gu et al., 2017). The transport mechanisms are regulated under stresses to keep the communication between cells, in plant growth and development (Schroeder et al., 2013), which improves the survival and competition under land conditions representing a mechanism of defense response developed by plants (Tegos et al., 2002). The membrane transporters systems are suggested to have arisen independently multiple times over an evolutionary time scale, resulting in a generic nature of the multidrug binding sites and their broad substrate specificity (Paulsen, 2003). The translocation of a diverse range of defense-related compounds across membranes is catalyzed by distinct groups of transporter genes, the primary and secondary active transporters in plants (Hwang et al., 2016).

In plants, the number of genes encoding membrane transporters is significantly larger than in other organisms (Hwang et al., 2016; Niño-González et al., 2019). Higher plants possess a multitude of transporters that group into three main distinct and ubiquitous families, the Multidrug And Toxic compound Extrusion (MATE) family, the ATP-

Binding Cassette (ABC) superfamily, and the Major Facilitator Superfamily (MFS) (Remy and Duque, 2014). Together, MATE, ABC, and MFS are plentiful, constituting on average more than 10% of the transporters in an organism (Paulsen, 2003).

The ABC members are primary transporters (Andolfo et al., 2015), while members of MATE and MFS superfamilies are secondary active transporters (Niño-González et al., 2019; Upadhyay et al., 2019). Primary transporters are membrane ATPases that use the hydrolysis of ATP to transport substances, whereas secondary transporters utilize proton gradients (gradient of H^+ in plants) as a driving force. The proteins structures of the MATE, ABC, and MFS members present large flexible hydrophobic cavities suggested to be the basis of multidrug recognition, which supports the accommodation of several compounds bounded via hydrogen bonding and/or electrostatic interactions, modulating the substrate specificities (Paulsen, 2003).

Moreover, the involvement of the membrane transporters proteins in the transport of a wide variety of defense-related molecules represents an evolutionary competition between micro-organisms and plants (Paulsen, 2003), considering the means of delivering the plant antimicrobial molecules into bacterial cells (Tegos et al., 2002). Despite their significance, especially their probably roles in the plant-pathogen interactions, genomic and transcriptomic-wide analyses of MATE, ABC, and MFS transporters in the Citrus species, are still lacking.

2.2.1 The Multi-Antimicrobial Extrusion Protein - MATE transporter family

The plant MATE proteins do the recognition and transport of specific substrates, acting in xenobiotics efflux, plant hormone signaling, alkaloids and flavonoids accumulation, leaf senescence, iron translocation, aluminum detoxification and other physiological functions (Takanashi et al., 2014b), transporting them either through the plasma membrane or into vacuoles (Omote et al., 2006). Substrate specificity between gene subfamily was found in *Arabidopsis thaliana,* whose genome includes 58 members grouped into five subfamilies (Li et al., 2002; Liu et al., 2016).

The evolution of the plant MATE family was probably different from that of other eukaryotes (Takanashi et al., 2014a). A mutation of a primordial polysaccharide-protein exporter within the prokaryotic domain probably leads to the arose of MATE family. Some members of this new family were vertically transmitted to eukaryotes or also during the endosymbiotic invasion of the eukaryotic cell by blue-green bacteria to give rise to

chloroplasts (Hvorup et al., 2003). The remarkable expansion of MATE proteins in plants is due to tandem and segmental duplications, resulting in a wide population among plant species (Upadhyay et al., 2019).

The H^+-driven MATE proteins include representatives in all three domains of life, which share a common domain, MatE domain (Pfam 01554, IIPR002528). The members are of about 450-550 amino acid residues in length and possess 12 putative transmembrane segments (TMS), as well as peaks of hydrophobicity well conserved (Hvorup et al., 2003). The first MATE transporter was identified in *Vibrio parahaemolyticus,* denoted as NorM (Morita et al., 1998). The NorM protein was classified into the major facilitator superfamily transporter and later reclassified as the novel multidrug transporter family called the MATE family (Brown et al., 1999).

The MATE family is arising as an important family in the establishment of plant disease resistance (Sun et al., 2011), since they contribute to stress tolerance under changing environmental conditions and can be required to mechanisms that allow plants to adapt better to abiotic and biotic stresses.

2.2.2 The ATP-Binding Cassette Transporters - ABC transporter family

For every type of molecule that must cross a cellular membrane, there is an ABC transporter with specificity for small and large molecules, inorganic ions, sugars, amino acids, proteins, and complex polysaccharides. Plants ABC transporters may translocate structurally unrelated substrates. Interference in the transport of a single substrate can impact multiple metabolic processes, including general metabolism and specific pathways such as resistance to drugs and toxins, resulting in distinct phenotypes from experimental data (Higgins, 2001; Lefèvre and Boutry, 2018).

ABC transporters mainly comprise two transmembrane domains (TMD) and two cytosolic nucleotide-binding domains (NBD), also known as ATP-binding cassettes or full-transporters. A half-transporter is formed by one TMD and one NBD (Higgins, 2001). The ABC signature, a specific sequence of motifs (LSGGQ), distinguishes ABC transporters from other ATP binding proteins (Higgins, 2001). The NBDs are between 200 and 300 amino acids in length and share conserved motifs involved either in ATP hydrolysis or in facilitating contact interfaces in the functionally assembled transporter (Dawson et al., 2007). In addition to these motifs, several functionally conserved residues coordinately

participate in the binding and hydrolysis of ATP (Higgins and Linton, 2004; Lefèvre, F.; Boutry, 2018).

The ABC transporter family is classified into eight subfamilies (ABC A to ABC I) according to the protein structure. In plants, the ABC H subfamily is absent. A total of 131 members were identified in the *A. thaliana* genome (Verrier et al., 2008). The diverse primary sequences of TMDs reflect the chemical and structural diversity of both efflux and uptake substrates. Different TDMs may translocate a very similar or the same substrate in the same direction across the membrane if they share significant sequence similarity (Dawnson et al., 2007).

The full structure transporters were originated by heterofusion and homofusion while the half transporters had at least four times the number of fusions with TMD and NBD. One of the four half structure transporters diverged into ABC C N-terminal, C-terminal, and ABC B half structure transporters. The ABC A, B, C, and G full structure transporters originated before the last eukaryotic common ancestor, and the ABC D family full structure transporter originated in the ancestor of land plants. The ABC F ABC 2 structure originated before the divergence of bacteria and archaea, and the ABC E family ABC 2 structure originated in archaea (Xiong et al., 2015).

The transport of molecules through the cell membrane against a concentration gradient requires energy that can be provided by ATP hydrolysis. The binding ATP promotes an outward-facing conformation while the release of the hydrolysis products ADP and phosphate promotes an inward-facing conformation (Dawnson et al., 2007). Such a process allows the proper distribution of defense-related molecules toward the plant surfaces, ensuring fast defense reactions of plants against pathogens (Berens et al., 2017; Khare et al., 2017).

2.2.3 The Major Facilitator Superfamily - MFS

The Major Facilitator Superfamily is a functionally diverse superfamily, representing the largest group of secondary active membrane transporters in plants. In the *Arabidopsis thaliana* genome this superfamily consists of 218 members, clustered in 22 families. The Sugar Transporter (STP) and the hitherto excluded NPF subfamilies account for nearly half of the 218 members (Niño-González et al., 2019).

The MFS members are secondary carriers, single-polypeptides capable of transporting small molecules across membranes using chemiosmotic gradients as an

energy source or acting as facilitators of substrate diffusion via uniport, symport, or antiport mechanism (Saier et al., 1999; Niño-González et al, 2019). The protein domain organization typically consists of 12 membrane-spanning segments, of which six membrane-spanning segments are located in one transmembrane domain, flanking a central hydrophilic pore. The transport channel pathway is constituted by the two halves forming a nearly flat interface at their boundary (Goswitz and Brooker, 1995; Hirai et al., 2003).

The MFS proteins are probably the result of a gene duplication arisen by intragenic duplication of an adjacent hairpin, multiple times during evolution. The MFS proteins may have developed from a single 2-TMS hairpin structure that triplicated to give a 6-TMS unit that duplicated to a 12-TMS protein (Reddy et al., 2012), primordial helix-triplets that formed functional transporters (Madej et al., 2013). The highly sequence diversity within the MFS members may be a result of the functional segments' assembling in a different consecutive order (Madej et al., 2013), whose some of them were characterized to be involved in biotic stresses (Büttner, 2010; Rottmann et al., 2018).

The MFS proteins are involved in the transport of a variety of molecule across the membranes, including sugars, inorganic ions, and amino acids across the cell membrane, particularly transport of macronutrients, such as Carbon, Nitrogen, and Phosporus (Reddy et al., 2012; Niño-González et al, 2019), playing an essential role in regulating the level of substances involved in plant growth and development, like repressing lateral root growth at low nitrate availability (Krouk et al., 2010).

The Sugar Transporter subfamily mediates the uptake and response to hexoses and are involved in biotic stresses such as in import sugars for component systems of secondary products and degradative enzymes important in plant-insect interactions (STP8 member, Rottmann et al., 2018) and in the recycling of sugars derived from cell wall degradation (STP7 and STP14 members, Poschet et al., 2010; Rottmann et al., 2018). Moreover, the ERD6-like subfamily is the largest *Arabidopsis thaliana* STP subfamily, suggested to transport substrates other than sugars, such as ESL1 and ESL6 members (Niño-González et al, 2019), which highlight the broad diversity and versatility of MFS transporters.

Since a handful of MATE, ABC, and MFS transporters are involved in the defense mechanism of plants and represents a useful resource to understand the processes triggered during plant-pathogen interaction, we aimed to identify the members of MATE, ABC, and MFS transporters in the *Citrus sinensis* genome and to detect and understand

the transcriptional changes underlying *Xanthomonas citri* subsp. *citri* infection. Moreover, proposing their roles in Citrus-Xac and other plant-pathogen interactions, highlighting members with potential biotechnology interest.

3. MATERIAL AND METHODS

3.1 Identification of MATE, ABC, and MFS genes in the *C. sinensis* genome

The *Citrus sinensis* 'Valencia' genome version 2.0 HZAU was retrieved from the Citrus Genome DB (https://www.citrusgenomedb.org/analysis/186). The MATE, ABC, and MFS transporters genes from *C. sinensis* (CsMATE, CsABC, and CsMFS, respectively) were retrieved by keyword search using the nomenclature systems for MATE (Brown, 1999), ABC (Verrier et al., 2018), and MFS (Niño-González et al, 2019). Since some of the genes could not be computationally annotated in the current and available version of *Citrus sinensis* annotation, we conducted two additional searches. Firstly, a tblastN using the sequences previously identified in the first search as query against the *C. sinensis* amino acid sequences. Secondly, a blastp using *Arabidopsis thaliana* MATE, ABC, and MFS amino acid sequences from UniProt database (Consortium, 2019) against the *C. sinensis* amino acid sequences. In both blast results, the sequences with more than 70% of similarity were added to the set for further verification. The presence of MATE, ABC, and MFS-related protein domains (Table 3) in the potential *C. sinensis* genes identified were manually verified using InterProScan results. A total of 11 MATE, 40 ABC, and 12 MFS were considered as false-positives and were removed from the further analyses.

Table 3. MATE, ABC, and MFS-related Domains.

Family	Accession	Name	Integrated Signatures	GO Terms
ABC	IPR000515	ABC transporter type 1, transmembrane domain MetI-like	PF00528, cd06261, PS50928	GO:0055085,GO:0016020
	IPR002491	ABC transporter periplasmic binding domain	PF01497, PS50983	
	IPR003439	ABC transporter-like	PF00005, PS50893	GO:0005524,GO:0016887
	IPR003760	ABC transporter substrate-binding protein PnrA-like	PF02608	GO:0005886
	IPR003838	ABC transporter permease protein domain	PF02687	GO:0016020

Table 3. MATE, ABC, and MFS-related Domains.

Family	Accession	Name	Integrated Signatures	GO Terms
ABC	IPR010929	CDR ABC transporter	PF06422	GO:0005524,GO:0042626,GO:0055085,GO:0016021
	IPR011527	ABC transporter type 1, transmembrane domain	PF00664, PF06472, PF13748, PS50929	GO:0005524,GO:0042626,GO:0055085,GO:0016021
	IPR013563	Oligopeptide/dipeptide ABC transporter, C-terminal	TIGR01727,PF08352	GO:0000166,GO:0005524,GO:0015833
	IPR013581	Plant PDR ABC transporter associated	PF08370	
	IPR022182	ABC transporter phosphate permease PstC, N-terminal domain	PF12501	GO:0006817
	IPR032524	ABC transporter Uup, C-terminal	PF16326	GO:0003677
	IPR032550	PBP-dependent ABC transporters TM subunit, N-terminal	PF16296	
	IPR040856	Glucose ABC transporter, C-terminal	PF17847	
MATE	IPR002528	Multi antimicrobial extrusion protein	PF01554,TIGR00797,PIRSF006603	GO:0015297,GO:0042910,GO:0055085,GO:0016020
MFS	IPR036259	MFS transporter superfamily	SSF103473	
	IPR011701	Major facilitator superfamily	PF07690	GO:0022857,GO:0055085
	IPR020846	Major facilitator superfamily domain	PS50850	GO:0022857
	IPR020846	Major facilitator superfamily domain	PS50850	GO:0022857
	IPR024989	Major facilitator superfamily associated domain	PF12832	
	IPR005828	Major facilitator, sugar transporter-like	PF00083	GO:0022857,GO:0055085,GO:0016021
	IPR000109	Proton-dependent oligopeptide transporter family	PTHR11654 PF00854	GO:0022857,GO:0055085,GO:0016020
	IPR004768	Oligopeptide transporter	TIGR00926	GO:0035673,GO:0006857,GO:0016021
	IPR004813	Oligopeptide transporter, OPT superfamily	TIGR00728,PF03169	GO:0055085
	IPR004814	Oligopeptide transporter OPT	TIGR00733	
	IPR004316	SWEET sugar transporter	PF03083	GO:0016021
	IPR005828	Major facilitator, sugar transporter-like	PF00083	GO:0022857,GO:0055085,GO:0016021
	IPR007271	Nucleotide-sugar transporter	PIRSF005799, PF04142, PTHR10231	GO:0015165,GO:0090481,GO:0000139,GO:0016021
	IPR012404	Nucleotide-sugar transporter-related	PIRSF036436	GO:0016021
	IPR018180	Sugar transporter SWEET1	PTHR10791:SF44, PTHR10791:SF155	GO:0051119
	IPR025601	ATP-binding sugar transporter-like protein	PF13856	
	IPR008509	Molybdate-anion transporter	PF05631, PTHR23516	GO:0015098,GO:0015689,GO:0016021

The homologous chromosomal regions events in *C. sinensis* were inferred using the Duplicate Gene Classifier from MCXScan toolkit (Wang et al., 2012), categorizing genes into singletons, dispersed duplicates, tandem genes, and whole-genome/segmental duplication (WGD) derived. The anchor genes in collinear blocks (genes in the same order) were named WGD genes, while the paralogs far each other on chromosomes without show conserved synteny were named dispersed duplicates, and two gene copies that are closely located on the chromosome but separated by up ten genes like tandem genes. The genes distribution and their likely duplication events were mapped to *C. sinensis* nine chromosomes (and one additional, the Unplaced) based on the chromosome size.

3.2 Transcriptome-wide identification of MATE, ABC, and MFS transcripts in Citrus species

The Citrus Reference Transcriptome was retrieved from CitrusKB (http://bioinfo.deinfo.uepg.br/citrus/). The CRT includes data from eight Citrus species of divergent Citrus Canker susceptibility levels (Table 4), whose leaves were inoculated with a suspension of Xac isolate (treatment) or sterile water (control). Leaves were collected at 24, 48 and 72 hours after inoculation (HAI) and the mRNA was isolated for cDNA synthesis. In vitro cloning was performed, the samples were then multiplexed and sequenced in HiScanSQ high throughput sequencing machine (Illumina, Ca, USA).

Table 4. The Citrus Reference Transcriptome species and its respective abbreviation used in the Figures of this work.

Susceptibility level	Commom name	Specie	Abbreviation
Less Susceptible	‘Kumquat’	*Fortunella* spp.	K
	Mandarin ‘Ponkan’	*C. reticulata*	PK
	Mandarin ‘Satsuma’	*C. unshiu*	S
Susceptible	Sweet orange ‘Pera Rio’	*C. sinensis*	PR
	Sweet orange ‘Hamlin’	*C. sinensis*	H
	Sweet orange ‘Bahia’	*C. sinensis*	BA
	Sweet orange ‘Valencia’	*C. sinensis*	V
Highly Susceptible	Acid Lime ‘Galego’	*C. aurantifolia*	LG

The raw data of each library were filtered to remove bad quality, adaptors and contaminated sequences. The libraries were aligned to the *Citrus sinensis* reference genome and the identification of novel transcripts and isoforms was performed using the reference transcriptome annotation of *Citrus sinensis* reference genome. The data were analyzed using a suite of bioinformatic tools. The high quality reads were mapped against

the *Citrus sinensis* reference genome, whose the absolute numbers of aligned reads were extracted for each transcript from the created transcriptome which loci was associated to the reference genome, using a read counting approach over the mapped libraries.

The CRT was re-annotated with Blast2GO using UniProt Viridiplantae database, and InterProScan. Searches to select potential MATE, ABC, and MFS sequences expressed by Citrus species (CstMATE, CstABC, and CstMFS, respectively) were conducted in the same way as genomic sequence searches. A total of 13 MATE, 16 ABC, and 16 MFS were considered as false-positives and were removed from the further analyses. The sequence length, isoelectric point value, and molecular weight of MATE, ABC, and MFS amino acid sequences were predicted by EMBOSS-PepStat (Madeira et al., 2019), and the subcellular location was predicted by WoLF PSORT (Horton et al., 2007).

Each CstMATE, CstABC, and CstMFS transcript was mapped in the *C. sinensis* genome using tBlastN tool to identify their corresponding genes. The results of the alignments were manually investigated (using a minimum of identity 90%, minimal alignment length of 100 amino acids, and expect value 10^{-5}) to find all the possible transcripts generated by membrane transporter genes families, and to propose the occurrence of potential alternative splicing (AS) events and isoforms generation.

3.3 Phylogenetic analyses of MATE, ABC, and MFS genomic and transcriptomic sequences

MATE, ABC, and MFS amino acid sequences identified in the *C. sinensis* genomic data were aligned using the multiple sequence aligner MAFFT version 7.4 (Nakamura et al., 2018), with standard parameters. The best evolutionary model LG+G+F (Le and Gascuel, 2008) was estimated for both ABC and MFS datasets, while WAG+G+F (Whelan and Goldman, 2001) for MATE dataset (PhyML 3.0, Guindon et al., 2010), considering the Akaike Information Criteria (AIC). Similarly, the MATE, ABC, and MFS amino acid sequences from the CRT were aligned using MAFFT, with standard parameters. The best phylogenetic model LG+G+F (Le and Gascuel, 2008) was estimated for both MATE and ABC datasets, while VT+G+F (Müller and Vingron, 2001) for MFS dataset (PhyML 3.0 , Uindon and Ranc, 2010), considering the AIC criteria.

Phylogenetic analyses were conducted in the Portal CIPRES v. 3.3 (Miller et al., 2015). The RaxML-HPC2 (Stamatakis, 2014) tool was chosen for Maximum Likelihood (ML) approach. The branches' support of the ML trees was evaluated by bootstrap with

1000 replicates. Clades without values correspond to the absence of statistical support in the bootstrap.

3.4 MATE, ABC, and MFS gene expression analysis based on CitrusKB Knowledge Base

Gene expression data from *C. reticulata, C. unshiu, C. sinensis* (‘Pera Rio’, ‘Valencia’, ‘Hamlin’, and ‘Bahia’ cultivars), *C. aurantifolia* and Fortunella spp. species were obtained from CitrusKB (Ferrasa et al., 2019, no prelo). To filter the deferentially expressed (DE) transcripts that probably most impacted the plant defense responses under Citrus-Xac infection we applied a filter of p-value <0.05 and $\log_2$fold-change (log2FC) values higher than 1 (up-regulated) or lower than -1 (down-regulated) (DESeq package, Anders and Huber, 2010). Heatmaps of DEs expression profiles were constructed using the ComplexHeatmap package in R (Gu et al., 2016). The gene expression data of the transcripts were displayed in three heatmaps (24, 48, and 72 HAI) for each family (MATE, ABC, and MFS), which were clustered by the Ward’s method (Murtagh and Legendre, 2014). Besides, the expression and significance values of DE transcripts from the less and the highly susceptible cultivars (‘Kumquat’ and ‘Galego’, respectively) were plotted using the ggplot2 package in R (Wickham and Chang, 2016).

4. RESULTS

4.1 Identification of MATE, ABC, and MFS genes in the *C. sinensis* genome

A total of 67 CsMATE, 91 CsMFS, and 143 CsABC genes were identified in the *C. sinensis* genome. The genes distribution and their homologous chromosomal regions, corresponding to dispersed, tandem, proximal and WGD events were mapped to *C. sinensis* chromosomes (2n = 18) showing an uneven distribution (Fig 1). The Unplaced chromosome was ignored in the following results. Most of the CsMATE, CsABC, and CsMFS genes were located in Chr2, Chr 1, and Chr 4, respectively. Mostly CsMATE and CsMFS genes correspond to tandem duplicates, while the dispersed genes correspond to the majority of CsABC genes (Fig 2). Interestingly, a smaller fraction of all membrane transporter genes were derived from WGD (Fig 2), supporting for their origin related to the ancient γ triplication event shared by all core eudicots (Jiao et al., 2011).

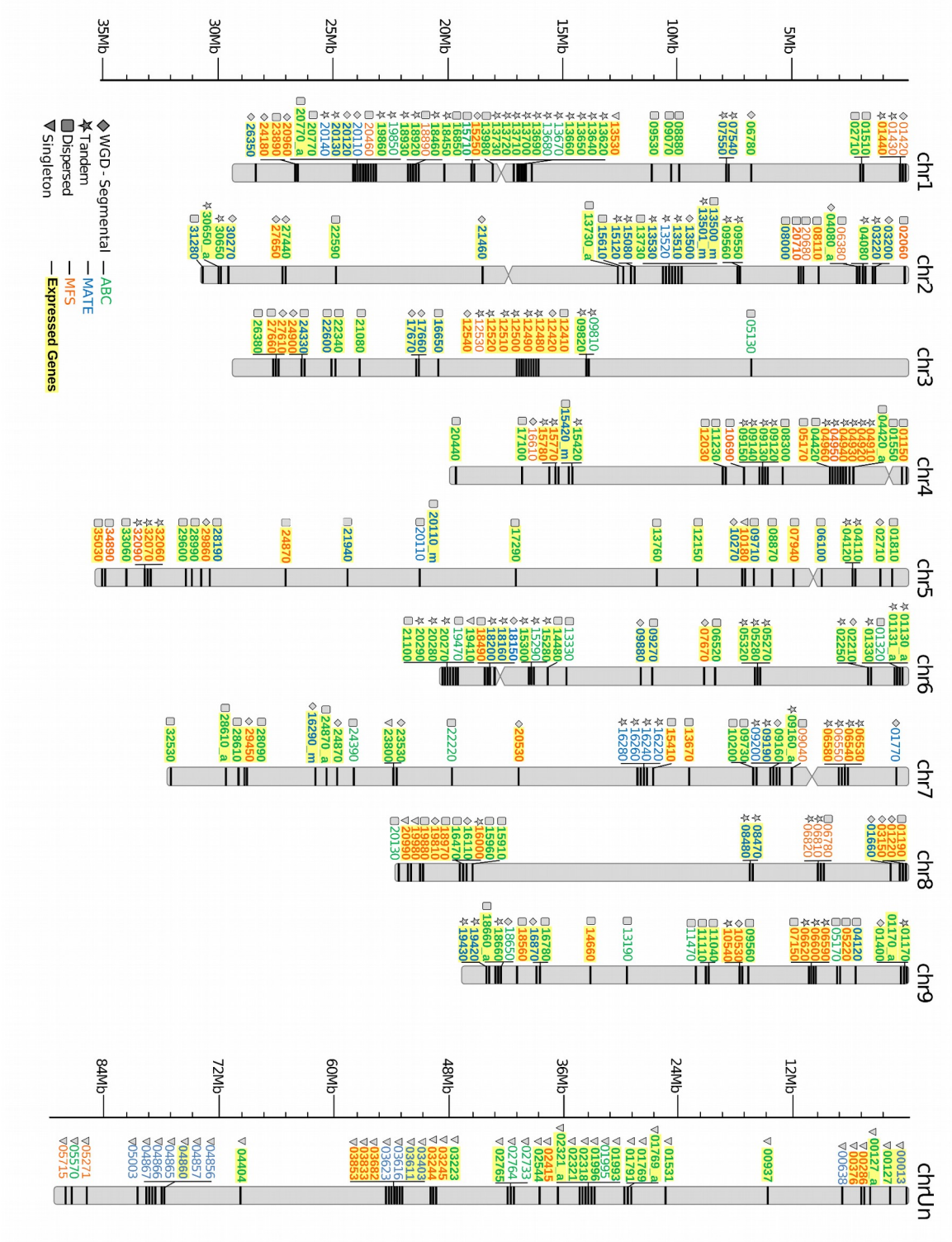

Figure 1. Genome distribution and gene duplication events of MATE, ABC, and MFS genes from *Citrus sinensis*. The size of a chromosome is indicated by its relative length given in Mb. Chromosome numbers (Chr) are indicated at the top of each chromosome. Gene duplication events are indicated with symbols. Genes with transcriptomic evidence from the Citrus Reference Transcriptome under Xac infection were shaded using yellow color and bold letters. The *C. sinensis* unplaced chromosome (chrUn) was not considered in the genome comparative analyses.

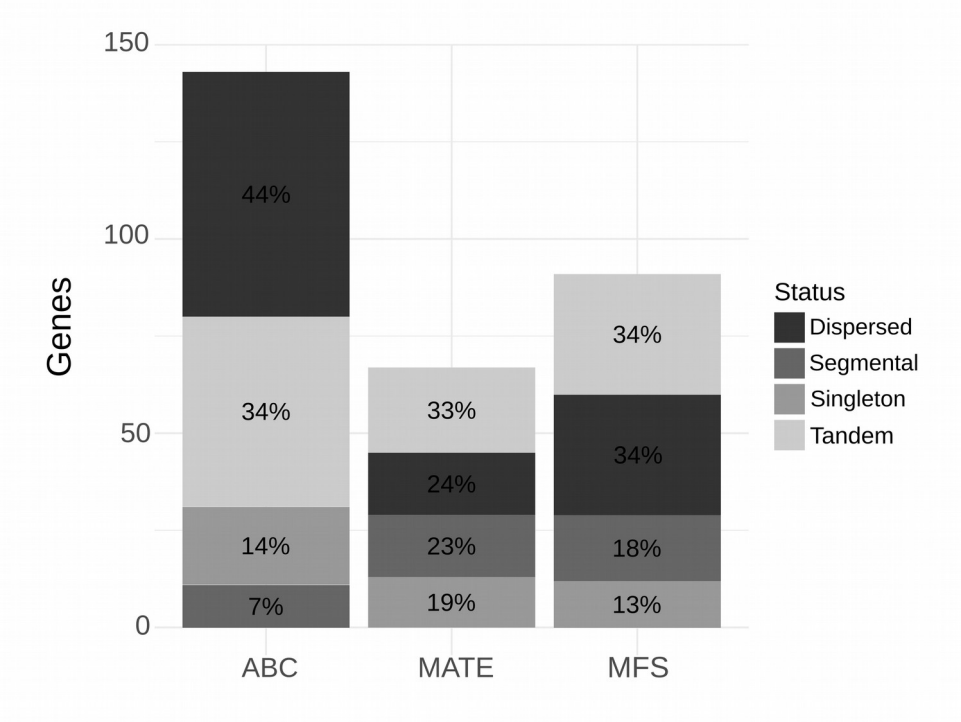

Figure 2. Duplication events of MATE, ABC, and MFS genes in the *Citrus sinensis* genome.

4.2 Transcriptome-wide identification of MATE, ABC, and MFS transcripts in Citrus species

The re-annotation of the CRT allowed us to identify a total of 82 MATE, 139 MFS, and 226 ABC transcripts. Conserved TMD and NDB domains and motifs related to MATE, ABC, and MFS proteins were found in all selected and annotated transcripts sequences. The length of the CstMATE sequences varied from 92 to 611 aa, the predicted molecular weight (MW) and isoelectric point (pI) ranged from 10 to 65.5 kDa, from 4.2 to 10.5, respectively. The length of the CstABC sequences varied from 114 to 1841 aa, the predicted MW and pI ranged from 12 to 205 kDa, from 4.3 to 11, respectively. The length of the CstMFS sequences varied from 87 to 747 aa, the predicted MW and pI ranged from 9.6 to 80.1 kDa, from 6.6 to 10.3, respectively. Both CstMATE, CstABC, and CstMFS sequences were mostly located on the plasma membrane. Few ABC members were located in the chloroplast (10%), while 15% of MATE and MFS was located in the vacuole (Table A1).

4.3 Phylogenetic analyses of MATE, ABC, and MFS genomic and transcriptomic sequences

The ML method was used to construct phylogenetic trees using datasets from genomic and transcriptomic sequences. The MATE genomic (Fig 3) and transcriptomic (Fig A1) sequences were assigned into five clades designated MATE I - MATE V. The ABC genomic (Fig 4) and transcriptomic (Fig A2) sequences were placed in eight clades in the phylogenetic tree, distributed according to the eight ABC subfamilies in plants (ABC A - ABC G, and ABC I). The MFS family harbors 14 subfamilies, whose genomic (Fig 5) and transcriptomic (Fig A3) sequences were assigned into the clades. The highest number of members of both trees with sequences from *Citrus sinensis* genome and CRT correspond to MATE I, ABC G, and STP subfamilies.

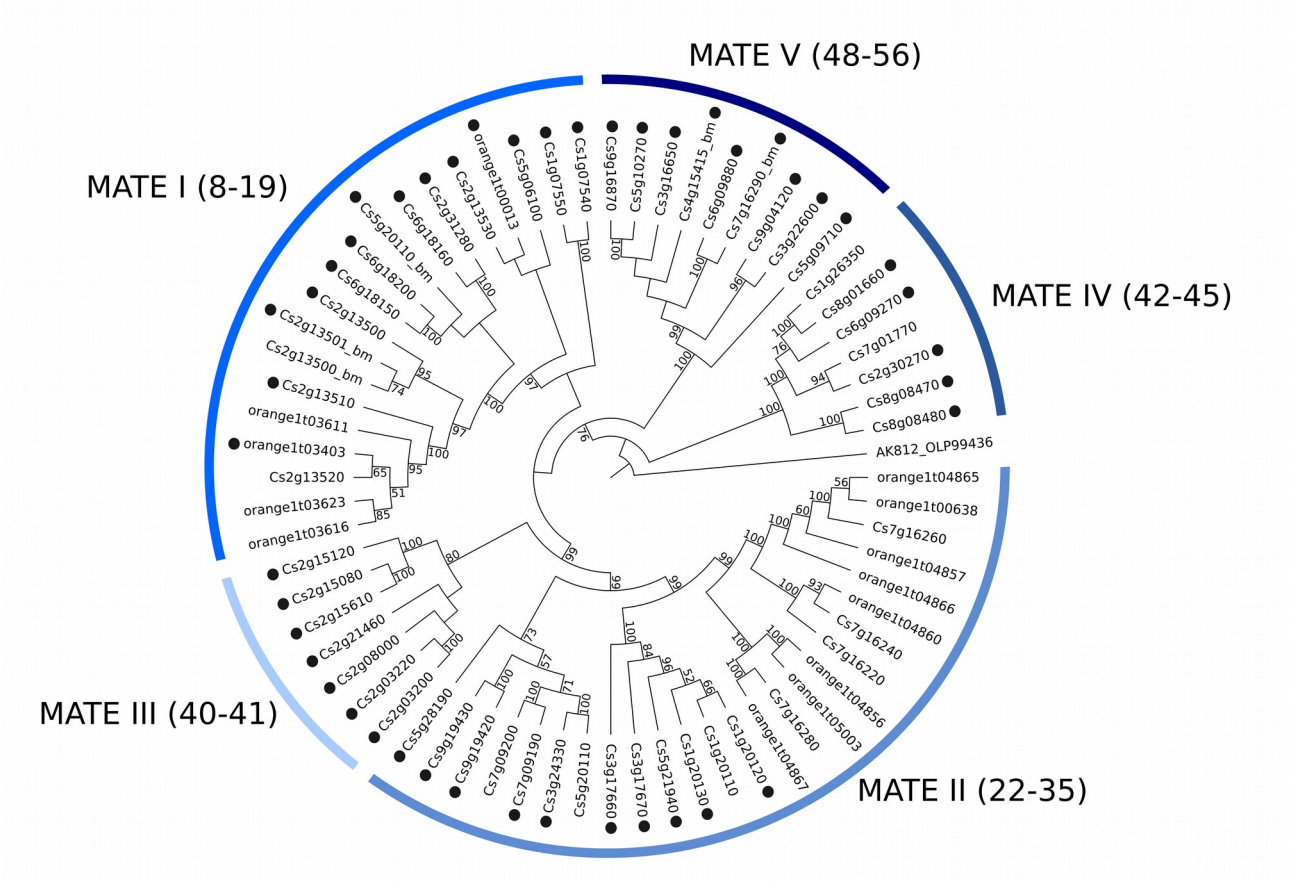

Figure 3. Maximum Likelihood tree of 67 MATE amino acid sequences from *Citrus sinensis* genome. Numbers above the branches represent bootstrap values. The black circles represent genes that have an associated transcript sequence in the CRT. AK812_OLP99436 was used as outgroup (*Symbiodinium microadriaticum str. CCMP2467,* Gene: slc47a1, Multidrug and toxin extrusion protein 1).

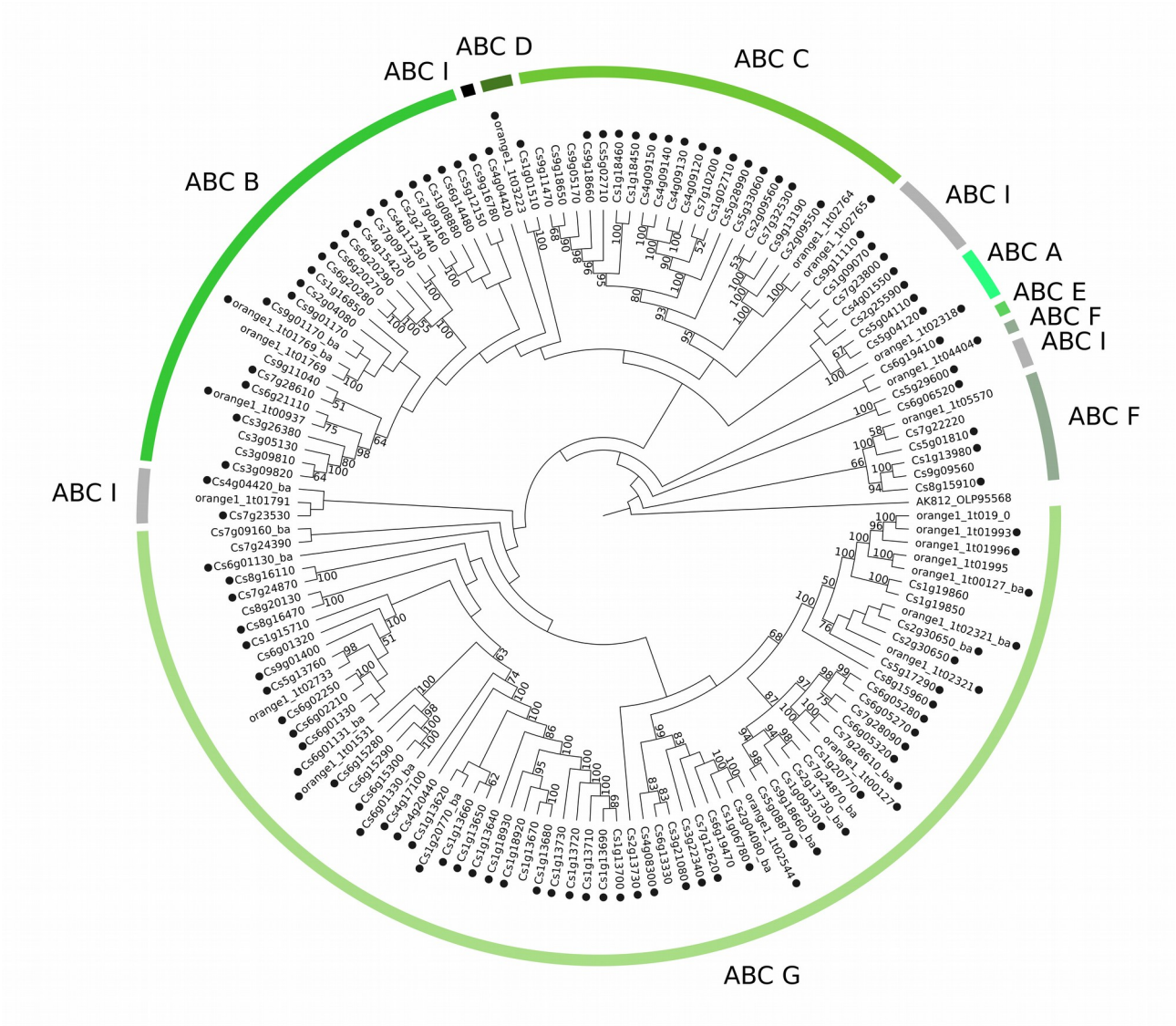

Figure 4. Maximum Likelihood tree of 143 ABC amino acid sequences from *Citrus sinensis* genome. Numbers above the branches represent bootstrap values. The black circles represent genes that have an associated transcript sequence in the CRT. AK812_OLP95568 was used as outgroup (*Symbiodinium microadriaticum str. CCMP2467,* Gene ABCF3, ATP-binding cassette subfamily F member 3).

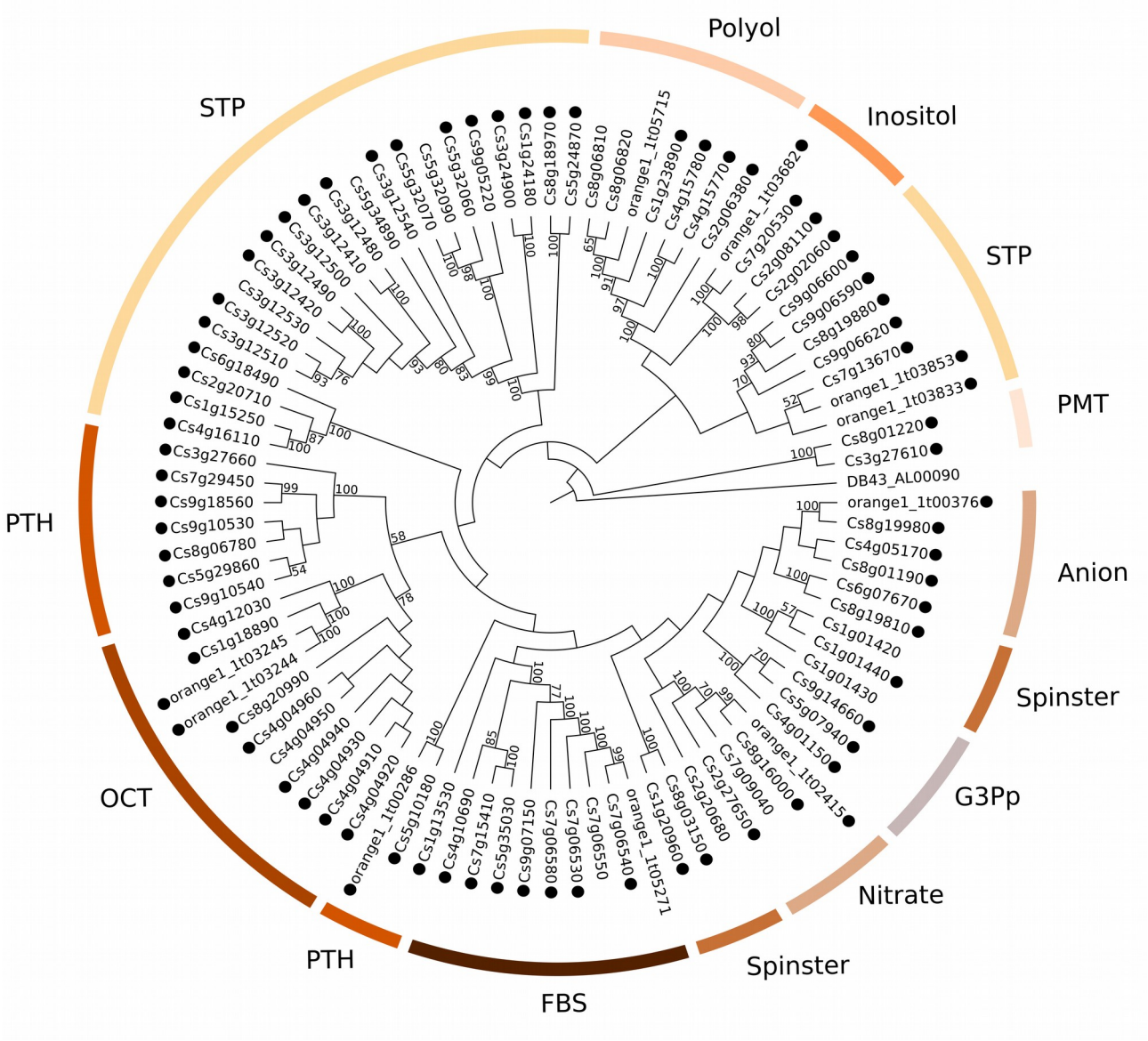

Figure 5. Maximum Likelihood tree of 91 MFS amino acid sequences from *Citrus sinensis* genome. Numbers above the branches represent bootstrap values. The black circles represent genes that have an associated transcript sequence in the CRT. DB43_AL00090 was used as outgroup (*Parachlamydia acanthamoebae,* Gene ywtG, putative metabolite transport protein YwtG).

4.4 Comparison between MATE, ABC, and MFS genomic and transcriptomic data

The transcriptional evidence of putative corresponding genes MATE, ABC, and MFS from the identified transcripts revealed that approximately 72% of CsMATE, 94% of CsABC, and 76% of CsMFS genes were transcribed under the Citrus-Xac interaction (Fig 1). Three CstABC transcripts showed no corresponding genes in the *C. sinensis* genome, which indicates a gap in the *Citrus sinensis* version 2.0 assembly. Moreover, most

transcripts were expressed by genes located on the Chr2, Chr1, and Chr4 for MATE, ABC, and MFS families, respectively (Fig 1, Table A2). Putative alternative splicing events supported by the RNA-Seq data were predicted in genes correspondents to multiples transcripts in more than 40% of both CsMATE (22 out of 48) and CsABC (51 out of 132), and CsMFS (28 out of 78) expressed genes (Table A2). Similarly, 26% of the gene models encoded two or more transcript isoforms in the *C. sinensis* genome in normal growth coditions (Xu et al., 2013). Also, the dispersed duplicates were the most predominant duplication events in the expressed genes from both families (Table A2). In general, most genes that possibly underwent alternative splicing events produced 2 or 3 isoforms. Most isoforms identified belonged to ABC G (37%), and STP (26%) subfamilies while in MATE they were proportionally distributed between the subfamilies (Table A2).

4.5 MATE, ABC, and MFS gene expression analysis based on CitrusKB Knowledge Base

A total of 29 CstMATE, 100 CstABC, and 45 CstMFS transcripts were classified as differentially expressed in CitrusKB. The transcripts were clustered into two main groups (the up-regulated and the down-regulated) showing distinguishable patterns of gene expression after Xac infection (Fig 6, 7, and 8), suggesting a high complex involvement of both transporters families in defense-related processes against Xac. Similarly, the membrane transporters seem to be under a complex global regulation in response to stresses or co-regulated with other genes (Paulsen 2003).

In general, the cultivars were clustered into two groups, which separated the contrasting cultivars to CC susceptibility level in different groups according to their patterns of gene expression. Moreover, we observed a crescent intensity of expression log2FC values in the most part of transcripts during/between the three time points (HAI), which iniciated in 24 HAI to 72 HAI more expressive in Kumquat while a pontual response in 48 HAI were observed in Galego, whose log2FC values decreased in 72 HAI.

The highest number of DE transcripts belonged to the subfamilies MATE I (23 DE, Fig 6), ABC G (63 DE, Fig 9), and STP (20 DE, Fig 8). Among the up-regulated genes, the highest log2FC values were exhibited by members from the subfamily I and subfamilies C and G, which can reflect a potential for high mRNA accumulation and protein production. It suggests a great importance of the MATE I and ABC G subfamilies in the Citrus species response to Xac, whose functions are discussed further.

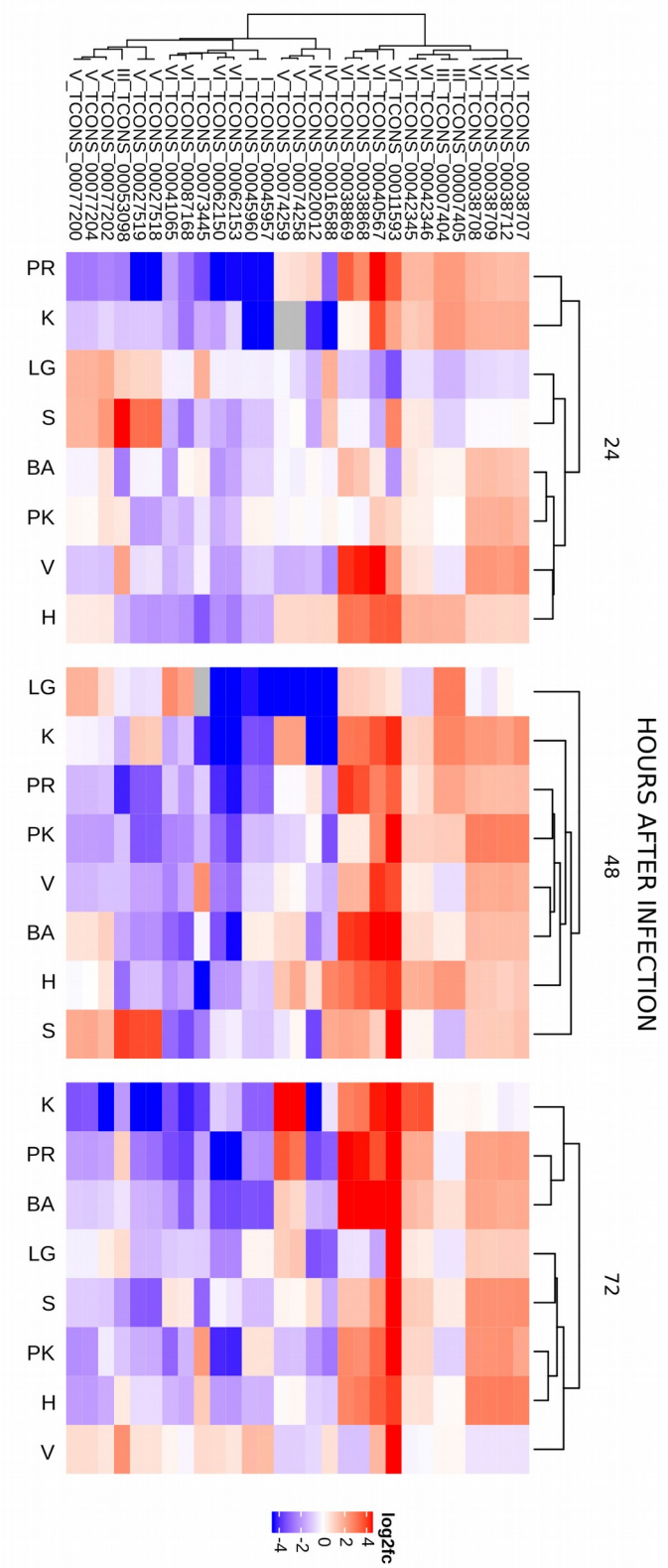

Figure 6. Heatmap of expression profiles of MATE transcripts differentially expressed on at least one HAI in a cultivar. K: ‘Kumquat’, PK: ‘Ponkan’, S: ‘Satsuma’, PR: ‘Pera Rio’, H: ‘Hamlin’, BA: ‘Bahia’, V: ‘Valencia’, LG:‘Galego’, log2fc: expression values in Log_2Fold-change. The subfamily of each transcript precedes its respective identification number.

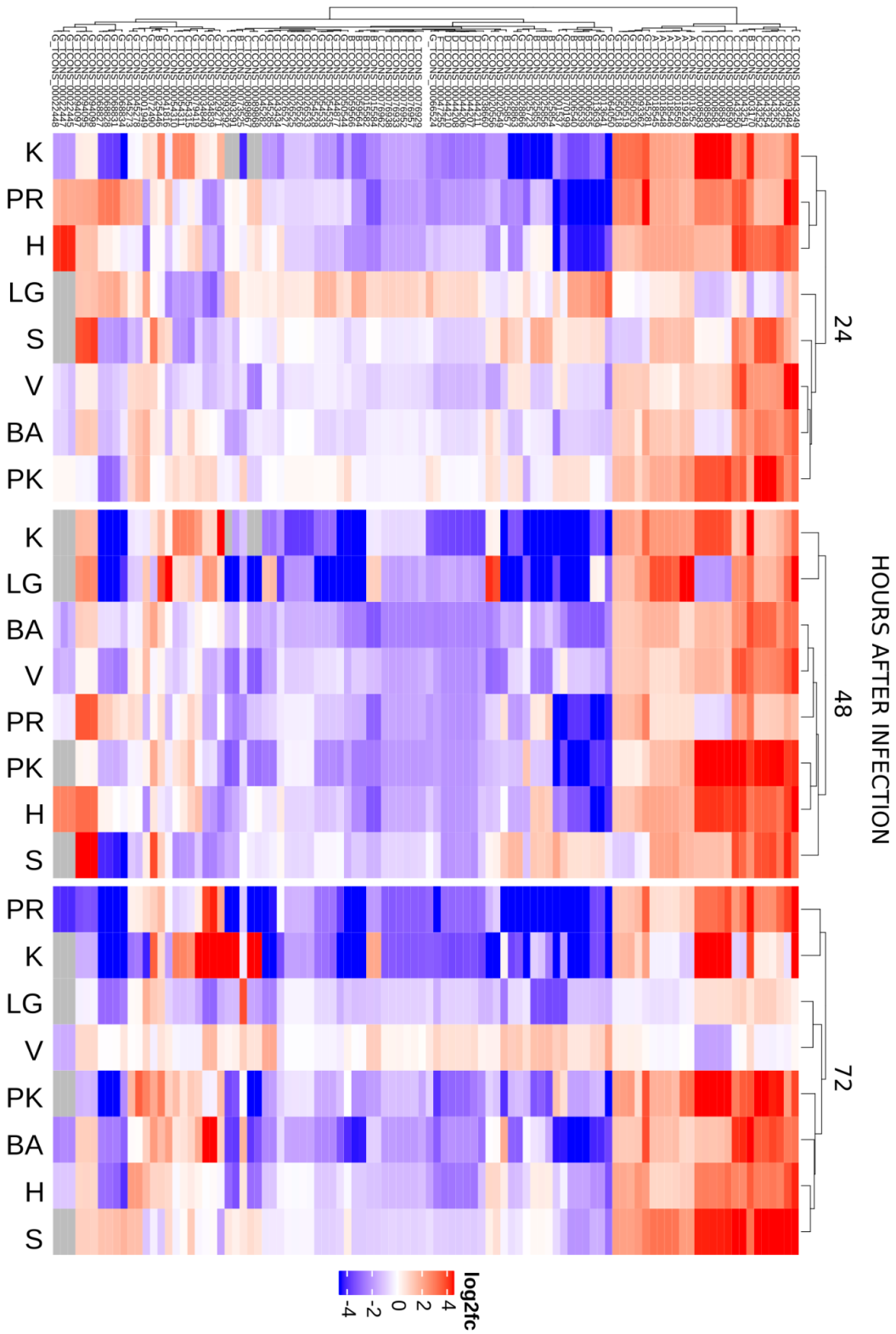

Figure 7. Heatmap of expression profiles of ABC (B)transcripts differentially expressed on at least one HAI in a cultivar. K: 'Kumquat', PK: 'Ponkan', S: 'Satsuma', PR: 'Pera Rio', H: 'Hamlin', BA: 'Bahia', V: 'Valencia', LG: 'Galego', log2fc: expression values in Log_2Fold-change.. The subfamily of each transcript precedes its respective identification number.

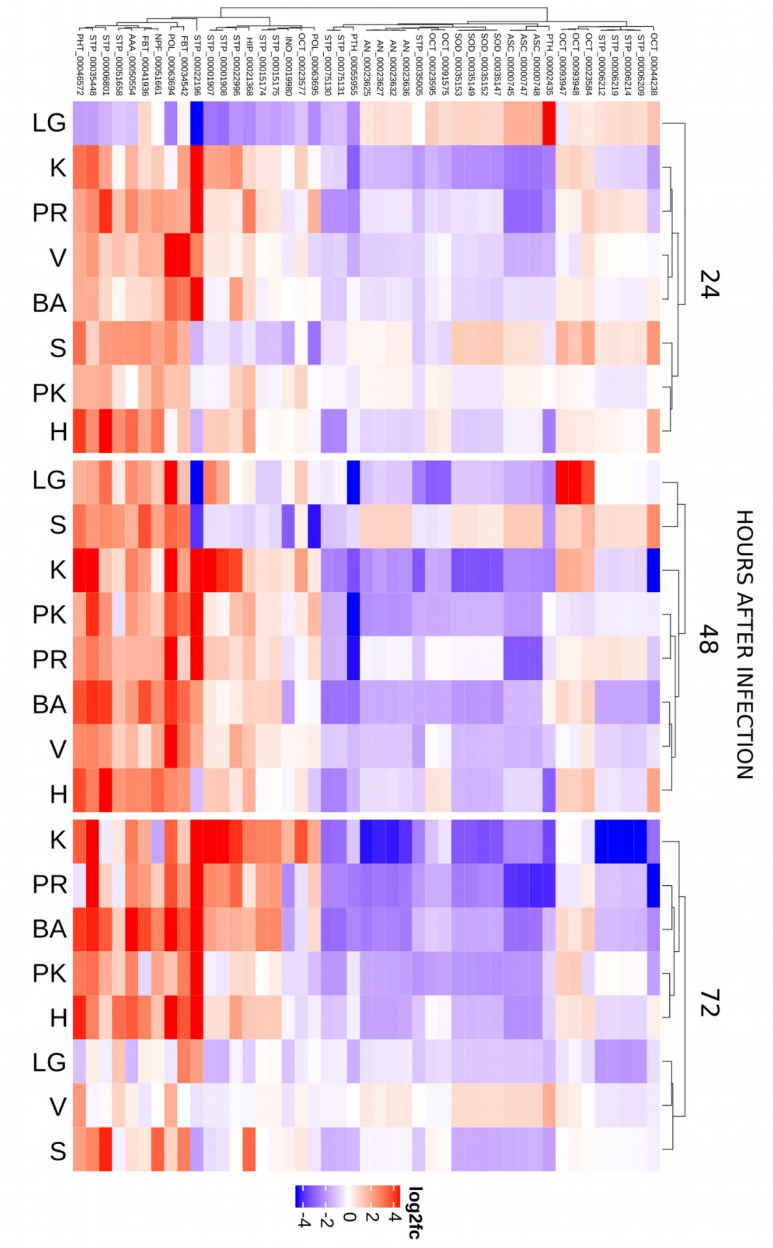

Figure 8. Heatmap of expression profiles of MFS transcripts differentially expressed on at least one HAI in a cultivar. K: 'Kumquat', PK: 'Ponkan', S: 'Satsuma', PR: 'Pera Rio', H: 'Hamlin', BA: 'Bahia', V: 'Valencia', LG: 'Galego', HAI: Hours After bacterial Inoculation. The subfamily of each transcript precedes its respective identification number.

Interestingly, the cultivars 'Kumquat' and 'Galego' presented contrasting numbers of DE transcripts and different sets of transcripts in each HAI (Fig 9), which can reflect their opposite levels of citrus canker susceptibility ('Galego' is more susceptible to CC than 'Kumquat'), and different molecular patterns of plant defense against *Xanthomonas citri* subsp. *citri*. The great part of the transcripts belonged to 'Kumquat', which were expressed

at all HAI, while the cultivar ‘Galego’ presented no up-regulated ABC transcripts at 24 HAI (Fig 9), which can be related to a late response in the highly susceptible cultivar to CC.

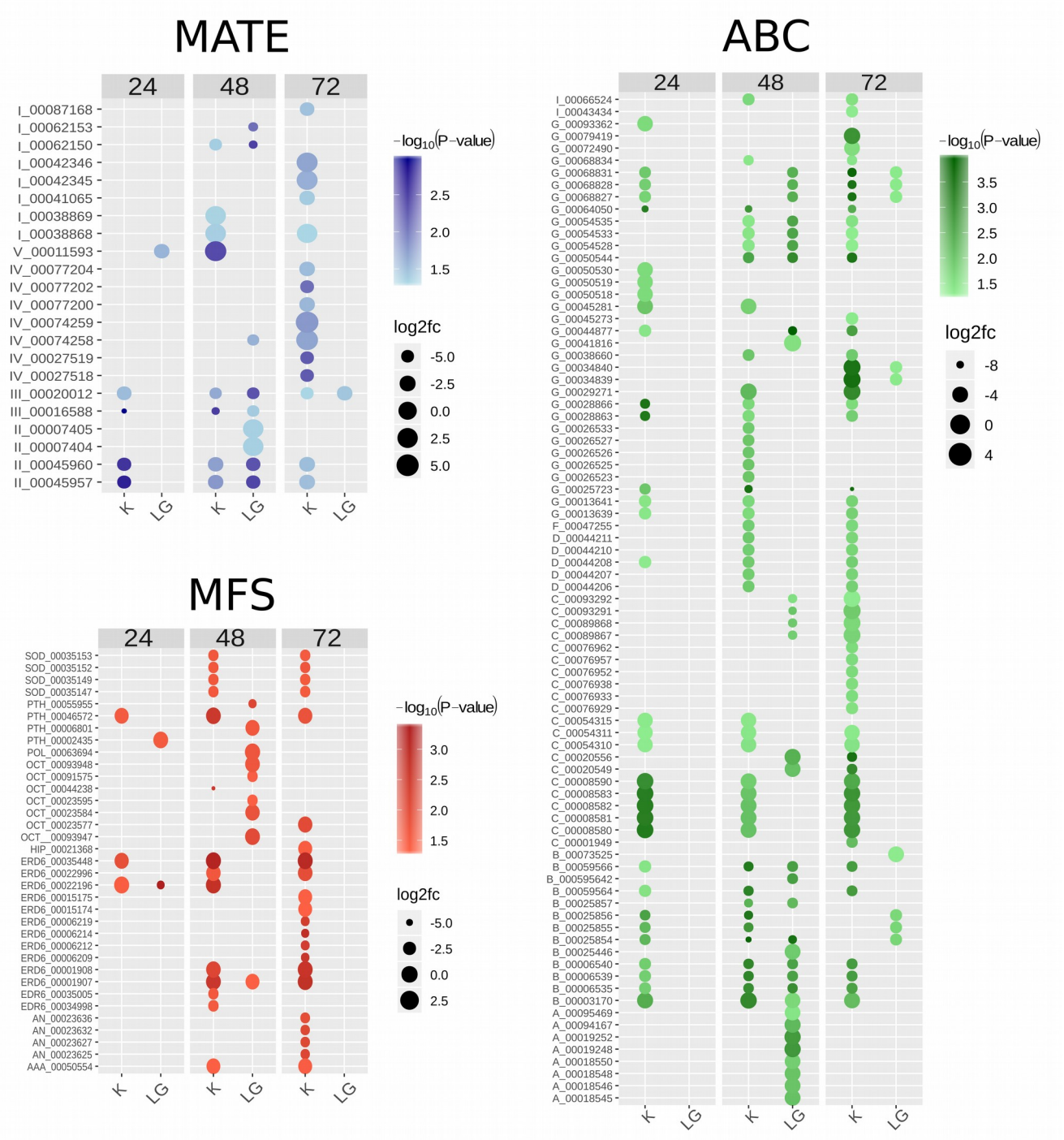

Figure 9. Bubble chart of MATE, ABC, and MFS transcripts differentially expressed in response to Xac infection in 24, 48, and 72 hours after bacterial inoculation. K: ‘Kumquat’, LG: Lima Ácida ‘Galego’. The color of markers represents the -log$_{10}$(p-value) values and the size is proportional to the log2FC values.

5. DISCUSSION

5.1 Identification of MATE, ABC, and MFS genes in the *C. sinensis* genome

We identified 67 MATE, 143 ABC, and 91 MFS genes in the *Citrus sinensis* genome, which were unevenly distributed into the *C. sinensis* chromosomes (Fig 1), consistent with previous reports on the distribution of MATE and ABC genes in plant species (Andolfo et al., 2015; Liu et al., 2016; Mishra et al., 2019). The Chr2 harbors about 24% of the CsMATE genes, likewise, 19% of MATE gene family in *G. arboreum* was located in Crh10 and 17% in Chr12 of *G. raimondii* genomes (Xu et al., 2019). In contrast, approximately 18% of CsMFS genes are located in Chr9. The greatest numbers of CsABC genes were found on Chr1 (about 17% of the annotated genes), similarly to the 20% of rice ABC genes in Chr1, while 15% of Solanaceae ABC genes are located in Chr12, 30% of *A. thaliana* ABC genes in Chr3, and 26% of grape ABC genes in Chr9 (Andolfo et al., 2015).

A variable number of membrane transporter genes are found in other genomes of plant species, whose differences in the gene family size and distribution across species may be a result of lineage-specific expansions (Panchy Lehti-Shiu, and Shiu, 2016). That diversity may imply the expansion and diversification of membrane transporter families since ABC transporters and secondary active transporters (including MATE and MFS) are largely found in plants from distinct environments, which require different sets of transporters to maintain the basic metabolism under changing conditions, highlighting the relevance of the transport mechanisms in the plant kingdom (Hwang et al., 2016).

Moreover, we conducted a gene classification to infer the homologous chromosomal regions of CsMATE, CsABC, and CsMFS genes. Approximately 21% of both CsMATE and CsABC genes and 10% of CsMFS were classified as singletons (Fig 2). In other words, more than 75% of CsMATE, CsABC, and CsMFS genes exist in duplicate copies. On average, 65% of annotated genes in 41 land plant genomes have a duplicate copy (Panchy, Lehti-Shiu, and Shiu, 2016). Gene duplication is a source of genetic novelty, acting in gene family expansion and protein functional diversification in large gene families (Cannon et al., 2004). Distinct groups of transporter genes were expanded during the evolution of plants, multiplied to enable many aspects of a sessile plants' lifestyle (Hwang et al., 2016) by sending information between cells and exchanging substances and toxic compounds (Wang et al., 2016a).

The tandem duplicates were the abundant gene duplicates identified in CsMATE genes, comprising 37% of the duplications that occurred in the gene family (Fig 2). In-tandem events constituted about 36% of MATE gene duplications occurred in Arabidopsis (Wang et al., 2016), 21% in soybean (Liu et al., 2016), 20% in rice and 55% in tomato (dos Santos et al., 2017), indicating a considerable implication of this evolutionary mechanism in the expansion of the MATE family and suggesting a similar expansion process in *C. sinensis*. The tandem clusters harbors genes involved in plant stress tolerance (Panchy, Lehti-Shiu, and Shiu, 2016), which may indicate that tandem duplication played a major role in members function from CsMATE family. In contrast to MATE, the most duplicates of CsABC and CsMFS genes were classified as dispersed duplicates (Fig 2). Tandem and dispersed duplicates may arise by unequal crossing over between similar alleles, and translocations originated by Transposable Elements, respectively (Panchy, Lehti-Shiu, and Shiu, 2016). Taken together, these findings strongly suggest for genomic evolution in the opposite direction for the membrane transporters' families and a probably contribution of gene duplications to the plants' traits linked to the biotic responses as a source of novelties and diversity.

5.2 Transcriptome-wide identification of MATE, ABC, and MFS transcripts in Citrus species

The keyword searches allowed us to identify 82 MATE, 226 ABC, and 139 MFS transporters in the re-annotated Citrus Reference Transcriptome. The amino acid sequences length varied from 89 to 611 aa in CstMATE sequences, from 77 to 1841 aa in CstABC sequences, and from 87 to 747 aa in CstMFS sequences. More than 60% of both CstMATE, and CstABC, and CstMFS sequences showed pI values higher than 7.0 (Table A1), indicating an overall global basic character. A variation in physicochemical and molecular properties like sequence length, molecular weight and, pI was previously reported in MATE and ABC sequences from monocot and dicot plant species (Andolfo et al., 2015; Wang et al., 2016). Furthermore, the subcellular localization of a transporter protein is central in its function. The plasma membrane was the main cell membrane system identified by the prediction of the three families subcellular locations (Table A1). The two primary sites of plant MATE transporters are either the plasma membranes or the vacuolar membranes (Jeong and Guerinot, 2009). However, the localization of Citrus species membrane transporters requires further functional validation.

It is also interesting to notice the higher number of membrane transporters transcripts compared to the number of membrane transporters genes. The majority of MATE, ABC, and MFS transcripts corresponding genes had transcriptional evidence associated from CRT while some genes were supposed to not be transcribed (Fig 1). The putative non-expression of some genes can reflect an energy-saving action underlying specific environmental conditions or a tissue-specific expression since a tissue-specific expression was reported for some MATE and ABC genes in maize (Nguyen et al., 2014; Zhu et al., 2016). Thus, is tempting to speculate that the set of non-expressed genes may be nonessential in the context of Citrus-Xac interaction.

Moreover, more than one Citrus transcript from MATE, ABC, and MFS families were associated with the same gene identification from the *C. sinensis* genome (Table A1 and A2), which indicates that alternative splicing events occurred during the transcription of the genes. Stress conditions frequently induce alternative splicing events in plant species including crop plants exposed to environmental stress (Staiger and Brown, 2013). In biotic stresses, the main AS-based regulation mechanism in plant responses is the rearrangement of exons and modular domains, which represent a source of transcriptome and proteome diversity, influence the amount of functional proteins produced, and quantitatively regulate the gene expression (Mastrangelo et al., 2012). However, further studies are required to determine which of the Citrus AS events are indeed biologically relevant during the Citrus-Xac interaction and what is the adaptive significance of novel structures and functions that are derived from gene duplication.

5.3 Phylogenetic based classification and gene expression analyses

Phylogenetic analyses were conducted for MATE, ABC, and MFS using genes (Fig 3, 4, and 5) and transcripts sequences (Fig A1, A2, and A3). The transporters functions and substrate specificity typically correlate with clades, and together with computational annotation analyses provide a satisfactory base for making functional and evolutionary predictions (Sugiyama et al., 2006; Liu et al., 2013; Wang et al., 2016a; Zhu et al., 2016; Lu et al., 2018; Ofori et al., 2018; Mishra et al., 2019; Xu et al., 2019). For instance, our results supported for 60% in average of amino acid conservation between *Citrus species* and *A. thaliana* MATE, ABC, and MFS proteins. Moreover, the gene expression analysis using the CRT data contributed to shedding light on the involvement of the membrane transporters members in the Citrus-Xac interaction.

5.3.1 Phylogenetics and gene expression analyses of MATE sequences

The five main clades were shaped in the MATE phylogenetics trees (Fig 3, A1), which were designated as subfamilies MATE I-V. In soybean and potato, six MATE subfamilies were identified according to the phylogenetic trees, whereas four subfamilies were identified in rice, Arabidopsis, and tomato, and three in cotton (Wang et al., 2016; Lu et al., 2018; Li et al., 2019), suggesting a diversification among plant species and an extensive performance of membrane transporters in the complex plant processes.

The MATE I subfamily contains 19 genomic sequences from *C. sinensis*, of which 14 have at least one transcript associated in the CRT (Fig 3), and a total of 26 transcripts annotated as DTX (Detoxification Proteins, as the classification of *A. thaliana* MATE members; Brown, 1999) 8-19 from the CRT (Table A1). Four transcripts were annotated as DTX19 isoforms and associated with Cs1g07550 gene and two with Cs1g07540 gene were identified. The genes were arranged in tandem in Chr1 of *C. sinensis*. A direct role in either the vacuolar sequestration or the cellular efflux of toxins was proposed to AtDTX19, as well as the ability to sequester the toxic cation tetramethylammonium, expressed and required in different tissues (Diener et al., 2001), which can explain the plasma membrane and endomembrane system locations predicted for the eight CstDTX19.

In general, the MATE I subfamily is strongly recruited by the less susceptible cultivars to Xac infection at 48 and 72HAI (Table A3, Fig 9) probably due to the valuable and broad utility of their transported substrates, which likely provides efficient adaptive stress responses to citrus canker by the tolerance towards xenobiotics, cellular homeostasis, and regulation of a variety of developmental processes. Considering the contrasting cultivars, K and LG, the two isoforms from Cs1g07540 were highly DE at 72 HAI in ‘Kumquat’. Then, the CstDTX19 transcripts may regulate the sequestration and, consequently, the tolerance towards xenobiotics after three days in Xac infection.

The MATE II subfamily contains 25 genomic sequences from *C. sinensis*, of which 10 have at least one transcript associated in the CRT (Fig 3), and a total of 22 transcripts annotated as (DTX 22-35) from the CRT (Table A1). Eight CstDTX27 transcripts share at least 70% of similarity with OsMATE1, which were reported to negatively regulate disease tolerance apart from governing growth and development in maize (Tiwari et al., 2014). The variation in gene expression profiles among different citrus cultivars observed in the MATE II transcripts (Fig 6) can potentially facilitate a stress-related response. Then, we speculate

an involvement of CstDTX27 transcripts in disease tolerance regulation, which were shown to be promising candidates for further exploitation.

Both TCONS_00053097 e TCONS_00053098 transcripts (annotated as DTX35 members) share 73% and 84% of identity to AtDTX35 , respectively. They were probably transcribed from Cs9g19420 and Cs9g19430 genes, which were arranged in tandem duplicates. Transporters reported to be involved in secondary metabolites transport from diverse species share from 68% to 83% of sequence similarity with both CstDTX35 sequences, including VvAM1 and VvAM3, responsible for anthocyanin-acyl glucosides uptake (Gomez et al., 2009), MtMATE2, for transport of glycosylated flavonoids (Zhao et al., 2011), AtDTX35, for flavonoid levels and metabolism changes (Thompson et al., 2010), and SlMTP77 for transport of anthocyanins into the vacuole (Mathews et al., 2003), suggesting a role for CstDTX34 and CstDTX35 transporters in anthocyanin sequestration in vegetative tissues. Changings in secondary metabolite levels during plant-pathogen interaction has been observed in Citrus species (Hijaz et al., 2013; Chin et al., 2014). In leaves from ‘Hamlin’ and ‘Valencia’ sweet oranges, flavonoid glycosides, polymethoxylated flavones, and hydroxycinnamates compounds levels increased more than 10-fold after *Candidatus* Liberibacter infection (Chin et al., 2014). Similarly, MATE II members showed differential expression after Xac infection (Fig 6), which could represent a great involvement of the secondary metabolites secretory pathway in Citrus defense response to Xac infection.

The MATE III subfamily contains 07 genomic sequences from *C. sinensis*, of which all of them have at least one transcript associated in the CRT (Fig 3), and a total of 9 transcripts annotated as (DTX 40-41) from the CRT (Table A1). Relatively, to take up apoplasmic precipitated iron, Citrus plants could secrete phenolics by CstDTX40 transporters, acting in metal detoxification and tolerance due to its close relation with characterized non-citrate transporters. Rice increases the production and release of phenolic compounds to the rhizosphere through the rice phenolic exporter OsPEZ1 phenolic efflux transporter (Ishimaru et al., 2011). Among the Citrus transcripts expressed in this group, two CstDTX40 members (TCONS_00020012, TCONS_00016588) showed a significant down-regulation after Xac infection in citrus cultivars with diverse levels of susceptibility, suggesting prioritization of the defense-related responses rather than keep the plant growth and development.

The MATE IV subfamily contains 07 genomic sequences from *C. sinensis*, of which 05 have at least one transcript associated in the CRT (Fig 3), and a total of 15 transcripts

annotated as (DTX 42-46) from the CRT (Table A1). Some DTX46 transcripts from the CRT and the AtDTX46 are localized at the chloroplast, which is proposed to most likely transports related substances such as phenolic acids (Parinthawong et al., 2015). Inducible citrate transporters are able to provide tolerance to Al^{3+} toxicity in other plant species, including BoMATE from *Brasicca oleracea* (Wu et al., 2014), HvAACT1 from *Hordeum vulgare* (Zhou et al., 2013), EcMATE1-4 from *Eucalyptus camaldulensis* (Sawaki et al., 2013), LjMATE from *Lotus japonicus* (Takanashi et al., 2013), MtMATE67 from *Medicago truncatula* (Kryvoruchko et al., 2018), AtDTX42 from *A. thaliana* (Liu et al., 2009), among others. The gene expression of seven CstMATE V members was mostly negatively regulated after Xac infection in the less and intermediate susceptible citrus cultivars (‘Kumquat’, ‘Ponkan’, and ‘Pera Rio’), indicating that Al^{3+} toxicity tests can be performed to better conclusions in Citrus-Xac impact.

The MATE V subfamily contains 09 genomic sequences from *C. sinensis*, of which all of them have at least one transcript associated in the CRT (Fig 3), and a total of 10 transcripts annotated as (DTX 48-56) from the CRT (Table A1). The CstDTX48 and CstDTX49 transcripts share the most significant alignments with MtMATE55 (82% of SS and 96% of SC and 78% of SS and 97% of SC, respectively), an transporter member involved in iron homeostasis (Wang et al., 2017), similar to AtDTX48, whose function is linked, among others, to Abscisic Acid (ABA)-mediated stress responses (Zhang et al., 2014). The gene expression values of CstDTX48 after bacterial infection were high and increasing, especially in 72 HAI, reaching more than 128 fold times in expression, suggesting a great involvement of this member in Citrus ABA-mediated stress responses and cellular homeostasis.

5.3.2 Phylogenetics and gene expression analyses of ABC sequences

Based on the phylogenetic relationships, eight ABC subfamilies were identified (ABC A - ABC G, except ABC H - Fig 4, A2), a conserved structure in plant species (Andolfo et al., 2015). Moreover, it allowed us to propose a subfamily for the ten ABC transcripts previously not completely annotated using BLAST2GO tool. We identified 3 genomic sequences from ABC A subfamily in the *C. sinensis* genome, of which all of them have at least one transcript associated in the CRT (Fig 4), and a total of 08 transcripts from the CRT (Table A1). Members belonging to subfamily ABC A were reported to be involved in salt stress and lipid metabolism by mediating the transport of fatty acids to the

endoplasmic reticulum (Kim et al., 2013). The fatty acid metabolism represents a point of convergence and modulation of crosstalk between diverse defense signaling cascades involving salicylic acid and jasmonic acid (Kachroo et al., 2001). Eight CstABC A members were identified in Citrus species, whose six members exhibited a great impact in their gene expression after Xac infection, which were up-regulated at 48 and 72HAI (Fig 6, Table A3). The transport of the fatty acids in Citrus species seems to be mainly positively regulated before 2 days of infection, which probably positively influenced the metabolic enzymes involved in fatty acid and signal molecules during the defense response to Xac.

A total of 26 and 21 genomic sequences from ABC B and ABC C subfamilies, respectively, were identified in the *C. sinensis* genome, which were enriched by gene duplications (Fig 1) as previously found in seven plant genomes (Andolfo et al., 2015). A total of 40 ABC B and 40 ABC C transcripts were identified in the CRT (Table A1), which could indicate the importance of these subfamilies in the Citrus species defense responses. Both subfamilies members are involved with the transport of plant metabolites. The ABC B subfamily is reported to be involved in auxin transport, translocation of xenobiotics and alkaloids (Geisler et al., 2005; Ramel et al., 2007), while ABC C members are involved in the transport of glutathione conjugates and vacuolar transporter of anthocyanins (Lu et al., 1997; Goodman et al., 2004). Nine ABC B transcripts were DE at 24 HAI in ‘Kumquat’, while no transcript in ‘Galego’, suggesting a faster response in the less susceptible cultivar (Fig 9). Patterns of high gene expression were identified in ABC C transcripts, especially in the less susceptible Citrus cultivars (Fig 7, Fig 9), which suggests a more powerful generation of anthocyanins and conjugated metabolites to control/cease the bacterial infection.

The wide range of putative transporters of plant metabolites differentially expressed after Xac infection can represent a substantial effect of Xac mechanisms on the metabolite composition of the Citrus plants and a reason for a large number of ABC B, ABC C, and MATE II transporters expressed by Citrus species under Xac infection, suggesting a contribution with the secreted compounds to pathogen defense at the leaf surface of Citrus plants. Thus, considering the gene expression pattern of these families in Citrus species, as well the previously substrates identified for their members in plants, and the fact that different transporter families may act mutually to transport a particular metabolite (Takanashi et al., 2014; Shoji et al., 2014), we also speculate a cooperative transport mediated by the ABC B, ABC C, and MATE II members for the extrusion of defense-related molecules in Citrus species.

The ABC subfamilies comprising the smallest numbers of members were ABC D, ABC E, and ABC F. A total of 02 genomic sequences from ABC D were identified in the *C. sinensis* genome (Fig 4). Both genes have at least one transcript associated in the CRT, and 08 transcripts were identified in the CRT (Table A1). A peroxisomal import of substrates for β-oxidation and the glyoxylate cycle, jasmonic acid precursors and/or its acyl-CoA derivative into the peroxisome has been suggested to ABC D subfamily (Park et al., 2013). The TCONS_00044207 was predicted to be located in peroxisomes while the other ABC D members in the chloroplast. The DE transcripts were expressed by two of the less susceptible cultivars ‘Ponkan’ and ‘Kumquat’, and no regulation was observed in the highly susceptible cultivar ‘Lima Galego’ (Table A3, Fig 9), suggesting a role of ABC D members in the detoxification mechanismsamplifying the stress-induced signalling pathway through feedback regulation of the transcrptional level of the less susceptibles Citrus plants to CC in response to Xac infection.

Just one and eight genomic sequences from ABC E and ABC F subfamilies, respectively, were identified in the *C. sinensis* genome and 02 and 07 transcripts were identified in the CRT (Table A1). The ABC E subfamily was also found to be the smallest amongst the ABC subfamilies in *A. thaliana*, rice, maize, grape, and tomato, represented in most genomes by a single-copy (Garcia et al., 2004; Çakir and Kiliçkaya, 2013; Liu et al., 2013; Ofori et al., 2018). The ABC E members are involved in ribosome biogenesis and recycling in eukaryotes, however, the mutant phenotypes in plants remain to be explained (Navarro-Quiles, Mateo-Bonmatí and Micol, 2018). The SlABCE1 in tomato is suggested to play roles in ribosome biogenesis, control of translation and gene silencing regulation (Ofori et al., 2018). Alignments using sequences of ABC E members from the CRT featured TCONS_00025710 as the best hit with AtABCE1, sharing 89% of SS and 94% of SC, which suggests a similar role in ribosome controlling of gene expression regulation. Nevertheless, no DE transcript belonging to subfamily E was found, which might represent a slight function of ABC E subfamily in Citrus-Xac interaction. The seven ABC F members identified in the CRT, on the other hand, exhibited negative log2FC values, and only TCONS_00047255 were down-regulated (Table A3). The LrABCF1 gene from *Lilium regale* functions as a positive regulator of plant defense against Cucumber mosaic virus, Tobacco rattle virus, and *Botrytis cinerea* in petunia (Sun et al., 2016). Then, ABC F members might be involved in stress-associated control during Citrus-Xac interaction, acting as a late negative regulator of plant defense.

We identified 72 genomic sequences from ABC G subfamily in the *C. sinensis* genome, of which 57 of them have at least one transcript associated in the CRT (Fig 4), and a total of 102 transcripts from the CRT (Table A1), representing more than 40% of annotated CstABC transporters. In addition to the largest number of members, a high rate of gene duplication was identified in *C. sinensis* genome (Fig 1) and in *A. thaliana, O. sativa, S. lycopersicum, S. tuberosum,* and *V. Vinifera* genomes (Andolfo et al., 2015), Moreover, the subfamily G harbors the largest number of DE transcripts and the genes that most underwent AS events, which can represent a family diversification in combination with gene duplication impacts. Its outstanding diversification is thought to be linked to the requirement of a reliable system to address molecules as nutrients or secondary metabolites to the appropriate cellular compartments for adaptation and survival of plants on the land environment (Hwang et al., 2016).

The ABC G subfamily is constituted of the reverse-oriented full-sized pleiotropic drug resistance homologs (PDRs) and the half-sized white-brown complex homolog proteins (WBCs) (Verrier et al. 2008; Pang et al. 2013). Proteins belonging to the ABC G full-transporters are involved in response to biotic stress and contribute to the transport of signaling molecules or secretion defense-related metabolites and a wide diversity of substrates (Kuromori et al., 2010; Ruocco et al., 2011). For instance, the mRNA level of AtABCG36 is elevated during plant infection with virulent and avirulent strains of the bacterial pathogen *Pseudomonas syringae* (Stein et al., 2006) as observed in the less susceptible cultivar (‘Kumquat’), which up-regulated a higher number of ABC G transcripts than the highly susceptible cultivar (‘Galego’) (Fig 9).

It was also shown that ABCG32 in *Arabidopsis* and HvABCG31 in barley are required for the formation of a functional cuticle, acting as the first barrier against abiotic and biotic stresses (Bessire et al., 2011; Chen et al., 2011). Still comparing the contrasting cultivars, the ABCG32 related transcripts from CRT were up-regulated at all HAI in ‘Kumquat’ and not deferentially expressed in ‘Galego’ whereas ABCG31 transcripts were up-regulated only at 72 HAI in both cultivars (Fig 9). Since the expression of ABC G proteins in plants is predominately in leaves and roots (Nuruzzaman et al., 2014), the expression patterns of ABC subfamily G members during Citrus-Xac interaction might indicate a role in the extrusion of defensive compounds and in barriers development in Citrus leaves, minimizing stress-induced damage and counteracting the pathogen.

The ABCI subfamily contains 09 genomic sequences from *C. sinensis*, of which 08 of them have at least one transcript associated in the CRT (Fig 4), and a total of 19

transcripts from the CRT (Table A1). The I subfamily is usually shorter in amino acid sequences, consisting of only one single ATP-binding domain, NBD, or accessory domains, rendering them difficult to identify and categorize (Verrier et al., 2008; Andolfo et al., 2015). The members of the ABCI subfamily were not clustered together but were distributed in spread clades, as previously observed in rice (Nguyen, Moon, and Jung, 2014), which reflects the assembling with other subunits in the cells to form functional ABC transport systems (Lefèvre and Boutry, 2018). Then, the sequence divergence between CstABC I members may correspond to the genetic fact of binding to play a functional role and consequently, to distinct functions performed in Citrus species. Moreover, the gene expression of two transcripts was negatively regulated in ‘Kumquat’ after Xac infection (Fig 9), suggesting a slight response of ABC I members in Citrus species to bacterial infection.

5.3.3 Phylogenetics and gene expression analyses of MFS sequences

The Major Facilitator Superfamily harbors the highest number of subfamilies (14) in *Citrus sinensis* comparing to the MATE and ABC families. The number of genomic sequences in the subfamilies varied from 2 to 23 in *Citrus sinenis* and from 3 to 38 transcriptomic sequences from the CRT. The largest subfamily, the Sugar Transporter Protein (STP), comprises 23 genes while 38 transcripts were expressed in the CRT. The STP family is also the larger MFS subfamily in *A. thaliana,* which includes 106 out of 218 members (Niño-González et al., 2019), mediating the uptake of a wide range of sugar substrates which are adjusted to the type of tissue, developmental stage, metabolic state, and environmental conditions (Rottmann et al., 2018).

Some STP members were characterized to be involved in biotic stresses, such as STP3 and STP4, involved in strikingly distinct induction kinetics by catalyzing monosaccharide import into classic sinks (Buttner et al., 2000). Moreover, leaf STP8 in import sugars for component systems of secondary products and degradative enzymes important in plant-insect interactions (Rottmann et al., 2018). Since Xac requires prolonged supply of carbon and other nutrients and induces sweet transporter of the cell plants by its effectors (Cohn et al., 2014), and the DE transcripts from STP family were highly recruited especially by the less susceptible cultivars to CC and in 48 and 72 HAI (Table A3, Fig 9), suggesting a role in depriving the apoplastically growing pathogens by limiting their sugar source

The Folate-Biopterin Transporter (FBT) subfamily harbors 10 genomic sequences from *C. sinensis* and 09 transcripts from the CRT (Table A1). The members are related to folate transport, which occurs by complex traffic between the organelles and the cytosol (Gorelova et al., 2017). The folate metabolism is involved in plant development (Mehrshahi et al., 2010), signaling cascades (Stokes et al., 2013), nitrogen and carbon metabolism (Meng et al., 2014), and abiotic stress (Baxter et al., 2007). Also, a biotic stress resistance by the accumulation of a folate precursor was observed in *A. thaliana* infected with *Pseudomonas syringae.* (Wittek et al., 2015). In the Citrus-Xac interaction, the expression of FBT members was not significantly affected, pointing out its likely importance and possible specific adjustment in other processes rather than Xac stress.

Curiously, the MFS members also act in the Inorganic phosphate (Pi) transport activities in the plant, which belong to the PHT subfamily (Phosphate Transporter). The PHT proteins in *A.* thaliana are involved in the transport of Pi between the cytosol and chloroplasts, heterotrophic plastids and the Golgi apparatus (Guo et al., 2008). We identified 7 genomic sequences in the *C. sinensis* genome and 10 transcripts expressed in the CRT, of whose four was DE (Table A3). In the less susceptible cultivar to CC, ‘Kumquat’, the transcript TCONS_00046572 was up-regulated after Xac infection in all the HAI while in the highly susceptible ‘Lima Galego’, three other transcripts were regulated 24 and 48 HAI (Fig 9). Then, the PHT members may be involved in the plant highly complex network of maintenance of Pi homeostasis through regulation of the abundance of PHTs in the Citrus leaves during the defense responses to Xac.

On the other hand, the smallest subfamilies (Spinster, PMT, NPF, INT, ASC, and Anion) are probably responsible for the transport of Anion, Inositol, Sphingolipids, and Lipids, which include 6 or fewer genes in the *C. sinensis* genome. Furthermore, the available information on these MFS subfamily members is still poorly investigated or not yet addressed experimentally. Despite that, we were able to infer based on previous experimental studies, genomic and transcriptomic data the potential of CsMFS members in meeting the carbohydrate demand of cells responding to bacterial stress, providing an efficient adaptive fit to the citrus canker disease. In conclusion, we hypothesize a complex strategy adopted by Citrus plants cells of regulation of multiple members from MATE II, ABC B, ABC C, ABC G, and STP subfamilies as the source of proper defense responses to Xac infection, highlighting 17 members as potential targets for functional studies (Table 5).

Table 5. Promising candidates for further exploitation based on their potential role in the Citrus-Xac interaction.

Gene	Acession Number	Subfamily in *C. sinensis*	Annotation	InterPro Family and Domains	InterPro Domains ID	Closest Homolog	*A. thaliana* Homolog	Potential role in the Citrus-Xac interaction
Cs1g07540	XP_006464779.1	MATE I	DTX19		IPR002528	*Herrania umbratica* DTX18	At3g23560	Regulation of the tolerance towards xenobiotics
Cs2g13530	XP_006468796.1	MATE I	DTX16		IPR002528	*Pistacia vera* DTX16	At5g52450	
Cs1g20130	XP_006466279.1	MATE II	DTX27		IPR002528	*Quercus lobata* DTX27	At5g65380	Disease tolerance regulation
Cs7g09190	XP_006483932.1	MATE II	DTX29		IPR002528	*Pistacia vera* DTX29	At3g26590	
Cs3g26380	XP_006473687.1	ABC B	ABC B13		IPR039421	*Pistacia vera* ABC B13	At1g27940	Transport of secondary metabolites (antocyanin, flavonoids, alkaloids, etc.)
Cs6g20270	XP_006482502.1	ABC B	ABC B15	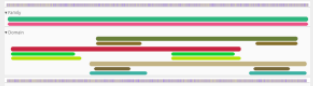	IPR039421	*Pistacia vera* ABC B15	At3g28345	
Cs7g10200	XP_006484035.1	ABC C	ABC C15		IPR003593, IPR003439, IPR011527	*Pistacia vera* ABC C15	At3g13080	
Cs1g18450	KDO65310.1	ABC C	ABC C8		IPR003593, IPR003439, IPR011527	*Populus alba* ABC C8	At3g21250	
orange1.1t02765	XP_006493359.1	ABC C	ABC C13		IPR003593, IPR003439, IPR011527	*Pistacia vera* ABC C13	At2g07680	
Cs5g17290	XP_006478168.1	ABC G	ABC G11		IPR003593, IPR003439, IPR011527	*Gossypium raimondii* ABC G11	At1g17840	Transport of signaling molecules, secretion of defensive compounds, and barriers development in Citrus leaves
Cs8g16470	XP_024958158.1	ABC G	ABC G31	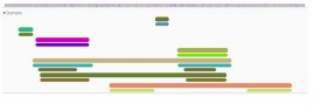	IPR013581, IPR029481, IPR003593, IPR003439, IPR011527, IPR034001, IPR034003	*Pistacia vera* ABC G31	At2g29940	
Cs9g01400	XP_015388954.1	ABC G	ABC G37	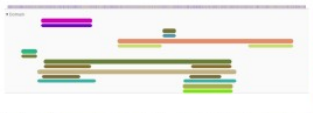	IPR013581, IPR029481, IPR003593, IPR003439, IPR011527, IPR034001, IPR034003	*Populus trichocarpa* ABC G37	At3g53480	
Cs4g17100	XP_006475761.1	ABC G	ABC G32	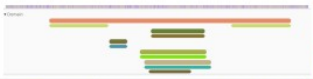	IPR013525, IPR003593, IPR013581, IPR034003, IPR003439	*Pistacia vera* ABC G32	At2g26910	
Cs3g24900	XP_006473508.3	STP	ERD6-like 6	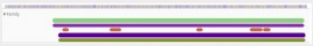	IPR003663, IPR005828	*Pyrus x bretschneideri* ERD6-like 6	At1g75220	Limit the sugar source of *Xanthomonas citri* subsp. *citri*
Cs1g24180	KDO79562.1	STP	ERD6-like 6		IPR003663, IPR005828	*Durio zibethinus* ERD6-like 6	At1g69650	
Cs5g32060	XP_006479807.1	STP	ERD6-like 7		IPR003663, IPR005828	*Pistacia vera* ERD6-like 7	At2g45820	

6. CONCLUSIONS

MATE, ABC, and MFS transporters are involved beyond development and survival processes in plants, are essential proteins under plant-pathogen interactions due to their role in the excretion or uptake of macronutrients, defense-related compounds, xenobiotics, and metabolic products. Five MATE, eight ABC, and fourteen MFS subfamilies were identified in *Citrus sinensis*, of which their putative roles and impact during the Citrus-Xac interaction revealed potential targets for functional studies and a common transport of secondary metabolites and xenobiotics. Moreover, the subfamilies MATE I and ABC G seem to be key players in the management of the compounds produced by plants during the defense responses. Altogether, the transcriptional evidence of both membrane transporter family members based on CRT data supports the proposal for a highly complex pattern of gene expression regulation during the Citrus-Xac interaction, which reflects the

intricate defense-related processes in CC susceptibility levels between Citrus cultivars. Also, alternative splicing and gene duplication events may represent evolutionary strategies to increase the membrane transporters' numbers and functional diversification in Citrus species for proper stress responses to Citrus Canker disease. Altogether the findings from this work offer useful information, highlighting membrane transporters for potential biotechnological applications, and representing a basis for the functional characterization of MATE, ABC, and MFS transporters in Citrus species, helping to address several biological questions concerning the plant membrane transporters families.

7. REFERENCES

Anders S and Huber W (2010) Differential expression analysis for sequence count data. **Nature Precedings** 11:1-12.

Andolfo G, Ruocco M, Di Donato A, Frusciante L, Lorito M, Scala F, Ercolano MR (2015) Genetic variability and evolutionary diversification of membrane ABC transporters in plants. **BMC Plant Biology** 15:51-66.

Bassanezi RB, Montesino LH, Gasparoto MCG, Filho AB, Amorim L (2011) Yield loss caused by huanglongbing in different sweet orange cultivars in São Paulo, Brazil. **European Journal of Plant Pathology** 130:577-586.

Baxter CJ, Redestig H, Schauer N, Repsilber D, Patil KR, Nielsen J, Selbig J, Liu J, Fernie AR, Sweetlove LJ (2007) The metabolic response of heterotrophic Arabidopsis cells to oxidative stress. **Plant Physiology** 143:312-325.

Behlau F, Belasque J, Graham JH, Leite RP (2010) Effect of frequency of copper applications on control of citrus canker and the yield of young bearing sweet orange trees. **Crop Protection** 29:300-305.

Berens ML, Berry HM, Mine A, Argueso CT, Tsuda K (2017) Evolution of Hormone Signaling Networks in Plant Defense. **Annual Review of Phytopathology** 55:401-425.

Bessire M, Borel S, Fabre G, Carraça L, Efremova N, Yephremov A, Cao Y, Jetter R, Jacquat A-C, Métraux J-P (2011) A Member of the PLEIOTROPIC DRUG RESISTANCE Family of ATP Binding Cassette Transporters Is Required for the Formation of a Functional Cuticle in Arabidopsis . **The Plant Cell** 23:1958-1970.

Burko Y, Geva Y, Refael-Cohen A, Shleizer-Burko S, Shani E, Berger Y, Halon E, Chuck G, Moshelion M, Ori N (2011) From organelle to organ: ZRIZI MATE-Type Transporter is an Organelle Transporter that Enhances Organ Initiation. **Plant and Cell Physiology** 52:518-527.

Brown MH, Paulsen IT and Skurray RA (1999) The multidrug efflux protein NorM is a prototype of a new family of transporters. **Molecular microbiology** 31:394-395.

Büttner M (2010) The Arabidopsis sugar transporter (AtSTP) family: an update. **Plant Biology** 12:35-41.

Çakir B, Kiliçkaya O (2013) Whole-genome survey of the putative ATP-binding cassette transporter family genes in *Vitis vinifera*. **PLoS ONE** 8:11-29.

Cannon SB, Mitra A, Baumgarten A, Young ND, May G (2004) The roles of segmental and tandem gene duplication in the evolution of large gene families in *Arabidopsis thaliana*. **BMC Plant Biology** 4:1-21.

Carbonell-Caballero J, Alonso R, Ibañez V, Terol J, Talon M, Dopazo J (2015) A phylogenetic analysis of 34 chloroplast genomes elucidates the relationships between wild and domestic species within the genus *Citrus*. **Molecular biology and evolution** 32:2015-2035.

de Carvalho SA, de Carvalho Nunes WM, Belasque J, Machado MA, Croce-Filho J, Bock CH, Abdo Z (2015) Comparison of Resistance to Asiatic Citrus Canker Among Different Genotypes of Citrus in a Long-Term Canker-Resistance Field Screening Experiment in Brazil. **Plant Disease** 99:207-218.

Chen G, Komatsuda T, Ma JF, Nawrath C, Pourkheirandish M, Tagiri A, Hu Y-G, Sameri M, Li X, Zhao X, et al. (2011) An ATP-binding cassette subfamily G full transporter is essential for the retention of leaf water in both wild barley and rice. **Proceedings of the National Academy of Sciences** 108:12354-12359.

Cheval C, Faulkner C (2018) Plasmodesmal regulation during plant-pathogen interactions. **New Phytologist** 217:62-67.

Chin EL, Mishchuk DO, Breksa AP, Slupsky CM (2014) Metabolite signature of candidatus liberibacter asiaticus infection in two citrus varieties. **Journal of Agricultural and Food Chemistry** 62:6585-6591.

Chiteka ZA, Gorbet DW, Knauft DA, Shokes FM, Kucharek TA (1988) Components of Resistance to Late Leafspot in Peanut. **Peanut Science** 15:76-81.

Conesa A, Götz S, García-gómez JM, Terol J, Talón M, Genómica D, Valenciano I, Agrarias DI, Valencia UP De (2005) Blast2GO : a universal tool for annotation , visualization and analysis in functional genomics research. **Bioinformatics** 21:3674-3676.

Cohn, M et al. (2014) *Xanthomonas axonopodis* virulence is promoted by a transcription activator-like effector–mediated induction of a SWEET sugar transporter in cassava. **Molecular Plant-Microbe Interactions**, 27:1186-1198.

Consortium TU (2019) UniProt : a worldwide hub of protein knowledge. **Bioinformatics** 47:506-515.

Dawson RJP, Hollenstein K, Locher KP (2007) Uptake or extrusion: Crystal structures of full ABC transporters suggest a common mechanism. **Molecular Microbiology** 65:250-257.

Diener AC, Gaxiola RA, Fink GR (2001) Arabidopsis ALF5, a Multidrug Efflux Transporter Gene Family Member, Confers Resistance to Toxins. **The Plant Cell** 13:1625.

Fath MJ, Kolter R (1993) ABC transporters: Bacterial exporters. **Microbiological Reviews** 57:995-1017.

Ferrasa, A et al. (2020) CitrusKB: A Comprehensive Knowledge Base for Transcriptome and Interactome of *Citrus* spp. Infected by *Xanthomonas citri* subsp. *citri* at Different Infection Stages. **bioRxiv**.

Garcia O, Bouige P, Forestier C, Dassa E (2004) Inventory and comparative analysis of rice and Arabidopsis ATP-binding cassette (ABC) systems. **Journal of Molecular Biology** 343:249-265.

Geisler M, Blakeslee JJ, Bouchard R, Lee OR, Vincenzetti V, Bandyopadhyay A, Titapiwatanakun B, Peer WA, Bailly A, Richards EL, et al. (2005) Cellular efflux of auxin catalyzed by the Arabidopsis MDR/PGP transporter AtPGP1. **Plant Journal** 44:179-194.

Gomez C, Terrier N, Torregrosa L, Vialet S, Fournier-Level A, Verriès C, Souquet J-M, Mazauric J-P, Klein M, Cheynier V, et al. (2009) Grapevine MATE-Type Proteins Act as Vacuolar H^+ -Dependent Acylated Anthocyanin Transporters . **Plant Physiology** 150:402-415.

Goodman CD, Casati P, Walbot V (2004) A Multidrug Resistance-Associated Protein Involved in Anthocyanin Transport in *Zea mays*. T**he Plant Cell** 16:1812-1826.

Gorelova V, Ambach L, Rébeillé F, Stove C, Van Der Straeten D (2017) Folates in plants: Research advances and progress in crop biofortification. **Frontiers in Chemistry** 5:1-20.

Goswitz VC, Brooker RJ (1995) Structural features of the uniporter/symporter/antiporter superfamily. **Protein Science** 4:534-537.

Gottwald TR, Graham JH, Schubert TS (2002) Citrus Canker : The Pathogen and Its Impact Plant Health Progress Plant Health Progress. **Plant Management Network.** 1993:48824.

Gregor Madej M, Dang S, Yan N, Ronald Kaback H (2013) Evolutionary mix-and-match with MFS transporters. **Proceedings of the National Academy of Sciences of the United States of America** 110:5870-5874.

Gu Y, Zavaliev R, Dong X (2017) Membrane Trafficking in Plant Immunity. **Molecular Plant** 10:1026-1034.

Gu Z, Eils R, Schlesner M (2016) Genome analysis Complex heatmaps reveal patterns and correlations in multidimensional genomic data. **Bioinformatics** 32:2847-2849.

Guo B, Jin Y, Wussler C, Blancaflor EB, Motes CM, Versaw WK (2008) Functional analysis of the Arabidopsis PHT4 family of intracellular phosphate transporters. **New Phytologist** 177:889-898.

H. Mathews, S. K. Clendennen, C. G. Caldwell, X. L. Liu, K. Connors, N. Matheis, D. K. Schuster, D. J. Menasco, W. Wagoner, J. Lightner and DW (2003) L'industrie de la Micoque. **The Plant Cell** 75:369-396.

Hasse CH (1915) *Pseudomonas citri,* the cause of citrus canker. **Journal of Agricultural Research** 4:97-104.

Higgins CF (2001) ScienceDirect.com - Research in Microbiology - ABC transporters: physiology, structure and mechanism - an overview. **Research in Microbiology** 152:205-210.

Higgins CF, Linton KJ (2004) The ATP switch model for ABC transporters. **Nature structural & molecular biology** 11:918-926.

Hijaz FM, Manthey JA, Folimonova SY, Davis CL, Jones SE, Reyes-De-Corcuera JI (2013) An HPLC-MS characterization of the changes in sweet orange leaf metabolite profile following infection by the bacterial pathogen Candidatus *Liberibacter asiaticus*. **PLoS ONE** 8:1-15.

Hirai T, Heymann JAW, Maloney PC, Subramaniam S (2003) Structural model for 12-helix transporters belonging to the major facilitator superfamily. **Journal of Bacteriology** 185:1712-1718.

Horton P, Park K, Obayashi T, Fujita N, Harada H, Nakai K (2007) WoLF PSORT: protein localization predictor. **Nucleic acids research** 35:585-587.

Hvorup RN, Winnen B, Chang AB, Jiang Y, Zhou X, Jr MHS (2003) The multidrug / oligosaccharidyl-lipid / polysaccharide (MOP) exporter superfamily. **European Journal of Biochemistry** 813:799-813.

Hwang J, Song W, Hong D, Ko D, Yamaoka Y, Jang S, Yim S, Lee E, Khare D, Kim K, et al. (2016) Plant ABC Transporters Enable Many Unique Aspects of a Terrestrial Plant' s Lifestyle. **Molecular Plant** 9:338-355.

Ishimaru Y, Kakei Y, Shimo H, Bashir K, Sato Y, Sato Y, Uozumi N, Nakanishi H, Nishizawa NK (2011) A rice phenolic efflux transporter is essential for solubilizing precipitated apoplasmic iron in the plant stele. **Journal of Biological Chemistry** 286:24649-24655.

Jeong J, Guerinot M Lou (2009) Homing in on iron homeostasis in plants. **Trends in Plant Science** 14:280-285.

Jiao Y, Wickett NJ, Ayyampalayam S, Chanderbali AS, Landherr L, Ralph PE, Tomsho LP, Hu Y, Liang H, Soltis PS, et al. (2011) Ancestral polyploidy in seed plants and angiosperms. **Nature** 473:97-100.

Jones JDG, Dangl JL (2006) The plant immune system. **Nature** 444:323-329.

Jones P, Binns D, Chang HY, Fraser M, Li W, McAnulla C, McWilliam H, Maslen J, Mitchell A, Nuka G, et al. (2014) InterProScan 5: Genome-scale protein function classification. **Bioinformatics** 30:1236-1240.

Kachroo P, Shanklin J, Shah J, Whittle EJ, Klessig DF (2001) A fatty acid desaturase modulates the activation of defense signaling pathways in plants. **Proceedings of the National Academy of Sciences of the United States of America** 98:9448-9453.

Khare D, Choi H, Huh SU, Bassin B, Kim J, Martinoia E, Sohn KH, Paek KH, Lee Y, Chrispeels MJ (2017) Arabidopsis ABCG34 contributes to defense against necrotrophic pathogens by mediating the secretion of camalexin. **Proceedings of the National Academy of Sciences of the United States of America** 114:E5712-E5720.

Kim S, Yamaoka Y, Ono H, Kim H, Shim D, Maeshima M, Martinoia E, Cahoon EB, Nishid I, Lee Y (2013) AtABCA9 transporter supplies fatty acids for lipid synthesis to the endoplasmic reticulum. **Proceedings of the National Academy of Sciences of the United States of America** 110:773-778.

Krouk G, Lacombe B, Bielach A, Perrine-Walker F, Malinska K, Mounier E, Hoyerova K, Tillard P, Leon S, Ljung K, et al. (2010) Nitrate-regulated auxin transport by NRT1.1 defines a mechanism for nutrient sensing in plants. **Developmental Cell** 18:927-937.

Kryvoruchko IS, Routray P, Sinharoy S, Torres-Jerez I, Tejada-Jiménez M, Finney LA, Nakashima J, Pislariu CI, Benedito VA, González-Guerrero M, et al. (2018) An Iron-Activated Citrate Transporter, MtMATE67, Is Required for Symbiotic Nitrogen Fixation. **Plant Physiology** 176:2315-2329.

Kuromori T, Miyaji T, Yabuuchi H, Shimizu H, Sugimoto E, Kamiya A, Moriyama Y, Shinozaki K (2010) ABC transporter AtABCG25 is involved in abscisic acid transport and responses. **Proceedings of the National Academy of Sciences of the United States of America** 107:2361-2366.

LBP Mendonça, L Zambolim JB (2017) Bacterial Citrus Diseases: Major Threats and Recent Progress. **Journal of Bacteriology & Mycology: Open Access** 5.

Le SQ, Gascuel O (2008) An improved general amino acid replacement matrix. **Molecular Biology and Evolution** 25:1307-1320.

Lefèvre, F.; Boutry M (2018) Topical Review on Substrates of ABC Transporters Towards Identification of the Substrates of ATP-Binding. **Plant Physiology** 178:18-39.

Li L, He Z, Pandey GK, Tsuchiya T, Luan S (2002) Functional cloning and characterization of a plant efflux carrier for multidrug and heavy metal detoxification. **Journal of Biological Chemistry** 277:5360-5368.

Liu J, Magalhaes J V., Shaff J, Kochian L V. (2009) Aluminum-activated citrate and malate transporters from the MATE and ALMT families function independently to confer Arabidopsis aluminum tolerance. **Plant Journal** 57:389-399.

Liu J, Li Y, Wang W, Gai J, Li Y (2016) Genome-wide analysis of MATE transporters and expression patterns of a subgroup of MATE genes in response to aluminum toxicity in soybean. **BMC Genomics** 17:1-15.

Liu M, Pang K, Yu Y, Li Y, Meng Z (2013) Inventory and general analysis of the ATP-binding cassette (ABC) gene superfamily in maize (*Zea mays* L.). **Gene** 526:411-428.

Lu P, Magwanga RO, Guo X, Kirungu JN, Lu H, Cai X, Zhou Z, Wei Y, Wang X, Zhang Z, et al. (2018) Genome-Wide Analysis of Multidrug and Toxic Compound Extrusion (MATE) Family in *Gossypium raimondii* and *Gossypium arboreum* and Its Expression Analysis Under Salt, Cadmium, and Drought Stress. **G3 Genes|Genomes|Genetics** 8:2483-2500.

Lu YP, Li ZS, Rea PA (1997) AtMRP1 gene of Arabidopsis encodes a glutathione S-conjugate pump: Isolation and functional definition of a plant ATP-binding cassette transporter gene. **Proceedings of the National Academy of Sciences of the United States of America** 94:8243-8248.

Madeira F, Park Y, Lee J, Buso N, Gur T, Madhusoodanan N, Basutkar P, Tivey ARN, Potter SC, Finn D, et al. (2019) The EMBL-EBI search and sequence analysis tools APIs in 2019. **Nucleic acids research** 47:636-641.

MAPA (2018) Ministério da Agricultura, Pecuária e Abastecimento. Instrução Normativa nº 21, de 25 de Abril de 2018. **AGROFIT: Sistema de Agrotóxicos Fitossanitários** 39-12

Mastrangelo AM, Marone D, Laidò G, De Leonardis AM, De Vita P (2012) Alternative splicing: Enhancing ability to cope with stress via transcriptome plasticity. **Plant Science** 185-186:40-49.

Mehrshahi P, Gonzalez-Jorge S, Akhtar TA, Ward JL, Santoyo-Castelazo A, Marcus SE, Lara-Núñez A, Ravanel S, Hawkins ND, Beale MH, et al. (2010) Functional analysis of folate polyglutamylation and its essential role in plant metabolism and development. **Plant Journal** 64:267-279.

Melotto M, Underwood W, Koczan J, Nomura K, He SY (2006) Plant Stomata Function in Innate Immunity against Bacterial Invasion. **Cell** 126:969-980.

Meng H, Jiang L, Xu B, Guo W, Li J, Zhu X, Qi X, Duan L, Meng X, Fan Y, et al. (2014) Arabidopsis plastidial folylpolyglutamate synthetase is required for seed reserve accumulation and seedling establishment in darkness. **PLoS ONE** 9.

Miller MA, Schwartz T, Pickett BE, He S, Klem EB, Scheuermann RH, Passarotti M, Kaufman S, Leary MAO (2015) A RESTful API for Access to Phylogenetic Tools via the CIPRES Science Gateway. **Evolutionary Bioinformatics** 11:43-48.

Mishra AK, Choi J, Rabbee MF, Baek KH, Shavrukov Y (2019) In Silico Genome-Wide Analysis of the ATP-Binding Cassette Transporter Gene Family in Soybean (*Glycine max* L.) and Their Expression Profiling. **BioMed Research International** 2019.

Morita Y, Kodama K, Shiota S, Mine T, Kataoka A, Mizushima T, Tsuchiya T (1998) NorM, putative multidrug efflux protein, of Vibrio parahaemolyticus and its homolog in Escherichia coli. **Antimicrobial Agents and Chemotherapy** 42:1778-1782.

Müller T, Vingron M (2001) Modeling amino acid replacement. **Journal of Computational Biology** 7:761-776.

Nakamura T, Yamada KD, Tomii K, Katoh K (2018) Sequence analysis Parallelization of MAFFT for large-scale multiple sequence alignments. **Bioinformatics** 34:2490-2492.

Navarro-Quiles C, Mateo-Bonmatí E, Micol JL (2018) ABCE proteins: From molecules to development. **Frontiers in Plant Science** 9:1-10.

Nguyen VNT, Moon S, Jung KH (2014) Genome-wide expression analysis of rice ABC transporter family across spatio-temporal samples and in response to abiotic stresses. **Journal of Plant Physiology** 171:1276-1288.

Niño-González M, Novo-Uzal E, Richardson DN, Barros PM, Duque P (2019) More Transporters, More Substrates: The Arabidopsis Major Facilitator Superfamily Revisited. **Molecular Plant** 12:1182-1202.

Nuruzzaman M, Zhang R, Cao HZ, Luo ZY (2014) Plant pleiotropic drug resistance transporters: Transport mechanism, gene expression, and function. **Journal of Integrative Plant Biology** 56:729-740.

Ofori PA, Mizuno A, Suzuki M, Martinoia E, Reuscher S, Aoki K, Shibata D, Otagaki S, Matsumoto S, Shiratake K (2018) Genome-wide analysis of atp binding cassette (abc) transporters in tomato. **PLoS ONE**.

Omote H, Hiasa M, Matsumoto T, Otsuka M, Moriyama Y (2006) The MATE proteins as fundamental transporters of metabolic and xenobiotic organic cations. **Trends in Pharmacological Sciences** 27:587-593.

Omura M, Shimada T (2016) Citrus breeding, genetics and genomics in Japan. **Breeding Science** 66:3-17.

Panchy N, Lehti-Shiu M, Shiu SH (2016) Evolution of gene duplication in plants. **Plant Physiology** 171:2294-2316.

Pang K, Li Y, Liu M, Meng Z and Yu Y (2013) Inventory and general analysis of the ATP-binding cassette (ABC) gene superfamily in maize (*Zea mays* L.). **Gene** 526:411-428.

Park S et al. (2013) The α/β hydrolase CGI-58 and peroxisomal transport protein PXA1 coregulate lipid homeostasis and signaling in Arabidopsis. **The Plant Cell** 5:1726-1739.

Parinthawong N, Cottier S, Buchala A, Nawrath C, Métraux JP (2015) Localization and expression of EDS5H a homologue of the SA transporter EDS5. **BMC Plant Biology** 15:1-10.

Paulsen IT (2003) Multidrug efflux pumps and resistance: Regulation and evolution. **Current Opinion in Microbiology** 6:446-451.

Peña L, Cervera M, Fagoaga C, Romero J, Ballester A, Soler N, Pons E, Rodr A, Peris J (2008) Citrus. **Compendium of transgenic crop plants** 1-62.

Ramel F, Sulmon C, Cabello-Hurtado F, Taconnat L, Martin-Magniette ML, Renou JP, El Amrani A, Couée I, Gouesbet G (2007) Genome-wide interacting effects of sucrose and herbicide-mediated stress in *Arabidopsis thaliana*: Novel insights into atrazine toxicity and sucrose-induced tolerance. **BMC Genomics** 8:1-20.

Reddy VS, Shlykov MA, Castillo R, Sun EI, Saier MH (2012) The major facilitator superfamily (MFS) revisited. **FEBS Journal** 279:2022-2035.

Rottmann T, Klebl F, Schneider S, Kischka D, Rüscher D, Sauer N, Stadler R (2018) Sugar transporter STP7 specificity for L-arabinose and D-xylose contrasts with the typical hexose transporters STP8 and STP12. **Plant Physiology** 176:2330-2350.

Ruocco M, Ambrosino P, Lanzuise S, Woo SL, Lorito M, Scala F (2011) Four potato (Solanum tuberosum) ABCG transporters and their expression in response to abiotic factors and *Phytophthora infestans* infection. **Journal of Plant Physiology** 168:2225-2233.

Saier MH, Beatty JT, Goffeau A, Harley KT, Heijne WHM, Huang SC, Jack DL, Jähn PS, Lew K, Liu J, et al. (1999) The major facilitator superfamily. **Journal of Molecular Microbiology and Biotechnology** 1:257-279.

dos Santos AL, Chaves-Silva S, Yang L, Maia LGS, Chalfun-Júnior A, Sinharoy S, Zhao J, Benedito VA (2017) Global analysis of the MATE gene family of metabolite transporters in tomato. **BMC Plant Biology** 17.

Sawaki Y, Kihara-Doi T, Kobayashi Y, Nishikubo N, Kawazu T, Kobayashi Y, Koyama H, Sato S (2013) Characterization of Al-responsive citrate excretion and citrate-transporting MATEs in *Eucalyptus camaldulensis*. **Planta** 237:979-989.

Schenk PM, Kazan K, Wilson I, Anderson JP, Richmond T, Somerville SC, Manners JM (2000) Coordinated plant defense responses in Arabidopsis revealed by microarray analysis. **Proceedings of the National Academy of Sciences of the United States of America** 97:11655-11660.

Schroeder JI, Delhaize E, Frommer WB, Guerinot M Lou, Harrison MJ, Herrera-Estrella L, Horie T, Kochian L V., Munns R, Nishizawa NK, et al. (2013) Using membrane transporters to improve crops for sustainable food production. **Nature** 497:60-66.

Seo PJ, Park J, Park M-J, Kim Y-S, Kim S-G, Jung J-H, Park C-M (2012) A Golgi-localized MATE transporter mediates iron homoeostasis under osmotic stress in Arabidopsis . **Biochemical Journal** 442:551-561.

Shitan N, Yazaki K (2013) New insights into the transport mechanisms in plant vacuoles. **International review of cell and molecular biology** Academic Press 305:383-433.

Shoji T (2014) ATP-Binding Cassette and Multidrug and Toxic Compound Extrusion Transporters in Plants. **International review of cell and molecular biology** Academic Press 309:303-346.

Staiger D, Brown JWS (2013) Alternative splicing at the intersection of biological timing, development, and stress responses. **Plant Cell** 25:3640-3656.

Stamatakis A (2014) RAxML version 8 : a tool for phylogenetic analysis and post-analysis of large phylogenies. **Bioinformatics** 30:1312-1313.

Stein M et al. (2006). Arabidopsis PEN3/PDR8, an ATP binding cassette transporter, contributes to nonhost resistance to inappropriate pathogens that enter by direct penetration. **The Plant Cell** 18:731-746.

Stokes ME, Chattopadhyay A, Wilkins O, Nambara E, Campbell MM (2013) Interplay between sucrose and folate modulates auxin signaling in Arabidopsis. **Plant Physiology** 162:1552-1565.

Sugiyama A, Shitan N, Sato S, Nakamura Y, Tabata S, Yazaki K (2006) Genome-wide analysis of ATP-binding cassette (ABC) proteins in a model legume plant, *Lotus japonicus*: Comparison with Arabidopsis ABC protein family. **DNA Research** 13:205-228.

Sun X, Gilroy EM, Chini A, Nurmberg PL, Hein I, Lacomme C, Birch PRJ, Hussian A, Yun B and Loake, GJ (2011) ADS1 encodes a MATE transporter that negatively regulates plant disease resistance. **New Phytologist** 192:471-482.

Sun D, Zhang X, Li S, Jiang CZ, Zhang Y and Niu, L (2016). LrABCF1, a GCN-type ATP-binding cassette transporter from *Lilium regale*, is involved in defense responses against viral and fungal pathogens. **Planta** 244:1185-1199.

Takanashi K, Yokosho K, Saeki K, Sugiyama A, Sato S, Tabata S, Ma JF, Yazaki K (2013) LjMATE1: A citrate transporter responsible for iron supply to the nodule infection zone of *Lotus japonicus*. **Plant and Cell Physiology** 54:585-594.

Takanashi K, Shitan N, Yazaki K (2014) The multidrug and toxic compound extrusion (MATE) family in plants. **Plant Biotechnology** 31:417-430.

Tegos G, Stermitz FR, Lomovskaya O, Lewis K (2002) Multidrug pump inhibitors uncover remarkable activity of plant antimicrobials. **Antimicrobial Agents and Chemotherapy** 46:3133-3141.

Thompson EP, Wilkins C, Demidchik V, Davies JM, Glover BJ (2010) An Arabidopsis flavonoid transporter is required for anther dehiscence and pollen development. **Journal of Experimental Botany** 61:439-451.

Tiwari M, Sharma D, Singh M, Tripathi RD, Trivedi PK (2014) Expression of OsMATE1 and OsMATE2 alters development, stress responses and pathogen susceptibility in Arabidopsis. **Scientific Reports** 4:1-12.

Uchida N, Tasaka M (2010) Intersections between immune responses and morphological regulation in plants. **Journal of Experimental Botany** 61:2539-2547.

Uindon PG, Ranc JEAN (2010) New Algorithms and Methods to Estimate Maximum-Likelihood Phylogenies : Assessing the Performance of PhyML 3.0. **Systematic Biology** 59:307-321.

United States Department of Agriculture USDA: Foreign Agricultural Service. Citrus: Word Markets and Trade. 1-13.

Upadhyay N, Kar D, Deepak Mahajan B, Nanda S, Rahiman R, Panchakshari NA, Bhagavatula L, Datta S (2019) The multitasking abilities of MATE transporters in plants. **Journal of Experimental Botany**.

Verrier PJ, Bird D, Burla B, Dassa E, Forestier C, Geisler M, Klein M, Kolukisaoglu Ü, Lee Y, Martinoia E, et al. (2008) Plant ABC proteins - a unified nomenclature and updated inventory. **Trends in Plant Science** 13:151-159.

Wang J, Hou Q, Li P, Yang L, Sun X, Benedito VA, Wen J, Chen B, Mysore KS, Zhao J (2017) Diverse functions of multidrug and toxin extrusion (MATE) transporters in citric acid efflux and metal homeostasis in *Medicago truncatula*. **Plant Journal** 90:79-95.

Wang L, Bei X, Gao J, Li Y, Yan Y, Hu Y (2016a) The similar and different evolutionary trends of MATE family occurred between rice and *Arabidopsis thaliana*. **BMC Plant Biology** 16:1-20.

Wang R, Liu X, Liang S, Ge Q, Li Y, Shao J, Qi Y, An L, Yu F (2015) A subgroup of MATE transporter genes regulates hypocotyl cell elongation in Arabidopsis. **Journal of Experimental Botany** 66:6327-6343.

Wang WM, Liu PQ, Xu YJ, Xiao S (2016b) Protein trafficking during plant innate immunity. **Journal of Integrative Plant Biology** 58:284-298.

Wang Y, Tang H, Debarry JD, Tan X, Li J, Wang X, Lee T, Jin H, Marler B, Guo H, et al. (2012) MCScanX : a toolkit for detection and evolutionary analysis of gene synteny and collinearity. **Nucleic acids research** 40:1-14.

Whelan S, Goldman N (2001) A general empirical model of protein evolution derived from multiple protein families using a maximum-likelihood approach. **Molecular Biology and Evolution** 18:691-699.

Wickham H (2016) ggplot2: elegant graphics for data analysis. **Springer** 17:160-167.

Wittek F, Kanawati B, Wenig M, Hoffmann T, Franz-Oberdorf K, Schwab W, Schmitt-Kopplin P, Vlot AC (2015) Folic acid induces salicylic acid-dependent immunity in Arabidopsis and enhances susceptibility to *Alternaria brassicicola*. **Molecular Plant Pathology** 16:616-622.

Wu X, Li R, Shi J, Wang J, Sun Q, Zhang H, Xing Y, Qi Y, Zhang N, Guo YD (2014) Brassica oleracea MATE encodes a citrate transporter and enhances aluminum tolerance in *Arabidopsis thaliana*. **Plant and Cell Physiology** 55:1426-1436.

Wu GA et al. (2018) Genomics of the origin and evolution of Citrus. **Nature**, 554:311-316.

Xiong J, Feng J, Yuan D, Zhou J, Miao W (2015) Tracing the structural evolution of eukaryotic ATP binding cassette transporter superfamily. **Scientific Reports** 5:1-15.

Xu L, Shen ZL, Chen W, Si GY, Meng Y, Guo N, Sun X, Cai YP, Lin Y, Gao JS (2019) Phylogenetic analysis of upland cotton MATE gene family reveals a conserved subfamily involved in transport of proanthocyanidins. **Molecular Biology Reports** 46:161-175.

Zhang H, Zhu H, Pan Y, Yu Y, Luan S, Li L (2014) A DTX/MATE-type transporter facilitates abscisic acid efflux and modulates ABA sensitivity and drought tolerance in Arabidopsis. **Molecular Plant** 7:1522-1532.

Zhao J, Huhman D, Shadle G, He X-Z, Sumner LW, Tang Y, Dixon RA (2011) MATE2 Mediates Vacuolar Sequestration of Flavonoid Glycosides and Glycoside Malonates in *Medicago truncatula*. **The Plant Cell** 23:1536-1555.

Zhou G, Delhaize E, Zhou M, Ryan PR (2013) The barley MATE gene, HvAACT1, increases citrate efflux and Al3+ tolerance when expressed in wheat and barley. **Annals of Botany** 112:603-612.

Zhu H, Wu J, Jiang Y, Jin J, Zhou W, Wang Y, Han G, Zhao Y, Cheng B (2016) Genome-wide analysis of MATE-type gene family in maize reveals microsynteny and their expression patterns under aluminum treatment. **Journal of Genetics** 95:691-704.

APPENDIX

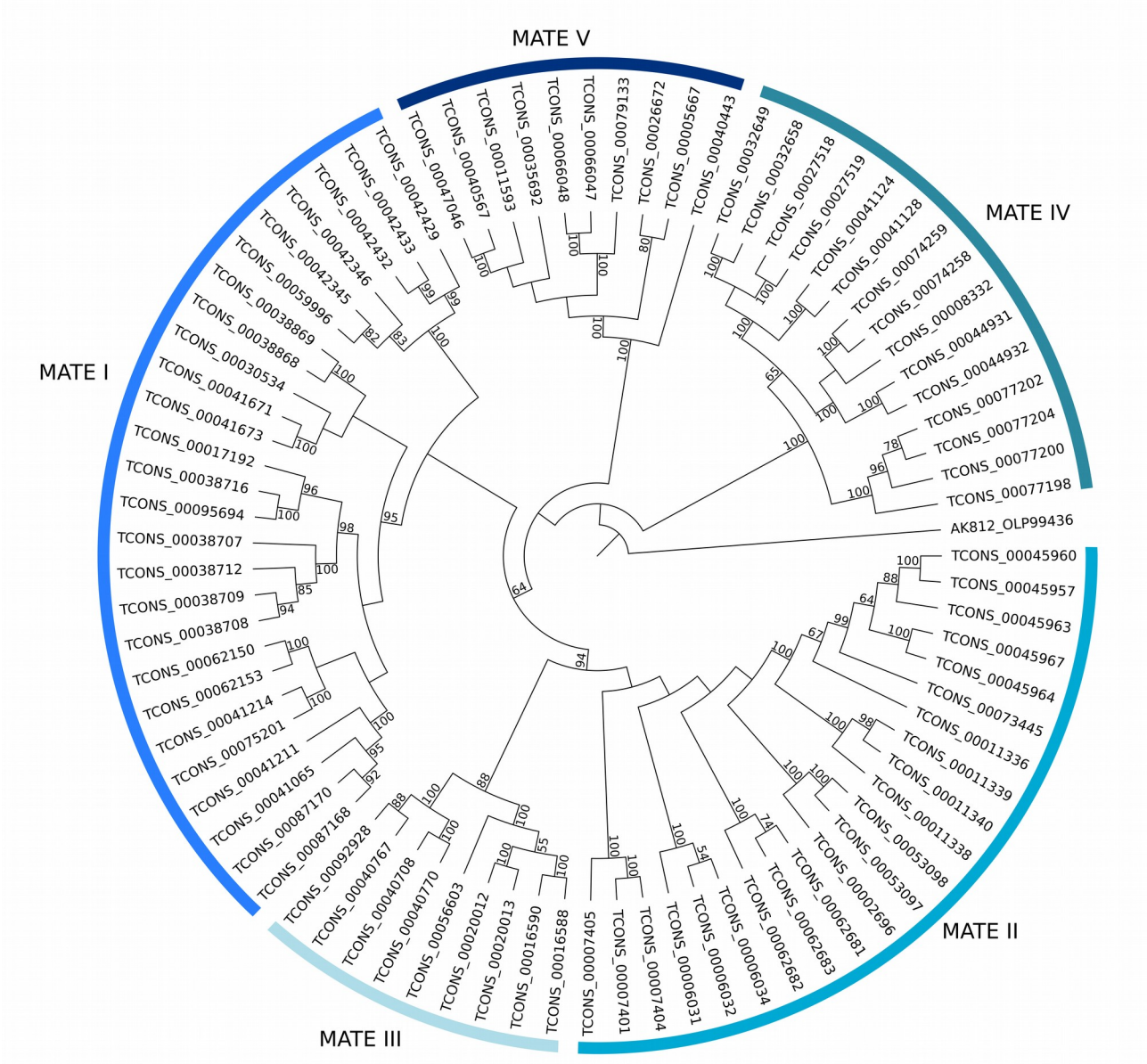

Fig A1. Maximum Likelihood tree of MATE amino acid sequences expressed by Citrus spp. identified in the Citrus Reference Transcriptome

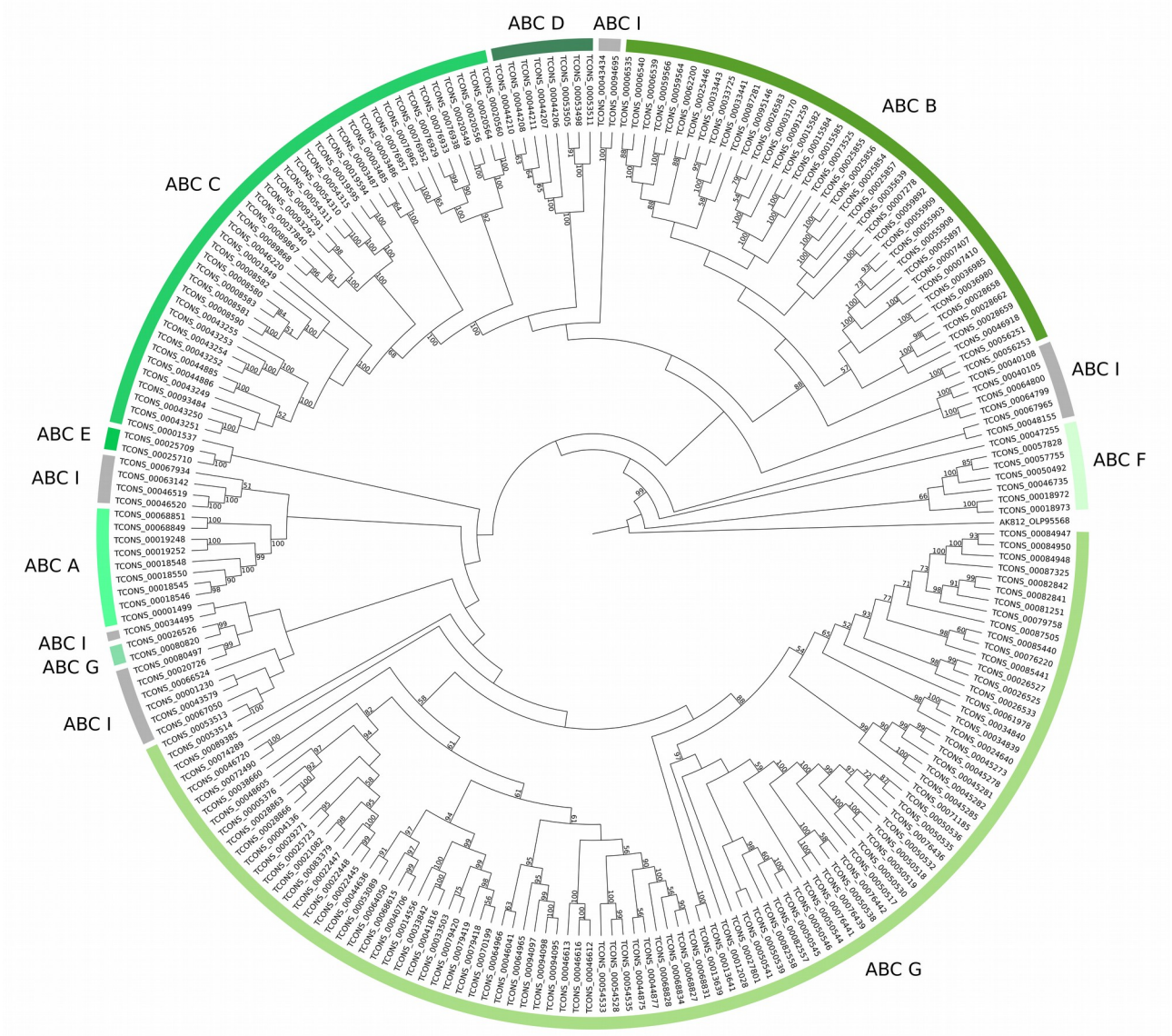

Fig A2. Maximum Likelihood tree of ABC amino acid sequences expressed by Citrus spp. identified in the Citrus Reference Transcriptome

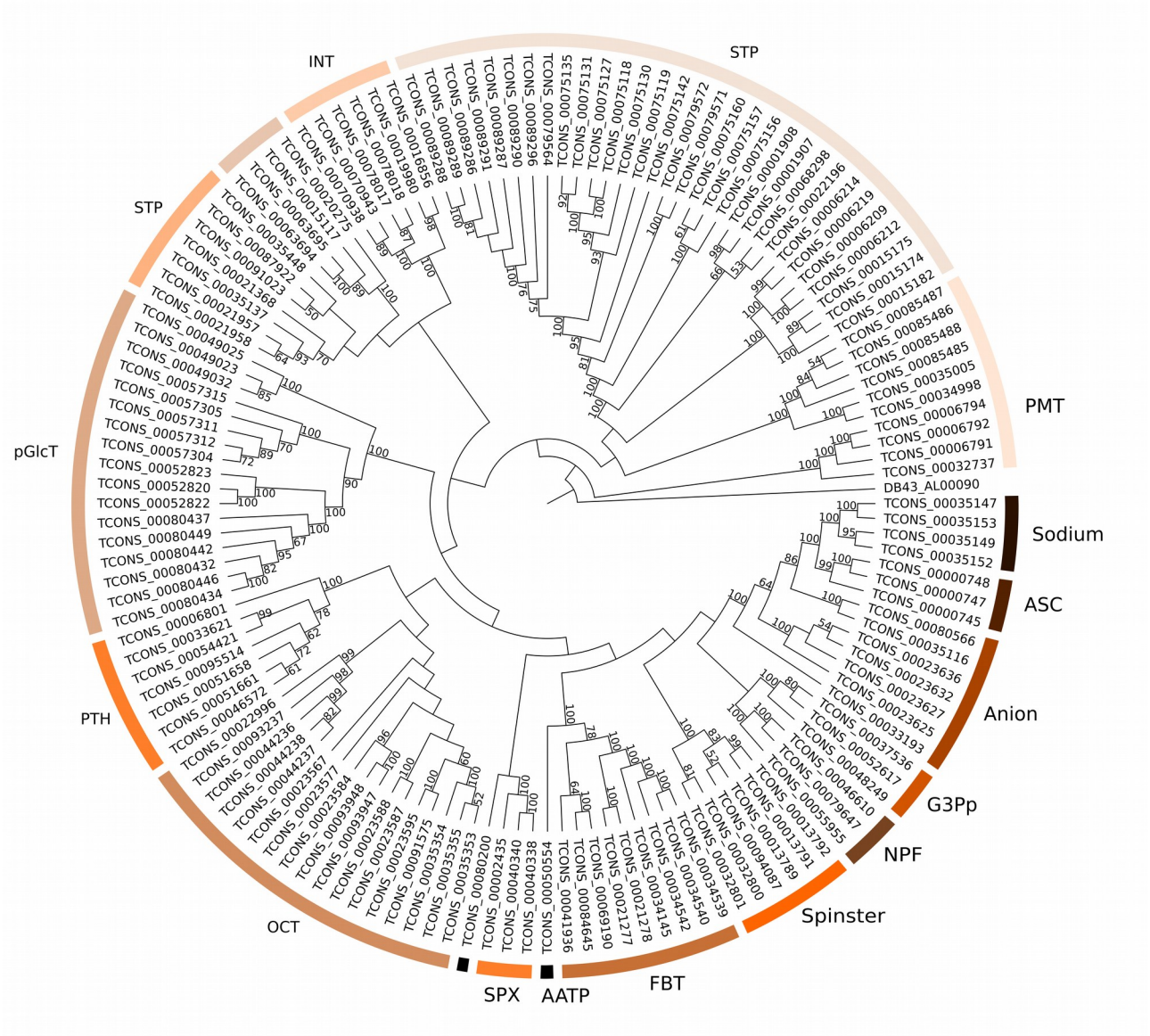

Fig A3. Maximum Likelihood tree of MFS amino acid sequences expressed by Citrus spp. identified in the Citrus Reference Transcriptome

Table A1. MATE, ABC, and MFS transcripts expressed by Citrus spp., Molecular Weigh, Isoelectric Point, Sequence Length, Subcellular Localization, and Putative Gene Name from *Citrus sinensis*

Transcript	Molecular Weigh	Isoelectric Point	Sequence Length	Sublocalization	Annotation	Subfamily	Putative Gene
TCONS_00059996	10086,59	6,7034	92	E.R.	DTX_19	I	Cs1g07550
TCONS_00095694	11907,74	4,1957	111	chloroplast	DTX_14	I	Cs2g13500
TCONS_00042429	19791,22	7,9528	179	vacuole	DTX_19	I	Cs1g07550
TCONS_00087168	20442,32	8,3374	183	E.R.	DTX_8	I	Cs6g18200
TCONS_00041065	24054,11	8,2445	223	vacuole	DTX_8	I	Cs6g18200
TCONS_00038707	27145,14	6,8017	244	plasma membrane	DTX_12	I	Cs2g13510
TCONS_00087170	27328,25	4,5576	244	plasma membrane	DTX_8	I	Cs6g18200
TCONS_00017192	27457,82	4,5817	250	plasma membrane	DTX_14	I	Cs2g13501_m
TCONS_00041214	28026,83	8,5859	256	plasma membrane	DTX_12	I	Cs6g18160
TCONS_00062153	31277,78	8,6791	287	vacuole	DTX_14	I	Cs5g20110_m
TCONS_00042432	34605,57	9,2806	309	plasma membrane	DTX_19	I	Cs1g07550
TCONS_00038712	35180,52	5,2449	320	plasma membrane	DTX_12	I	Cs2g13510
TCONS_00041673	36382,45	8,3743	328	plasma membrane	DTX_16	I	orange1.1t00013
TCONS_00042345	40783,02	6,4827	371	E.R.	DTX_19	I	Cs1g07540
TCONS_00038868	41382,29	8,2776	375	plasma membrane	DTX_16	I	Cs2g13530
TCONS_00062150	49446,92	8,9154	454	plasma membrane	DTX_14	I	Cs5g19630
TCONS_00038709	50403,38	7,9799	461	plasma membrane	DTX_12	I	Cs2g13510
TCONS_00075201	49998,52	8,6245	461	plasma membrane	DTX_12	I	Cs2g31280
TCONS_00030534	52006,38	7,9821	476	plasma membrane	DTX_16	I	Cs5g06100
TCONS_00042346	52550,9	6,6813	481	plasma membrane	DTX_19	I	Cs1g07540
TCONS_00038716	54731,49	5,0645	500	plasma membrane	DTX_14	I	Cs2g13500
TCONS_00038708	54657,3	8,1167	502	plasma membrane	DTX_12	I	Cs2g13510
TCONS_00038869	54635,28	7,7156	502	plasma membrane	DTX_16	I	Cs2g13530
TCONS_00042433	56145,07	8,2104	506	plasma membrane	DTX_19	I	Cs1g07550
TCONS_00041211	56198,51	7,1551	513	plasma membrane	DTX_8	I	Cs6g18150
TCONS_00041671	58872,46	7,8564	538	plasma membrane	DTX_16	I	orange1.1t00013
TCONS_00006031	18326,51	6,8755	173	vacuole	DTX_33	II	Cs3g24330
TCONS_00011338	19623,33	7,1645	183	vacuole	DTX_27	II	Cs3g17660
TCONS_00006032	25481,81	8,4818	230	vacuole	DTX_33	II	Cs3g24330
TCONS_00045963	27335,12	7,9173	244	plasma membrane	DTX_27	II	Cs1g20120
TCONS_00062681	30391,1	7,1433	278	vacuole	DTX_33	II	Cs5g28190
TCONS_00011339	36043,5	7,4298	323	plasma membrane	DTX_27	II	Cs3g17660
TCONS_00045964	37221,95	5,2667	335	E.R.	DTX_27	II	Cs1g20120
TCONS_00045957	37170	7,8896	338	plasma membrane	DTX_27	II	Cs1g20130
TCONS_00007401	37381,19	6,8374	341	plasma membrane	DTX_29	II	Cs7g09190
TCONS_00006034	43126,5	7,8135	398	vacuole	DTX_33	II	Cs3g24330
TCONS_00007405	51604,55	10,1562	464	plasma membrane	DTX_29	II	Cs7g09190
TCONS_00073445	52576,44	6,5865	476	plasma membrane	DTX_27	II	Cs5g21940
TCONS_00053097	52762,66	8,5186	482	plasma membrane	DTX_35	II	Cs9g19430
TCONS_00011340	53150,98	6,4797	487	plasma membrane	DTX_27	II	Cs3g17660
TCONS_00045967	54929,89	6,3298	499	plasma membrane	DTX_27	II	Cs1g20120
TCONS_00045960	54381,49	8,216	499	plasma membrane	DTX_27	II	Cs1g20130
TCONS_00062683	55735,5	5,2952	507	plasma membrane	DTX_33	II	Cs5g28190
TCONS_00053098	55726,9	6,7161	509	plasma membrane	DTX_35	II	Cs9g19420

Transcript	Molecular Weigh	Isoelectric Point	Sequence Length	Sublocalization	Annotation	Subfamily	Putative Gene
TCONS_00011336	56100,96	7,9652	512	plasma membrane	DTX_27	II	Cs3g17670
TCONS_00002696	57273,01	5,4118	524	plasma membrane	DTX_34	II	orange1.1t00390
TCONS_00062682	57912,19	7,837	525	plasma membrane	DTX_33	II	Cs5g28190
TCONS_00007404	57249,67	6,969	527	plasma membrane	DTX_29	II	Cs7g09190
TCONS_00016590	23209,71	9,9123	215	vacuole	DTX_40	III	Cs2g03200
TCONS_00040770	23852,96	6,4396	219	E.R.	DTX_41	III	Cs2g15080
TCONS_00020013	27074,17	5,6849	252	vacuole	DTX_40	III	Cs2g08000
TCONS_00040708	28640,73	7,2885	257	vacuole	DTX_41	III	Cs2g15610
TCONS_00092928	33423,65	8,6776	303	vacuole	DTX_41	III	Cs2g15080
TCONS_00020012	54024,08	7,6783	501	plasma membrane	DTX_40	III	Cs2g08000
TCONS_00040767	55481,7	7,5818	505	plasma membrane	DTX_41	III	Cs2g15120
TCONS_00016588	56297,17	6,0341	519	plasma membrane	DTX_40	III	Cs2g03220
TCONS_00056603	59547,18	8,1005	547	plasma membrane	DTX_40	III	Cs2g21460
TCONS_00008332	26412,55	10,2381	246	plasma membrane	DTX_43	IV	Cs1g26350
TCONS_00077202	28053,38	7,6464	257	chloroplast	DTX_46	IV	Cs8g08470
TCONS_00041128	29661,07	10,5478	279	chloroplast	DTX_44	IV	Cs6g09270
TCONS_00032658	30083,89	10,0467	282	plasma membrane	DTX_45	IV	Cs8g01660
TCONS_00044931	31956,05	5,1502	299	plasma membrane	DTX_42	IV	Cs2g30270
TCONS_00027519	35806,19	10,3576	330	chloroplast	DTX_45	IV	Cs1g26350
TCONS_00074259	40292,85	9,7167	375	plasma membrane	DTX_42	IV	orange1.1t03403
TCONS_00077200	43554,19	8,5898	398	plasma membrane	DTX_46	IV	Cs8g08470
TCONS_00041124	44027,12	10,24	413	chloroplast	DTX_44	IV	Cs6g09270
TCONS_00044932	57227,16	7,8844	535	plasma membrane	DTX_42	IV	Cs2g30270
TCONS_00074258	58134,83	7,4094	538	plasma membrane	DTX_42	IV	orange1.1t03403
TCONS_00077198	59496,73	7,7824	548	plasma membrane	DTX_46	IV	Cs8g08480
TCONS_00077204	60550,45	8,6079	557	chloroplast	DTX_46	IV	Cs8g08470
TCONS_00032649	63766,47	9,2068	602	plasma membrane	DTX_45	IV	Cs8g01660
TCONS_00027518	65503,16	9,2159	611	E.R.	DTX_45	IV	Cs1g26350
TCONS_00005667	37132,98	6,4647	336	plasma membrane	DTX_54	V	Cs3g22600
TCONS_00066047	36822,48	8,4209	337	plasma membrane	DTX_53	V	Cs6g09880
TCONS_00079133	50153,96	7,6444	465	vacuole	DTX_53	V	Cs7g16290_m
TCONS_00066048	53856,72	8,5624	496	plasma membrane	DTX_53	V	Cs6g09880
TCONS_00026672	54470,37	8,2021	501	plasma membrane	DTX_55	V	Cs9g04120
TCONS_00040567	56054,22	7,4348	513	plasma membrane	DTX_49	V	Cs5g10270
TCONS_00047046	57180,6	7,7634	525	plasma membrane	DTX_49	V	Cs9g16870
TCONS_00035692	57003,36	8,0683	531	plasma membrane	DTX_51	V	Cs4g15415_m
TCONS_00040443	58872,66	8,3841	543	plasma membrane	DTX_56	V	Cs5g09710
TCONS_00011593	61807,34	7,8303	586	plasma membrane	DTX_48	V	Cs3g16650

Transcript	Molecular Weigh	Isoelectric Point	Sequence Length	Sublocalization	Subfamily	Putative Gene
TCONS_00019248	53839,28	5,2737	483	plasma membrane	A	Cs5g04120
TCONS_00018548	65454,57	7,1179	589	plasma membrane	A	Cs5g04110
TCONS_00018550	70976,26	8,4755	637	plasma membrane	A	Cs5g04110
TCONS_00019252	78376,39	7,2099	706	plasma membrane	A	Cs5g04120
TCONS_00018545	101276,4	7,2179	908	plasma membrane	A	Cs5g04110
TCONS_00018546	106798,08	8,0549	956	plasma membrane	A	Cs5g04110
TCONS_00068851	188525,17	7,0271	1695	plasma membrane	A	orange1.1t02318
TCONS_00068849	205029,33	7,8267	1841	plasma membrane	A	orange1.1t02318
TCONS_00028658	17715,28	7,1293	160	cytosol	B	Cs6g14480
TCONS_00007410	37102,54	10,0755	326	plasma membrane	B	Cs7g09160
TCONS_00055908	46192,76	7,4341	407	mitocondria	B	Cs2g27440
TCONS_00033725	46021,68	9,9774	412	chloroplast	B	Cs7g28610
TCONS_00055897	52723,24	9,3561	467	plasma membrane	B	Cs2g27440
TCONS_00095146	51233,21	7,3486	478	plasma membrane	B	Cs2g04080
TCONS_00028662	63740,34	8,6188	582	plasma membrane	B	Cs6g14480
TCONS_00028659	64880,75	9,341	592	plasma membrane	B	Cs6g14480
TCONS_00036985	64853,55	8,4383	611	plasma membrane	B	Cs5g12150
TCONS_00015585	68155,5	7,0146	632	plasma membrane	B	Cs2g04070
TCONS_00025854	71274,68	7,2363	647	plasma membrane	B	Cs6g20270
TCONS_00036980	68987,4	8,6972	647	plasma membrane	B	Cs5g12150
TCONS_00025855	73470,79	8,2938	668	vacuole	B	Cs6g20270
TCONS_00055903	76001,21	8,5797	677	plasma membrane	B	Cs2g27440
TCONS_00056253	77986,37	9,6879	702	plasma membrane	B	Cs1g08880
TCONS_00091259	76008,04	7,8674	703	plasma membrane	B	Cs9g01170
TCONS_00055909	79846,69	8,3853	709	plasma membrane	B	Cs2g27440
TCONS_00056251	81372,51	10,0389	731	plasma membrane	B	Cs1g08880
TCONS_00033441	82815,6	5,4403	747	plasma membrane	B	Cs7g28610
TCONS_00006540	85588,31	7,1752	789	plasma membrane	B	Cs3g26380
TCONS_00046918	86191,02	9,387	791	plasma membrane	B	Cs9g16780
TCONS_00006535	88318,42	7,5953	819	plasma membrane	B	Cs3g26380
TCONS_00015582	91599,66	9,194	837	plasma membrane	B	Cs2g04080
TCONS_00007407	96751,66	9,7628	854	plasma membrane	B	Cs7g09160
TCONS_00059566	99686,33	8,6588	903	plasma membrane	B	Cs3g09820
TCONS_00025856	112925,74	8,4603	1027	plasma membrane	B	Cs6g20280
TCONS_00087281	124578,86	7,0244	1139	plasma membrane	B	Cs9g11040
TCONS_00007278	133938,42	9,0203	1224	plasma membrane	B	Cs7g09730
TCONS_00035639	134759,42	9,172	1230	plasma membrane	B	Cs4g15420
TCONS_00026583	133450,29	7,2295	1236	plasma membrane	B	Cs9g01170_a
TCONS_00025857	136076,59	7,5088	1247	plasma membrane	B	Cs6g20290
TCONS_00025446	136438,12	8,5551	1253	plasma membrane	B	Cs6g21110
TCONS_00059892	137715,87	9,0217	1255	plasma membrane	B	Cs4g11230
TCONS_00006539	136639,36	8,4429	1260	plasma membrane	B	Cs3g26380
TCONS_00059564	142127,25	8,645	1292	plasma membrane	B	Cs3g09820
TCONS_00003170	140125,78	6,6978	1299	plasma membrane	B	orange1.1t01769_a

Transcript	Molecular Weigh	Isoelectric Point	Sequence Length	Sublocalization	Subfamily	Putative Gene
TCONS_00033443	144915,27	7,2087	1303	plasma membrane	B	Cs7g28610
TCONS_00015584	144638,8	8,1973	1332	plasma membrane	B	Cs2g04080
TCONS_00062200	148975,56	8,3082	1359	plasma membrane	B	orange1.1t00937
TCONS_00073525	171667,2	9,2634	1560	plasma membrane	B	Cs1g16850
TCONS_00093292	19006,58	10,4364	161	plasma membrane	C	Cs1g18450
TCONS_00093291	21974,13	9,6543	191	plasma membrane	C	Cs1g18450
TCONS_00076929	30369,87	7,6572	273	chloroplast	C	orange1.1t02765
TCONS_00089867	37479,06	7,5084	332	nucleus	C	Cs1g18450
TCONS_00043250	47502,63	5,656	425	chloroplast	C	Cs4g09140
TCONS_00003485	48814,36	7,1194	435	chloroplast	C	Cs5g33060
TCONS_00043249	56270,37	9,0061	501	plasma membrane	C	Cs4g09150
TCONS_00093484	56051,65	6,1313	508	plasma membrane	C	Cs4g09150
TCONS_00076933	59151,17	6,8578	530	plasma membrane	C	orange1.1t02765
TCONS_00020549	61168,52	9,6605	543	plasma membrane	C	Cs7g32530
TCONS_00044885	61122,26	8,0095	547	plasma membrane	C	Cs4g09140
TCONS_00089868	61573,8	8,5267	555	chloroplast	C	Cs1g18450
TCONS_00008581	87533,28	8,4347	779	plasma membrane	C	Cs7g10200
TCONS_00008590	87945,08	9,2257	781	plasma membrane	C	Cs7g10200
TCONS_00019594	89232,09	6,1392	799	plasma membrane	C	Cs5g02710
TCONS_00003487	90298,15	6,2127	807	plasma membrane	C	Cs5g33060
TCONS_00076938	94373,23	7,9232	835	plasma membrane	C	orange1.1t02765
TCONS_00043253	98197,19	5,9232	885	plasma membrane	C	Cs4g09130
TCONS_00008582	99974,37	6,9255	893	plasma membrane	C	Cs7g10200
TCONS_00054310	99858,66	8,8131	895	plasma membrane	C	Cs9g18660
TCONS_00076952	110325,28	6,7756	980	plasma membrane	C	orange1.1t02765
TCONS_00020564	127020,95	5,5519	1142	plasma membrane	C	Cs2g09550
TCONS_00044886	129092,47	7,5305	1156	plasma membrane	C	Cs1g13700
TCONS_00054315	137138,23	8,3994	1234	plasma membrane	C	Cs9g18660
TCONS_00019595	141203,84	6,6556	1261	plasma membrane	C	Cs5g02710
TCONS_00043251	145109,16	6,4705	1300	nucleus	C	Cs4g09140
TCONS_00020556	147399,58	9,2353	1307	plasma membrane	C	Cs2g09560
TCONS_00046220	149463,19	7,5066	1343	plasma membrane	C	Cs5g28990
TCONS_00076962	160756,62	6,6066	1433	plasma membrane	C	orange1.1t02765
TCONS_00008580	162302,14	8,4242	1444	plasma membrane	C	Cs7g10200
TCONS_00076957	164017,51	6,6624	1465	plasma membrane	C	orange1.1t02765
TCONS_00043252	163674,91	7,1965	1469	plasma membrane	C	Cs1g13720
TCONS_00008583	165591,13	8,4506	1472	plasma membrane	C	Cs7g10200
TCONS_00037840	164345,38	8,7054	1475	plasma membrane	C	Cs1g18460
TCONS_00054311	165306,37	8,1658	1485	plasma membrane	C	Cs9g18660
TCONS_00043254	166553,59	7,1469	1495	plasma membrane	C	Cs4g09130
TCONS_00043255	165906,5	6,5071	1496	plasma membrane	C	Cs4g09120
TCONS_00003486	169310,85	7,6464	1513	plasma membrane	C	Cs5g33060
TCONS_00001949	168678,36	7,849	1514	plasma membrane	C	Cs1g02710
TCONS_00020560	183757,62	6,5966	1635	plasma membrane	C	Cs2g09550

Transcript	Molecular Weigh	Isoelectric Point	Sequence Length	Sublocalization	Subfamily	Putative Gene
TCONS_00044210	35136,86	7,4169	314	nucl_plas	D	orange1.1t03223
TCONS_00044208	53120,39	6,0318	472	chloroplast	D	orange1.1t03223
TCONS_00044207	58140,61	9,0197	510	peroxissome	D	orange1.1t03223
TCONS_00053511	57332,25	9,1375	513	cytosol	D	Cs1g01510
TCONS_00044206	59869,57	5,4323	532	E.R.	D	orange1.1t03223
TCONS_00044211	88875,29	7,4742	788	chloroplast	D	orange1.1t03223
TCONS_00053498	96849,32	7,3367	865	cytosol	D	Cs1g01510
TCONS_00053505	155020,14	9,3954	1384	plasma membrane	D	Cs1g01510
TCONS_00025709	37972,64	6,2521	335	cytosol	E	Cs6g19410
TCONS_00025710	72131,23	7,9791	639	hloroplast_mitocondri	E	Cs6g19410
TCONS_00018972	12084,95	10,238	114	chloroplast	F	Cs5g01810
TCONS_00057828	14732,98	10,6387	134	nucleus	F	Cs9g09560
TCONS_00057755	17521,35	8,1524	158	golgi	F	Cs1g13980
TCONS_00018973	29364,85	8,145	266	mitocondria	F	Cs5g01810
TCONS_00046735	66209,91	6,6092	593	cytosol	F	Cs8g15910
TCONS_00047255	79816,03	7,9346	708	chloroplast	F	orange1.1t04404
TCONS_00050492	83228,16	6,2344	747	cytosol	F	Cs1g13980
TCONS_00068834	13370,37	10,9972	122	cytosol	G	orange1.1t02321_a
TCONS_00082841	17329,96	9,9551	149	nucleus	G	Cs6g02250
TCONS_00089385	15598,15	5,5119	149	vacuole	G	Cs1g01420
TCONS_00085440	18175,52	6,887	159	vacuole	G	Cs5g13760
TCONS_00001499	22256,97	9,7118	198	nucleus	G	orange1.1t01659
TCONS_00064965	25345,04	7,3462	223	plasma membrane	G	orange1.1t01996
TCONS_00026526	25722,7	10,3057	224	cytosol	G	Cs9g01400
TCONS_00080820	26350,81	9,8679	231	cytosol	G	Cs6g02250
TCONS_00087505	26682,38	6,9439	233	plasma membrane	G	Cs6g01131_a
TCONS_00005376	27256,27	7,9397	243	plasma membrane	G	Cs3g21080
TCONS_00094097	29178,53	7,8791	255	plasma membrane	G	orange1.1t01993
TCONS_00079420	29858,47	9,0717	263	vacuole	G	Cs6g05320
TCONS_00076436	30907,98	10,1429	265	cytosol	G	?
TCONS_00022447	35552,84	8,0065	309	plasma membrane	G	Cs1g06780
TCONS_00053513	37178,16	6,849	329	cytosol	G	Cs1g01500
TCONS_00068831	37862,85	7,9148	330	plasma membrane	G	orange1.1t02321
TCONS_00022445	38000,1	8,3426	345	chloroplast	G	Cs1g06780
TCONS_00087325	41403,15	5,8926	363	E.R.	G	Cs6g01330
TCONS_00082842	42303,44	9,0279	364	plasma membrane	G	Cs6g02250
TCONS_00094098	41685,77	6,4893	369	plasma membrane	G	orange1.1t01993
TCONS_00068828	41946,33	8,0557	376	mitocondria	G	orange1.1t02321
TCONS_00046041	43833,54	8,0435	396	nucleus	G	Cs1g19860
TCONS_00026527	45575,32	8,0846	397	cytosol	G	Cs9g01400
TCONS_00001537	44936,87	7,1453	399	cytosol	G	Cs5g33740
TCONS_00094095	45512,18	6,8219	401	plasma membrane	G	orange1.1t01993
TCONS_00033842	45799,06	8,5341	406	plasma membrane	G	Cs7g28610_a
TCONS_00021082	45553,87	10,0202	413	chloroplast	G	Cs2g04080_a

Transcript	Molecular Weigh	Isoelectric Point	Sequence Length	Sublocalization	Subfamily	Putative Gene
TCONS_00079758	46775,38	6,8769	422	plasma membrane	G	Cs6g02250
TCONS_00064966	49804,12	8,8014	449	golgi	G	orange1.1t00127_a
TCONS_00046613	53455,62	8,9756	487	plasma membrane	G	Cs8g15960
TCONS_00028863	54444,1	8,2338	490	plasma membrane	G	?
TCONS_00054535	55518,6	9,4559	493	plasma membrane	G	Cs5g17290
TCONS_00054533	54966,21	8,2126	500	cytosol	G	Cs5g17290
TCONS_00022448	57413,25	8,6982	520	plasma membrane	G	Cs1g06780
TCONS_00082557	58835,62	7,0814	521	cytosol	G	Cs1g13620
TCONS_00033503	58962,31	9,9116	525	plasma membrane	G	Cs7g28090
TCONS_00027801	60334,67	7,243	531	plasma membrane	G	Cs1g20770_a
TCONS_00070199	66615,51	8,7726	592	plasma membrane	G	Cs6g05270
TCONS_00053514	67987,7	6,2911	604	cytosol	G	Cs1g01500
TCONS_00083379	66930,45	9,2959	604	plasma membrane	G	orange1.1t02544
TCONS_00053089	67472,76	9,1039	605	plasma membrane	G	Cs9g18660_a
TCONS_00040706	69007,7	9,431	610	plasma membrane	G	Cs2g13730_a
TCONS_00068615	68722,2	9,2709	612	plasma membrane	G	Cs7g24870_a
TCONS_00038660	68983,76	9,1971	622	chloroplast	G	Cs2g13730
TCONS_00044636	71045,37	7,8188	627	plasma membrane	G	Cs5g08870
TCONS_00025723	70994,53	9,0574	637	plasma membrane	G	Cs6g19470
TCONS_00050518	72409,85	7,2202	640	plasma membrane	G	Cs1g13720
TCONS_00014556	72039,37	9,8131	646	plasma membrane	G	Cs1g20770
TCONS_00064050	73309,61	8,6615	648	plasma membrane	G	Cs1g09530
TCONS_00079418	72483,81	8,092	651	plasma membrane	G	Cs6g05270
TCONS_00044875	73989,92	9,3344	661	plasma membrane	G	Cs2g30650_a
TCONS_00048605	76380,14	9,2969	674	plasma membrane	G	Cs4g08300
TCONS_00004136	75199,05	9,0489	679	plasma membrane	G	Cs3g22340
TCONS_00068827	76953,72	8,2362	683	plasma membrane	G	orange1.1t02321
TCONS_00046612	77511	9,1194	697	plasma membrane	G	Cs8g15960
TCONS_00044877	77939,37	9,6856	697	plasma membrane	G	Cs2g30650
TCONS_00029271	77528,86	8,7514	698	golgi	G	Cs7g12620
TCONS_00054528	79707,16	8,6803	715	plasma membrane	G	Cs5g17290
TCONS_00046616	80359,31	8,9366	723	plasma membrane	G	Cs8g15960
TCONS_00079419	81275,02	8,0374	737	plasma membrane	G	Cs6g05280
TCONS_00028866	85084,45	9,3389	772	plasma membrane	G	?
TCONS_00084950	86749,31	6,5015	775	plasma membrane	G	Cs6g01330
TCONS_00082558	93748,86	9,3593	829	plasma membrane	G	Cs1g13620
TCONS_00034839	94000,45	9,4414	836	plasma membrane	G	Cs8g16470
TCONS_00074289	95598,55	7,8067	846	plasma membrane	G	Cs6g01130_a
TCONS_00041816	94991,58	9,531	846	plasma membrane	G	orange1.1t00127
TCONS_00045278	100677,11	7,2409	889	plasma membrane	G	Cs6g01330_a
TCONS_00013639	101491,62	9,3168	893	plasma membrane	G	Cs4g17100
TCONS_00050546	101744,58	9,5249	899	plasma membrane	G	Cs1g13620
TCONS_00045282	110790,16	8,918	988	plasma membrane	G	Cs6g15280
TCONS_00050530	111391,01	8,5203	993	plasma membrane	G	Cs1g13720

Transcript	Molecular Weigh	Isoelectric Point	Sequence Length	Sublocalization	Subfamily	Putative Gene
TCONS_00050530	111391,01	8,5203	993	plasma membrane	G	Cs1g13720
TCONS_00026525	119657,27	7,0831	1051	plasma membrane	G	Cs9g01400
TCONS_00026533	122293,91	7,9901	1086	plasma membrane	G	Cs9g01400
TCONS_00072490	124041,34	8,8628	1111	plasma membrane	G	Cs7g24870
TCONS_00046720	123969,03	8,822	1118	plasma membrane	G	Cs8g16110
TCONS_00085441	132593,43	7,8679	1174	plasma membrane	G	Cs5g13760
TCONS_00084948	137934,65	6,5931	1218	plasma membrane	G	Cs6g01330
TCONS_00084947	141227,66	6,6279	1247	plasma membrane	G	Cs6g01330
TCONS_00024640	140163,24	8,5262	1250	plasma membrane	G	Cs8g16470
TCONS_00076220	144152,63	8,9493	1280	plasma membrane	G	Cs5g13760
TCONS_00076439	144892,13	7,7566	1283	plasma membrane	G	Cs1g18930
TCONS_00076441	148195,03	7,9792	1311	plasma membrane	G	Cs1g18930
TCONS_00061978	148436,35	7,7382	1314	plasma membrane	G	Cs1g15710
TCONS_00050539	148567,09	8,8585	1315	plasma membrane	G	Cs1g13660
TCONS_00076442	149230,7	7,7144	1326	plasma membrane	G	Cs1g18920
TCONS_00050517	150420,48	8,3174	1332	plasma membrane	G	Cs1g13730
TCONS_00045273	158528,42	7,0977	1403	plasma membrane	G	Cs6g15300
TCONS_00045281	159327,4	7,339	1403	plasma membrane	G	orange1.1t01531
TCONS_00050541	159978,23	8,6815	1412	plasma membrane	G	Cs1g13650
TCONS_00013641	161335,96	9,1147	1422	plasma membrane	G	Cs4g17100
TCONS_00050544	160180,46	8,1096	1425	plasma membrane	G	Cs1g13640
TCONS_00034840	159924,72	9,1767	1427	plasma membrane	G	Cs8g16470
TCONS_00050535	162134,52	8,3761	1435	plasma membrane	G	Cs1g13700
TCONS_00012028	162300,73	7,0452	1436	plasma membrane	G	Cs4g20440
TCONS_00050538	162306,23	7,3781	1436	plasma membrane	G	Cs1g13680
TCONS_00050536	163592,29	7,9602	1446	plasma membrane	G	Cs1g13690
TCONS_00050545	164163,46	8,8657	1455	plasma membrane	G	Cs1g13620
TCONS_00081251	165085,24	8,2034	1458	plasma membrane	G	Cs6g02210
TCONS_00045285	164392,97	8,8255	1458	plasma membrane	G	Cs6g15300
TCONS_00050532	164929,9	8,1443	1459	plasma membrane	G	Cs1g13710
TCONS_00050519	165990,72	8,3549	1469	plasma membrane	G	Cs4g09130
TCONS_00071185	166799,14	8	1472	plasma membrane	G	orange1.1t01531
TCONS_00094695	16011,68	6,7221	146	cytosol	I	Cs4g04420
TCONS_00040105	18404,9	10,7889	168	chloroplast	I	Cs2g25590
TCONS_00064799	19497,76	9,619	177	chloroplast	I	Cs1g09070
TCONS_00067050	23654,66	5,5354	199	chloroplast	I	Cs5g33740_a
TCONS_00046519	23299,67	5,9505	201	cytosol	I	Cs5g29600
TCONS_00043579	22787,67	10,0709	206	vacuole	I	Cs4g04420_a
TCONS_00048155	27477,28	10,4245	245	chloroplast	I	Cs4g01550
TCONS_00064800	29884,54	7,4136	273	chloroplast	I	Cs1g09070
TCONS_00034495	32847,23	10,5325	291	E.R.	I	Cs7g09160_a
TCONS_00046520	32993,69	6,3034	294	nucleus	I	Cs5g29600
TCONS_00040108	33348,38	9,8604	304	chloroplast	I	Cs2g25590
TCONS_00043434	34979,9	7,246	317	plasma membrane	I	Cs4g04420
TCONS_00067965	36406,82	6,9638	332	chloroplast	I	Cs7g23800

Transcript	Molecular Weigh	Isoelectric Point	Sequence Length	Sublocalization	Subfamily	Putative Gene
TCONS_00063142	39195,32	8,494	349	cytosol	I	Cs6g06520
TCONS_00067934	45051,76	4,3434	394	cytosol	I	Cs7g23530
TCONS_00080497	54738	7,0896	497	chloroplast	I	Cs7g22890
TCONS_00020726	62921,7	5,439	565	chloroplast	I	Cs2g07970
TCONS_00001230	67732,03	4,9734	614	chloroplast	I	orange1.1t01791
TCONS_00066524	87011,44	5,8905	791	plasma membrane	I	Cs9g11110

Transcript	Molecular Weigh	Isoelectric Point	Seq. Len.	Sublocalization	Annotation	Subf.	Putative Gene
TCONS_00075142	9660.60	7.1045	87	cytosol	ERD6-like	STP	Cs3g12510
TCONS_00089286	10553.12	3.6463	106	extracellular space	ERD6-like	STP	Cs3g12500
TCONS_00089288	14512.28	10.3399	127	vacuole	ERD6-like	STP	Cs3g12490
TCONS_00001908	14411.12	7.0042	133	vacuole	ERD6-like	STP	Cs5g32070
TCONS_00089289	15826.60	10.1332	140	vacuole	ERD6-like	STP	Cs3g12490
TCONS_00089290	15851.97	9.4787	141	vacuole	ERD6-like	STP	Cs3g12510
TCONS_00089287	17976.93	4.1788	170	vacuole	ERD6-like	STP	Cs3g12510
TCONS_00075119	19638.09	9.3633	174	plasma membrane	ERD6-like	STP	Cs3g12510
TCONS_00075131	21252.06	8.6742	193	vacuole	ERD6-like	STP	Cs3g12510
TCONS_00075135	21854.92	9.5502	198	vacuole	ERD6-like	STP	Cs3g12510
TCONS_00089291	24114.36	6.2618	224	vacuole	ERD6-like	STP	Cs3g12510
TCONS_00075130	24761.96	6.6831	226	plasma membrane	ERD6-like	STP	Cs3g12520
TCONS_00006214	25287.62	9.0791	230	plasma membrane	ERD6-like	STP	Cs3g24900
TCONS_00015174	26326.06	9.4997	242	plasma membrane	ERD6-like	STP	Cs1g24180
TCONS_00075156	26943.60	7.1075	249	chloroplast	ERD6-like	STP	Cs3g12540
TCONS_00089296	32378.30	4.7276	305	vacuole	ERD6-like	STP	Cs3g12510
TCONS_00068298	34159.84	9.2197	308	plasma membrane	ERD6-like	STP	Cs9g05220
TCONS_00079564	33506.96	4.6451	312	plasma membrane	ERD6-like	STP	Cs3g12420
TCONS_00006212	34157.52	8.2489	316	plasma membrane	ERD6-like	STP	Cs3g24900
TCONS_00006209	34835.72	6.3963	321	plasma membrane	ERD6-like	STP	Cs3g24900
TCONS_00079571	35426.84	8.7952	323	plasma membrane	ERD6-like	STP	Cs3g12410
TCONS_00075160	35354.20	5.1028	335	vacuole	ERD6-like	STP	Cs3g12540
TCONS_00015182	37001.28	8.2215	339	plasma membrane	ERD6-like	STP	Cs1g24180
TCONS_00079572	37886.64	8.5662	343	plasma membrane	ERD6-like	STP	Cs3g12480
TCONS_00075118	38016.95	8.8851	345	plasma membrane	ERD6-like	STP	Cs3g12520
TCONS_00022196	38754.00	9.5455	355	plasma membrane	ERD6-like	STP	Cs9g05220
TCONS_00075127	40277.71	9.2776	366	plasma membrane	ERD6-like	STP	Cs3g12520
TCONS_00075157	51904.03	6.4758	488	vacuole	ERD6-like	STP	Cs3g12540
TCONS_00015175	53131.24	8.4353	490	plasma membrane	ERD6-like	STP	Cs1g24180

Transcript	Molecular Weigh	Isoelectric Point	Seq. Len.	Sublocalization	Annotation	Subf.	Putative Gene
TCONS_00001907	54498.57	7.7054	506	plasma membrane	ERD6-like	STP	Cs5g32060
TCONS_00006219	55197.80	9.0178	506	plasma membrane	ERD6-like	STP	Cs3g24900
TCONS_00087922	39182.79	4.9863	364	vacuole	Sugar	STP	orange1.1t03853
TCONS_00021958	47871.04	10.4165	435	plasma membrane	Sugar	STP	Cs9g06590
TCONS_00035137	49901.46	6.8871	458	plasma membrane	Sugar	STP	Cs8g19880
TCONS_00035448	56360.41	8.9078	514	plasma membrane	Sugar	STP	orange1.1t03833
TCONS_00091023	56188.34	8.5209	523	plasma membrane	Sugar	STP	Cs7g13670
TCONS_00021368	58006.20	9.4607	526	plasma membrane	Sugar	STP	Cs9g06620
TCONS_00021957	57487.21	9.3174	530	plasma membrane	Sugar	STP	Cs9g06600
TCONS_00094087	17718.65	5.6301	162	plasma membrane	Sphingolipid	Spinster	Cs8g03150
TCONS_00032800	31663.76	9.2530	283	plasma membrane	Sphingolipid	Spinster	Cs8g03150
TCONS_00032801	39484.82	9.8127	358	plasma membrane	Sphingolipid	Spinster	Cs8g03150
TCONS_00013789	43218.56	7.8872	402	plasma membrane	Sphingolipid	Spinster	Cs1g20960
TCONS_00013792	55268.53	6.0920	511	plasma membrane	Sphingolipid	Spinster	Cs1g20960
TCONS_00013791	59854.78	6.0936	555	plasma membrane	Sphingolipid	Spinster	Cs1g20960
TCONS_00080200	36297.97	6.9506	329	plasma membrane	Spinster	Spinster	Cs1g01440
TCONS_00040338	35145.90	8.1386	324	plasma membrane	SPX Domain	PTH8	Cs5g10180
TCONS_00040340	70058.08	5.9581	619	plasma membrane	SPX Domain	PTH5	Cs5g10180
TCONS_00002435	78745.00	6.6601	704	plasma membrane	SPX Domain	PTH5	orange1.1t00286
TCONS_00033621	44188.37	8.0427	402	plasma membrane	Inorganic Phosphate	PTH	Cs7g29450
TCONS_00051658	57030.88	9.0777	519	plasma membrane	Inorganic Phosphate	PTH	Cs9g10530
TCONS_00054421	59451.34	8.1361	534	plasma membrane	Inorganic Phosphate	PTH	Cs9g18560
TCONS_00046572	59253.94	8.9326	542	plasma membrane	Inorganic Phosphate	PTH	Cs5g29860
TCONS_00095514	37362.12	6.4038	338	plasma membrane	Phosphate	PTH	Cs8g06780
TCONS_00051661	56655.36	9.6122	520	plasma membrane	Phosphate	PTH	Cs9g10540
TCONS_00006801	59714.57	8.7491	538	plasma membrane	Phosphate	PTH	Cs3g27660
TCONS_00006791	56239.69	7.2794	509	vacuole	Monosaccharide-sensing	PMT	Cs3g27610
TCONS_00006792	57576.63	5.2352	525	plasma membrane	Monosaccharide-sensing	PMT	Cs3g27610
TCONS_00032737	78531.72	5.0690	736	plasma membrane	Monosaccharide-sensing	PMT	Cs8g01220
TCONS_00006794	80151.32	5.1906	747	plasma membrane	Monosaccharide-sensing	PMT	Cs3g27610

Transcript	Molecular Weigh	Isoelectric Point	Seq. Len.	Sublocalization	Annotation	Subf.	Putative Gene
TCONS_00015117	31335.97	10.3404	285	plasma membrane	Polyol	PMT	Cs1g23890
TCONS_00020275	55711.14	5.9938	519	plasma membrane	Polyol	PMT	Cs2g06380
TCONS_00063695	57461.27	7.7683	535	plasma membrane	Polyol	PMT	Cs4g15780
TCONS_00063694	58621.50	9.2732	541	plasma membrane	Polyol	PMT	Cs4g15770
TCONS_00080449	25266.33	8.6770	234	plasma membrane	Plastidic Glucose	pGlcT	Cs4g16110
TCONS_00057305	26365.00	8.0920	243	plasma membrane	Plastidic Glucose	pGlcT	Cs2g20710
TCONS_00057315	32360.57	4.6924	299	plasma membrane	Plastidic Glucose	pGlcT	Cs2g20710
TCONS_00080446	34604.22	6.7392	316	chloroplast	Plastidic Glucose	pGlcT	Cs4g16110
TCONS_00080437	39948.48	8.6022	364	plasma membrane	Plastidic Glucose	pGlcT	Cs4g16110
TCONS_00057304	40797.39	7.8636	372	plasma membrane	Plastidic Glucose	pGlcT	Cs2g20710
TCONS_00052820	42249.51	9.2611	401	plasma membrane	Plastidic Glucose	pGlcT	Cs1g15250
TCONS_00052822	44326.31	9.9976	420	plasma membrane	Plastidic Glucose	pGlcT	Cs1g15250
TCONS_00080442	54588.16	8.4681	504	endoplasmic reticulum	Plastidic Glucose	pGlcT	Cs4g16110
TCONS_00049023	56360.41	8.9078	514	plasma membrane	Plastidic Glucose	pGlcT	Cs6g18490
TCONS_00080432	57482.92	7.3998	526	plasma membrane	Plastidic Glucose	pGlcT	Cs4g16110
TCONS_00049025	59172.52	9.0540	547	chloroplast	Plastidic Glucose	pGlcT	Cs6g18490
TCONS_00057312	59681.48	7.4355	547	plasma membrane	Plastidic Glucose	pGlcT	Cs2g20710
TCONS_00080434	59681.48	7.4355	547	plasma membrane	Plastidic Glucose	pGlcT	Cs4g16110
TCONS_00057311	60456.87	8.5433	558	plasma membrane	Plastidic Glucose	pGlcT	Cs2g20710
TCONS_00049032	67072.51	10.1052	622	plasma membrane	Plastidic Glucose	pGlcT	Cs6g18490
TCONS_00052823	67072.51	10.1052	622	plasma membrane	Plastidic Glucose	pGlcT	Cs1g15250
TCONS_00085488	25587.50	10.4829	231	plasma membrane	D-xylose-proton	Other	Cs5g24870
TCONS_00085486	27290.24	8.9826	252	plasma membrane	D-xylose-proton	Other	Cs5g24870
TCONS_00085485	28525.64	7.0525	259	endoplasmic reticulum	D-xylose-proton	Other	Cs5g24870
TCONS_00034998	49308.64	9.2279	458	plasma membrane	D-xylose-proton	Other	Cs8g18970
TCONS_00085487	56188.34	8.5209	523	plasma membrane	D-xylose-proton	Other	Cs5g24870
TCONS_00035005	60537.00	9.8988	559	chloroplast	D-xylose-proton	Other	Cs8g18970
TCONS_00035147	28856.39	9.1738	265	endoplasmic reticulum	Sodium-dependent Phosphate	Other	Cs8g19980

Transcript	Molecular Weigh	Isoelectric Point	Seq. Len.	Sublocalization	Annotation	Subf.	Putative Gene
TCONS_00035152	29663.34	9.4923	268	plasma membrane	Sodium-dependent Phosphate	Other	Cs8g19980
TCONS_00035149	56898.38	8.7905	519	plasma membrane	Sodium-dependent Phosphate	Other	Cs8g19980
TCONS_00035153	58563.74	7.8722	539	plasma membrane	Sodium-dependent Phosphate	Other	Cs8g19980
TCONS_00093948	11507.44	4.2497	105	cytosol	Cation/carnitin	OCT	Cs4g04930
TCONS_00093947	20449.15	5.0770	189	vacuole	Organic Cation/carnitin	OCT	Cs4g04930
TCONS_00023567	27538.92	8.6440	255	vacuole	Organic Cation/carnitin	OCT	Cs4g04910
TCONS_00044238	38710.20	4.7590	352	plasma membrane	Organic Cation/carnitin	OCT	orange1.1t03244
TCONS_00023587	46584.12	9.3293	413	plasma membrane	Organic Cation/carnitin	OCT	Cs4g04940
TCONS_00093237	46214.88	9.7904	422	vacuole	Organic Cation/carnitin	OCT	Cs1g18890
TCONS_00035353	46687.91	9.1259	427	plasma membrane	Organic Cation/carnitin	OCT	Cs8g20990
TCONS_00044237	49867.44	9.2545	457	plasma membrane	Organic Cation/carnitin	OCT	orange1.1t03245
TCONS_00035355	50281.97	9.8426	460	plasma membrane	Organic Cation/carnitin	OCT	Cs8g20990
TCONS_00044236	51921.51	8.7318	473	plasma membrane	Organic Cation/carnitin	OCT	orange1.1t03244
TCONS_00091575	52470.82	8.5248	489	plasma membrane	Organic Cation/carnitin	OCT	Cs4g04960
TCONS_00022996	58555.62	7.6381	539	plasma membrane	Organic Cation/carnitin	OCT	Cs4g12030
TCONS_00023595	65079.63	9.2476	584	vacuole	Organic Cation/carnitin	OCT	Cs4g04960
TCONS_00023577	70058.08	5.9581	619	vacuole	Organic Cation/carnitin	OCT	Cs4g04920
TCONS_00023588	69186.39	9.2324	620	plasma membrane	Organic Cation/carnitin	OCT	Cs4g04940
TCONS_00023584	78745.00	6.6601	704	plasma membrane	Organic Cation/carnitin	OCT	Cs4g04930
TCONS_00035354	78531.72	5.0690	736	plasma membrane	Organic Cation/carnitin	OCT	Cs8g20990
TCONS_00046610	53994.25	6.4793	493	plasma membrane	e Nitrate	NPF	Cs8g16000
TCONS_00079647	57487.21	9.3174	530	plasma membrane	Nitrate	NPF	orange1.1t02415
TCONS_00055955	57942.40	9.2053	538	plasma membrane	Nitrate	NPF	Cs2g27650
TCONS_00070938	19476.51	5.5685	177	chloroplast	Inositol	INT	Cs7g20530
TCONS_00070943	24612.76	7.1867	227	plasma membrane	Inositol	INT	orange1.1t03682
TCONS_00078017	35324.40	5.7519	323	vacuole	Inositol	INT	orange1.1t03682
TCONS_00078018	54928.07	5.0839	511	plasma membrane	Inositol	INT	orange1.1t03682
TCONS_00016856	62789.41	8.2940	581	plasma membrane	Inositol	INT	Cs2g02060
TCONS_00019980	63731.35	9.2529	586	plasma membrane	Inositol	INT	Cs2g08110

Transcript	Molecular Weigh	Isoelectric Point	Seq. Len.	Sublocalization	Annotation	Subf.	Putative Gene
TCONS_00048249	54218.49	7.0189	499	plasma membrane	Glycerol-3-phosphate	G3Pp	Cs4g01150
TCONS_00052617	57942.40	9.2053	538	plasma membrane	Glycerol-3-phosphate	G3Pp	Cs5g07940
TCONS_00037536	59172.52	9.0540	547	plasma membrane	Glycerol-3-phosphate	G3Pp	Cs9g14660
TCONS_00021278	40658.16	4.9001	379	plasma membrane	Folate-Biopterin	FBT	Cs9g07150
TCONS_00069190	44647.85	9.4466	411	vacuole	Folate-Biopterin	FBT	Cs7g15410
TCONS_00034539	53060.91	8.6966	476	plasma membrane	Folate-Biopterin	FBT	Cs7g06540
TCONS_00034540	54750.77	8.7188	492	plasma membrane	Folate-Biopterin	FBT	Cs7g06540
TCONS_00041936	55065.03	10.2587	496	plasma membrane	Folate-Biopterin	FBT	Cs4g10690
TCONS_00034145	54711.45	5.2402	499	plasma membrane	Folate-Biopterin	FBT	Cs7g06580
TCONS_00034542	56388.42	7.7881	511	plasma membrane	Folate-Biopterin	FBT	Cs7g06530
TCONS_00021277	61865.69	8.2114	569	plasma membrane	Folate-Biopterin	FBT	Cs9g07150
TCONS_00084645	62349.91	10.0206	574	plasma membrane	Folate-Biopterin	FBT	Cs5g35030
TCONS_00000748	44855.05	9.5612	412	plasma membrane	Ascorbate	ASC	orange1.1t00376
TCONS_00000745	54291.40	9.6342	490	plasma membrane	Ascorbate	ASC	orange1.1t00376
TCONS_00000747	69186.39	9.2324	620	plasma membrane	Ascorbate	ASC	orange1.1t00376
TCONS_00050554	64111.66	10.0865	584	plasma membrane	Plastidic ATP/ ADP	AATP	Cs1g13530
TCONS_00080566	47904.98	8.7492	442	plasma membrane	Anion	Anion	Cs6g07670
TCONS_00033193	53111.68	6.6901	489	plasma membrane	Anion	Anion	Cs8g01190
TCONS_00023625	53190.22	4.8059	495	vacuole	Anion	Anion	Cs4g05170
TCONS_00023636	58006.20	9.4607	526	plasma membrane	Anion	Anion	Cs4g05170
TCONS_00035116	58078.05	10.0500	533	chloroplast	Anion	Anion	Cs8g19810
TCONS_00023627	76808.37	5.3881	715	cytosol	Anion	Anion	Cs4g05170
TCONS_00023632	80151.32	5.1906	747	plasma membrane	Anion	Anion	Cs4g05170

Seq. Len.: Sequence Length; Subf.: Subfamily

Table A2. MATE, ABC, and MFS expressed genes by Citrus spp., including gene duplication status, number of putative isoforms produced and the annotation

Gene ID	Duplication Status	Isof.	Subfamily	Gene ID	Duplication Status	Isof.	Subfamily
orange1t02318	Singleton	2	ABC A	Cs6g19470	Dispersed	1	ABC G
Cs5g04120	Tandem	2	ABC A	Cs7g12620	Dispersed	1	ABC G
Cs5g04110	Tandem	4	ABC A	Cs7g24870_a	Dispersed	1	ABC G
Cs1g16850	Dispersed	1	ABC B	Cs7g28090	Dispersed	1	ABC G
Cs4g11230	Dispersed	1	ABC B	Cs7g28610_a	Dispersed	1	ABC G
Cs6g06520	Dispersed	1	ABC B	Cs9g18660_a	Dispersed	1	ABC G

Gene ID	Duplication Status	Isof.	Subfamily	Gene ID	Duplication Status	Isof.	Subfamily
Cs6g21110	Dispersed	1	ABC B	orange1t00127_a	Dispersed	1	ABC G
Cs7g09730	Dispersed	1	ABC B	orange1t02321_a	Dispersed	1	ABC G
Cs9g11040	Dispersed	1	ABC B	Cs1g01500	Dispersed	2	ABC G
Cs9g16780	Dispersed	1	ABC B	Cs4g17100	Dispersed	2	ABC G
orange1t01769_a	Dispersed	1	ABC B	Cs5g13760	Dispersed	3	ABC G
Cs1g08880	Dispersed	2	ABC B	Cs5g17290	Dispersed	3	ABC G
Cs5g12150	Dispersed	2	ABC B	Cs8g15960	Dispersed	3	ABC G
Cs7g28610	Dispersed	3	ABC B	Cs8g16470	Dispersed	3	ABC G
Cs2g04080_a	Segmental	1	ABC B	Cs1g01420	Segmental	1	ABC G
Cs7g09160	Segmental	2	ABC B	Cs6g02210	Segmental	1	ABC G
Cs2g27440	Segmental	4	ABC B	Cs7g24870	Segmental	1	ABC G
orange1t00937	Singleton	1	ABC B	Cs8g16110	Segmental	1	ABC G
Cs6g19410	Singleton	2	ABC B	Cs1g06780	Segmental	3	ABC G
Cs3g26380	Singleton	3	ABC B	Cs9g01400	Segmental	4	ABC G
Cs6g14480	Singleton	3	ABC B	orange1t00127	Singleton	1	ABC G
Cs2g04070	Tandem	1	ABC B	orange1t01659	Singleton	1	ABC G
Cs3g09820	Tandem	1	ABC B	orange1t01996	Singleton	1	ABC G
Cs4g15420	Tandem	1	ABC B	orange1t02544	Singleton	1	ABC G
Cs6g20280	Tandem	1	ABC B	orange1t01531	Singleton	2	ABC G
Cs6g20290	Tandem	1	ABC B	orange1t01993	Singleton	3	ABC G
Cs9g01170	Tandem	1	ABC B	orange1t02321	Singleton	3	ABC G
Cs9g01170_a	Tandem	1	ABC B	Cs1g13640	Tandem	1	ABC G
Cs6g20270	Tandem	2	ABC B	Cs1g13650	Tandem	1	ABC G
Cs2g04080	Tandem	3	ABC B	Cs1g13680	Tandem	1	ABC G
Cs1g02710	Dispersed	1	ABC C	Cs1g13690	Tandem	1	ABC G
Cs5g28990	Dispersed	1	ABC C	Cs1g13710	Tandem	1	ABC G
Cs7g32530	Dispersed	1	ABC C	Cs1g13730	Tandem	1	ABC G
Cs5g33060	Dispersed	3	ABC C	Cs1g18920	Tandem	1	ABC G
Cs7g10200	Dispersed	5	ABC C	Cs1g19860	Tandem	1	ABC G
Cs5g02710	Segmental	2	ABC C	Cs2g30650	Tandem	1	ABC G
orange1t02765	Singleton	6	ABC C	Cs2g30650_a	Tandem	1	ABC G
Cs1g13720	Tandem	1	ABC C	Cs6g01130_a	Tandem	1	ABC G
Cs1g18460	Tandem	1	ABC C	Cs6g01131_a	Tandem	1	ABC G
Cs2g09560	Tandem	1	ABC C	Cs6g01330_a	Tandem	1	ABC G
Cs4g09120	Tandem	1	ABC C	Cs6g05280	Tandem	1	ABC G
Cs1g13700	Tandem	2	ABC C	Cs6g05320	Tandem	1	ABC G
Cs2g09550	Tandem	2	ABC C	Cs6g15280	Tandem	1	ABC G
Cs4g09150	Tandem	2	ABC C	Cs1g13660	Tandem	2	ABC G
Cs4g09130	Tandem	3	ABC C	Cs1g18930	Tandem	2	ABC G
Cs4g09140	Tandem	3	ABC C	Cs6g05270	Tandem	2	ABC G
Cs9g18660	Tandem	3	ABC C	Cs6g15300	Tandem	2	ABC G
Cs1g18450	Tandem	4	ABC C	Cs1g13720	Tandem	3	ABC G
Cs1g01510	Dispersed	3	ABC D	Cs1g13620	Tandem	4	ABC G
orange1t03223	Singleton	5	ABC D	Cs6g01330	Tandem	4	ABC G
Cs8g15910	Dispersed	1	ABC F	Cs6g02250	Tandem	4	ABC G
Cs9g09560	Dispersed	1	ABC F	Cs2g07970	Dispersed	1	ABC I
Cs1g13980	Dispersed	2	ABC F	Cs4g01550	Dispersed	1	ABC I

Gene ID	Duplication Status	Isof.	Subfamily	Gene ID	Duplication Status	Isof.	Subfamily
Cs5g01810	Dispersed	2	ABC F	Cs4g04420_a	Dispersed	1	ABC I
orange1t04404	Singleton	1	ABC F	Cs7g22890	Dispersed	1	ABC I
Cs1g09530	Dispersed	1	ABC G	Cs9g11110	Dispersed	1	ABC I
Cs1g15710	Dispersed	1	ABC G	Cs1g09070	Dispersed	2	ABC I
Cs1g20770	Dispersed	1	ABC G	Cs2g25590	Dispersed	2	ABC I
Cs1g20770_a	Dispersed	1	ABC G	Cs4g04420	Dispersed	2	ABC I
Cs2g13730	Dispersed	1	ABC G	Cs5g29600	Dispersed	2	ABC I
Cs2g13730_a	Dispersed	1	ABC G	Cs4g16980	Segmental	1	ABC I
Cs3g21080	Dispersed	1	ABC G	Cs7g23530	Segmental	1	ABC I
Cs3g22340	Dispersed	1	ABC G	Cs7g23800	Singleton	1	ABC I
Cs4g08300	Dispersed	1	ABC G	orange1t01791	Singleton	1	ABC I
Cs4g20440	Dispersed	1	ABC G	Cs5g33740_a	Tandem	1	ABC I
Cs5g08870	Dispersed	1	ABC G	Cs7g09160_a	Tandem	1	ABC I

Gene ID	Duplication Status	Isof.	Subfamily	Gene ID	Duplication Status	Isof.	Subfamily
Cs2g13500_m	Dispersed	1	MATE I	Cs9g19430	Tandem	1	MATE II
Cs2g31280	Dispersed	1	MATE I	Cs7g09190	Tandem	3	MATE II
Cs3g16650	Dispersed	1	MATE I	Cs2g15610	Dispersed	1	MATE III
Cs5g06100	Dispersed	1	MATE I	Cs2g08000	Dispersed	2	MATE III
Cs5g19630	Dispersed	1	MATE I	Cs2g03200	Segmental	1	MATE III
Cs5g20110_m	Dispersed	1	MATE I	Cs2g21460	Segmental	1	MATE III
Cs6g18150	Segmental	1	MATE I	Cs2g03220	Tandem	1	MATE III
Cs2g13500	Segmental	2	MATE I	Cs2g15120	Tandem	1	MATE III
orange1t00013	Singleton	2	MATE I	Cs2g15080	Tandem	2	MATE III
Cs6g18160	Tandem	1	MATE I	Cs6g09270	Dispersed	2	MATE IV
Cs1g07540	Tandem	2	MATE I	Cs2g30270	Segmental	2	MATE IV
Cs2g13530	Tandem	2	MATE I	Cs8g01660	Segmental	2	MATE IV
Cs6g18200	Tandem	3	MATE I	Cs1g26350	Segmental	3	MATE IV
Cs1g07550	Tandem	4	MATE I	orange1t03403	Singleton	2	MATE IV
Cs2g13510	Tandem	4	MATE I	Cs8g08480	Tandem	1	MATE IV
Cs5g21940	Dispersed	1	MATE II	Cs8g08470	Tandem	3	MATE IV
Cs3g17670	Segmental	1	MATE II	Cs3g22600	Dispersed	1	MATE V
Cs1g20120	Segmental	3	MATE II	Cs4g15415_m	Dispersed	1	MATE V
Cs3g17660	Segmental	3	MATE II	Cs5g09710	Dispersed	1	MATE V
Cs1g20130	Tandem	2	MATE II	Cs9g04120	Dispersed	1	MATE V
Cs3g24330	Dispersed	3	MATE II	Cs5g10270	Segmental	1	MATE V
Cs5g28190	Dispersed	3	MATE II	Cs7g16290_m	Segmental	1	MATE V
orange1t00390	Singleton	1	MATE II	Cs9g16870	Segmental	1	MATE V
Cs9g19420	Tandem	1	MATE II	Cs6g09880	Segmental	2	MATE V

Gene ID	Duplication Status	Isof.	Subfamily	Gene ID	Duplication Status	Isof.	Subfamily
Cs1g13530	Singleton	1	AATP	Cs6g18490	Dispersed	3	pGlcT
Cs4g05170	Dispersed	4	Anion	Cs1g23890	Dispersed	1	PMT
Cs6g07670	Segmental	1	Anion	Cs2g06380	Dispersed	1	PMT
Cs8g01190	Dispersed	1	Anion	Cs3g27610	Segmental	3	PMT
Cs8g19810	Segmental	1	Anion	Cs4g15770	Tandem	1	PMT
orange1.1t00376	Singleton	3	ASC	Cs4g15780	Tandem	1	PMT
Cs4g10690	Dispersed	1	FBT	Cs8g01220	Segmental	1	PMT
Cs5g35030	Dispersed	1	FBT	Cs3g27660	Dispersed	1	PTH
Cs7g06530	Tandem	1	FBT	Cs5g29860	Segmental	1	PTH
Cs7g06540	Tandem	2	FBT	Cs7g29450	Dispersed	1	PTH
Cs7g06580	Tandem	1	FBT	Cs8g06780	Dispersed	1	PTH
Cs7g15410	Dispersed	1	FBT	Cs9g10530	Segmental	1	PTH
Cs9g07150	Dispersed	2	FBT	Cs9g10540	Tandem	1	PTH
Cs4g01150	Dispersed	1	G3Pp	Cs9g18560	Dispersed	1	PTH
Cs5g07940	Dispersed	1	G3Pp	Cs5g10180	Singleton	2	PTH5
Cs9g14660	Dispersed	1	G3Pp	orange1.1t00286	Singleton	1	PTH5
Cs2g02060	Dispersed	1	INT	Cs1g01440	Tandem	1	Spinster
Cs2g08110	Dispersed	1	INT	Cs1g20960	Segmental	3	Spinster
Cs7g20530	Dispersed	1	INT	Cs8g03150	Segmental	3	Spinster
orange1.1t03682	Singleton	3	INT	Cs1g24180	Segmental	3	STP
Cs2g27650	Segmental	1	NPF	Cs3g12410	Segmental	1	STP
Cs8g16000	Tandem	1	NPF	Cs3g12420	Tandem	1	STP
orange1.1t02415	Singleton	1	NPF	Cs3g12480	Tandem	1	STP
Cs1g18890	Dispersed	1	OCT	Cs3g12490	Tandem	2	STP
Cs4g04910	Tandem	1	OCT	Cs3g12500	Tandem	1	STP
Cs4g04920	Tandem	1	OCT	Cs3g12510	Tandem	8	STP
Cs4g04930	Tandem	3	OCT	Cs3g12520	Tandem	3	STP
Cs4g04940	Tandem	2	OCT	Cs3g12540	Segmental	3	STP
Cs4g04960	Tandem	2	OCT	Cs3g24900	Segmental	4	STP
Cs4g12030	Dispersed	1	OCT	Cs5g32060	Tandem	1	STP
Cs8g20990	Dispersed	3	OCT	Cs5g32070	Tandem	1	STP
orange1.1t03244	Singleton	2	OCT	Cs7g13670	Dispersed	1	STP
orange1.1t03245	Singleton	1	OCT	Cs8g19880	Dispersed	1	STP
Cs5g24870	Dispersed	4	Other	Cs9g05220	Dispersed	2	STP
Cs8g18970	Dispersed	2	Other	Cs9g06590	Tandem	1	STP
Cs8g19980	Dispersed	4	Other	Cs9g06600	Tandem	1	STP
Cs1g15250	Segmental	3	pGlcT	Cs9g06620	Tandem	1	STP
Cs2g20710	Dispersed	5	pGlcT	orange1.1t03833	Singleton	1	STP
Cs4g16110	Segmental	6	pGlcT	orange1.1t03853	Singleton	1	STP

Isof.: Isoforms.

Table A3. MATE, ABC, and MFS differentially expressed, Log2FC values according to the time points after bacterial inoculation (HAI) and cultivars, p-value, and annotation

Transcript ID	Log2FC	HAI	P-value	Subf.
TCONS_00018545	2,80	S72	0,04	ABC A
TCONS_00018545	3,37	LG48	0,01	ABC A
TCONS_00018546	2,81	S72	0,04	ABC A
TCONS_00018546	3,32	LG48	0,01	ABC A
TCONS_00018548	2,80	S72	0,04	ABC A
TCONS_00018548	3,35	LG48	0,01	ABC A
TCONS_00018550	2,75	S72	0,04	ABC A
TCONS_00018550	3,09	LG48	0,01	ABC A
TCONS_00019248	2,79	PK72	0,03	ABC A
TCONS_00019248	4,28	LG48	0,00	ABC A
TCONS_00019252	2,79	PK72	0,03	ABC A
TCONS_00019252	4,22	LG48	0,00	ABC A
TCONS_00003170	2,68	H48	0,03	ABC B
TCONS_00003170	2,72	PR48	0,04	ABC B
TCONS_00003170	2,80	S72	0,04	ABC B
TCONS_00003170	2,88	LG48	0,02	ABC B
TCONS_00003170	2,92	V48	0,04	ABC B
TCONS_00003170	2,95	H24	0,03	ABC B
TCONS_00003170	3,17	H72	0,01	ABC B
TCONS_00003170	3,23	PK72	0,01	ABC B
TCONS_00003170	3,39	BA48	0,01	ABC B
TCONS_00003170	3,51	K72	0,01	ABC B
TCONS_00003170	3,63	PK48	0,00	ABC B
TCONS_00003170	3,82	K24	0,00	ABC B
TCONS_00003170	3,93	PR72	0,00	ABC B
TCONS_00003170	4,58	K48	0,00	ABC B
TCONS_00003170	5,20	BA72	0,00	ABC B
TCONS_00006535	-2,76	BA48	0,04	ABC B
TCONS_00006535	-2,96	H48	0,02	ABC B
TCONS_00006535	-3,11	K24	0,01	ABC B
TCONS_00006535	-3,47	PR48	0,01	ABC B
TCONS_00006535	-3,93	H24	0,00	ABC B
TCONS_00006535	-4,09	PK48	0,00	ABC B
TCONS_00006535	-4,09	BA72	0,00	ABC B
TCONS_00006535	-4,16	PR72	0,00	ABC B
TCONS_00006535	-4,22	K72	0,00	ABC B
TCONS_00006535	-4,25	PR24	0,01	ABC B
TCONS_00006535	-4,70	K48	0,00	ABC B
TCONS_00006535	-5,02	LG48	0,00	ABC B
TCONS_00006539	-2,78	BA48	0,04	ABC B
TCONS_00006539	-2,99	H48	0,02	ABC B
TCONS_00006539	-3,13	K24	0,01	ABC B
TCONS_00006539	-3,47	PR48	0,01	ABC B
TCONS_00006539	-3,88	H24	0,00	ABC B
TCONS_00054311	2,52	K48	0,04	ABC C
TCONS_00054315	2,44	K24	0,05	ABC C
TCONS_00054315	2,48	K48	0,04	ABC C
TCONS_00076929	-2,78	PR72	0,04	ABC C
TCONS_00076929	-2,84	K72	0,03	ABC C
TCONS_00076933	-2,81	PR72	0,04	ABC C
TCONS_00076933	-2,87	K72	0,03	ABC C
TCONS_00076938	-2,83	K72	0,03	ABC C
TCONS_00076938	-2,86	PR72	0,03	ABC C
TCONS_00076952	-2,81	PR72	0,04	ABC C
TCONS_00076952	-2,90	K72	0,02	ABC C
TCONS_00076957	-2,79	PR72	0,04	ABC C
TCONS_00076957	-2,87	K72	0,02	ABC C
TCONS_00076962	-2,81	PR72	0,04	ABC C
TCONS_00076962	-2,88	K72	0,02	ABC C
TCONS_00089867	-3,40	BA72	0,03	ABC C
TCONS_00089867	-4,81	PR72	0,01	ABC C
TCONS_00089867	-5,02	PK72	0,00	ABC C
TCONS_00089867	-5,96	LG48	0,01	ABC C
TCONS_00089867	5,43	K72	0,02	ABC C
TCONS_00089868	-2,98	BA72	0,05	ABC C
TCONS_00089868	-4,83	PR72	0,01	ABC C
TCONS_00089868	-5,05	PK72	0,00	ABC C
TCONS_00089868	-6,07	LG48	0,01	ABC C
TCONS_00089868	5,33	K72	0,02	ABC C
TCONS_00093291	-3,39	BA72	0,04	ABC C
TCONS_00093291	-5,23	PR72	0,01	ABC C
TCONS_00093291	-6,67	LG48	0,01	ABC C
TCONS_00093291	6,09	K72	0,01	ABC C
TCONS_00093292	-4,91	PR72	0,02	ABC C
TCONS_00093292	-6,07	LG48	0,03	ABC C
TCONS_00093292	5,23	K72	0,05	ABC C
TCONS_00093484	3,18	H24	0,03	ABC C
TCONS_00093484	3,33	H72	0,02	ABC C
TCONS_00093484	3,49	PR72	0,04	ABC C
TCONS_00093484	3,59	H48	0,01	ABC C
TCONS_00093484	3,64	PK48	0,01	ABC C
TCONS_00093484	3,83	S48	0,01	ABC C
TCONS_00093484	4,09	S72	0,01	ABC C
TCONS_00093484	4,39	PR24	0,01	ABC C
TCONS_00093484	6,50	V24	0,02	ABC C
TCONS_00044206	-2,60	PK72	0,04	ABC D
TCONS_00044206	-2,61	PR72	0,05	ABC D
TCONS_00044206	-3,09	K72	0,02	ABC D

Transcript ID	Log2FC	HAI	P-value	Subf.	Transcript ID	Log2FC	HAI	P-value	Subf.
TCONS_00006539	-4,09	PK48	0,00	ABC B	TCONS_00044206	-3,22	K48	0,01	ABC D
TCONS_00006539	-4,12	BA72	0,00	ABC B	TCONS_00044207	-2,59	PR72	0,05	ABC D
TCONS_00006539	-4,20	PR72	0,00	ABC B	TCONS_00044207	-2,62	PK72	0,04	ABC D
TCONS_00006539	-4,26	PR24	0,01	ABC B	TCONS_00044207	-3,02	K72	0,02	ABC D
TCONS_00006539	-4,31	K72	0,00	ABC B	TCONS_00044207	-3,18	K48	0,01	ABC D
TCONS_00006539	-4,40	LG48	0,00	ABC B	TCONS_00044208	-2,46	K24	0,05	ABC D
TCONS_00006539	-4,84	K48	0,00	ABC B	TCONS_00044208	-2,65	PR72	0,04	ABC D
TCONS_00006540	-2,77	BA48	0,04	ABC B	TCONS_00044208	-2,65	PK72	0,03	ABC D
TCONS_00006540	-2,97	H48	0,02	ABC B	TCONS_00044208	-3,15	K72	0,01	ABC D
TCONS_00006540	-3,16	K24	0,01	ABC B	TCONS_00044208	-3,20	K48	0,01	ABC D
TCONS_00006540	-3,46	PR48	0,01	ABC B	TCONS_00044210	-2,60	PR72	0,05	ABC D
TCONS_00006540	-3,89	H24	0,00	ABC B	TCONS_00044210	-2,63	PK72	0,03	ABC D
TCONS_00006540	-4,08	PK48	0,00	ABC B	TCONS_00044210	-3,02	K72	0,02	ABC D
TCONS_00006540	-4,12	BA72	0,00	ABC B	TCONS_00044210	-3,16	K48	0,01	ABC D
TCONS_00006540	-4,21	PR72	0,00	ABC B	TCONS_00044211	-2,72	PR72	0,04	ABC D
TCONS_00006540	-4,26	PR24	0,01	ABC B	TCONS_00044211	-2,99	K72	0,02	ABC D
TCONS_00006540	-4,30	K72	0,00	ABC B	TCONS_00044211	-3,28	K48	0,01	ABC D
TCONS_00006540	-4,40	LG48	0,00	ABC B	TCONS_00047255	-2,79	BA72	0,02	ABC F
TCONS_00006540	-4,82	K48	0,00	ABC B	TCONS_00047255	-2,84	K72	0,02	ABC F
TCONS_00015582	-2,69	PR48	0,05	ABC B	TCONS_00047255	-3,07	K48	0,01	ABC F
TCONS_00015582	-2,90	BA48	0,03	ABC B	TCONS_00047255	-3,46	PK72	0,01	ABC F
TCONS_00015582	-2,91	H48	0,02	ABC B	TCONS_00047255	-4,25	PR72	0,00	ABC F
TCONS_00015584	-2,70	PR48	0,05	ABC B	TCONS_00001537	-3,86	BA72	0,04	ABC G
TCONS_00015584	-2,91	BA48	0,03	ABC B	TCONS_00001537	-4,30	PR48	0,03	ABC G
TCONS_00015584	-2,92	H48	0,02	ABC B	TCONS_00001537	-4,60	H24	0,03	ABC G
TCONS_00025446	2,58	PK72	0,04	ABC B	TCONS_00001537	-4,72	PK48	0,01	ABC G
TCONS_00025446	3,36	LG48	0,01	ABC B	TCONS_00001537	-5,50	PR72	0,01	ABC G
TCONS_00025854	-3,14	LG72	0,02	ABC B	TCONS_00013639	-2,57	K24	0,04	ABC G
TCONS_00025854	-3,20	PK72	0,02	ABC B	TCONS_00013639	-2,87	BA48	0,03	ABC G
TCONS_00025854	-4,14	K24	0,01	ABC B	TCONS_00013639	-2,87	K48	0,02	ABC G
TCONS_00025854	-6,45	LG48	0,00	ABC B	TCONS_00013639	-3,09	K72	0,02	ABC G
TCONS_00025854	-7,87	K48	0,00	ABC B	TCONS_00013639	-3,14	PR72	0,02	ABC G
TCONS_00025855	-2,93	PK72	0,02	ABC B	TCONS_00013639	-3,39	PK48	0,01	ABC G
TCONS_00025855	-3,05	LG72	0,02	ABC B	TCONS_00013639	-3,69	BA72	0,00	ABC G
TCONS_00025855	-4,15	K24	0,01	ABC B	TCONS_00013639	-3,86	H24	0,00	ABC G
TCONS_00025855	-5,48	K48	0,00	ABC B	TCONS_00013639	-4,23	H48	0,00	ABC G
TCONS_00025856	-2,77	PK72	0,03	ABC B	TCONS_00013639	-4,57	PR48	0,00	ABC G
TCONS_00025856	-2,99	LG72	0,02	ABC B	TCONS_00013639	-5,57	PR24	0,00	ABC G
TCONS_00025856	-4,61	K24	0,00	ABC B	TCONS_00013641	-2,62	K24	0,04	ABC G
TCONS_00025856	-6,12	K48	0,00	ABC B	TCONS_00013641	-2,90	BA48	0,03	ABC G
TCONS_00025857	-3,53	PK72	0,01	ABC B	TCONS_00013641	-2,90	K48	0,02	ABC G
TCONS_00025857	-4,58	LG48	0,01	ABC B	TCONS_00013641	-3,09	K72	0,02	ABC G
TCONS_00025857	-5,60	PR72	0,00	ABC B	TCONS_00013641	-3,13	PR72	0,02	ABC G
TCONS_00025857	-6,25	K48	0,00	ABC B	TCONS_00013641	-3,38	PK48	0,01	ABC G
TCONS_00059564	-2,69	K24	0,03	ABC B	TCONS_00013641	-3,66	BA72	0,00	ABC G
TCONS_00059564	-3,83	BA72	0,00	ABC B	TCONS_00013641	-3,84	H24	0,00	ABC G
TCONS_00059564	-4,10	PR72	0,00	ABC B	TCONS_00013641	-4,21	H48	0,00	ABC G

Transcript ID	Log2FC	HAI	P-value	Subf.
TCONS_00059564	-4,42	LG48	0,00	ABC B
TCONS_00059564	-4,47	K72	0,00	ABC B
TCONS_00059564	-5,06	K48	0,00	ABC B
TCONS_00059566	-2,66	K24	0,04	ABC B
TCONS_00059566	-3,88	BA72	0,00	ABC B
TCONS_00059566	-4,10	PR72	0,00	ABC B
TCONS_00059566	-4,38	LG48	0,00	ABC B
TCONS_00059566	-4,45	K72	0,00	ABC B
TCONS_00059566	-5,30	K48	0,00	ABC B
TCONS_00073525	3,40	LG72	0,05	ABC B
TCONS_00001949	-3,74	K72	0,01	ABC C
TCONS_00001949	2,52	PK72	0,05	ABC C
TCONS_00008580	2,60	H72	0,03	ABC C
TCONS_00008580	2,83	PR72	0,03	ABC C
TCONS_00008580	3,28	PK24	0,01	ABC C
TCONS_00008580	3,41	K48	0,01	ABC C
TCONS_00008580	3,69	H48	0,00	ABC C
TCONS_00008580	3,85	S72	0,01	ABC C
TCONS_00008580	4,40	K72	0,00	ABC C
TCONS_00008580	5,04	K24	0,00	ABC C
TCONS_00008581	2,62	H72	0,03	ABC C
TCONS_00008581	2,99	PR72	0,03	ABC C
TCONS_00008581	3,29	PK24	0,01	ABC C
TCONS_00008581	3,42	K48	0,01	ABC C
TCONS_00008581	3,72	H48	0,00	ABC C
TCONS_00008581	3,87	S72	0,01	ABC C
TCONS_00008581	4,33	K72	0,00	ABC C
TCONS_00008581	4,93	K24	0,00	ABC C
TCONS_00008582	2,53	H72	0,04	ABC C
TCONS_00008582	2,82	PR72	0,03	ABC C
TCONS_00008582	3,28	PK24	0,01	ABC C
TCONS_00008582	3,44	K48	0,01	ABC C
TCONS_00008582	3,71	H48	0,00	ABC C
TCONS_00008582	3,87	S72	0,01	ABC C
TCONS_00008582	4,35	K72	0,00	ABC C
TCONS_00008582	4,98	K24	0,00	ABC C
TCONS_00008583	2,58	H72	0,04	ABC C
TCONS_00008583	2,84	PR72	0,03	ABC C
TCONS_00008583	3,28	PK24	0,01	ABC C
TCONS_00008583	3,38	K48	0,01	ABC C
TCONS_00008583	3,68	H48	0,00	ABC C
TCONS_00008583	3,85	S72	0,01	ABC C
TCONS_00008583	4,47	K72	0,00	ABC C
TCONS_00008583	4,94	K24	0,00	ABC C
TCONS_00008590	2,88	H72	0,02	ABC C
TCONS_00008590	3,29	K48	0,01	ABC C
TCONS_00008590	3,47	PR72	0,01	ABC C
TCONS_00008590	3,52	H48	0,01	ABC C
TCONS_00008590	3,63	PK24	0,01	ABC C
TCONS_00008590	3,90	S72	0,01	ABC C
TCONS_00008590	4,14	K72	0,00	ABC C
TCONS_00008590	4,86	K24	0,00	ABC C

Transcript ID	Log2FC	HAI	P-value	Subf.
TCONS_00013641	-4,58	PR48	0,00	ABC G
TCONS_00013641	-5,51	PR24	0,00	ABC G
TCONS_00022445	-3,61	PR72	0,02	ABC G
TCONS_00022445	3,82	H24	0,01	ABC G
TCONS_00022447	-3,60	PR72	0,02	ABC G
TCONS_00022447	3,85	H24	0,02	ABC G
TCONS_00022448	-3,52	PR72	0,03	ABC G
TCONS_00022448	3,72	H24	0,02	ABC G
TCONS_00025723	-3,96	K24	0,01	ABC G
TCONS_00025723	-5,61	PR72	0,00	ABC G
TCONS_00025723	-6,78	K48	0,00	ABC G
TCONS_00025723	-8,14	K72	0,00	ABC G
TCONS_00026525	-3,37	K48	0,01	ABC G
TCONS_00026526	-3,36	K48	0,01	ABC G
TCONS_00026527	-3,38	K48	0,01	ABC G
TCONS_00026533	-3,31	K48	0,01	ABC G
TCONS_00028863	-2,73	BA72	0,03	ABC G
TCONS_00028863	-2,93	K48	0,02	ABC G
TCONS_00028863	-3,23	K72	0,01	ABC G
TCONS_00028863	-4,99	PR72	0,00	ABC G
TCONS_00028863	-5,21	K24	0,00	ABC G
TCONS_00028866	-2,77	BA72	0,03	ABC G
TCONS_00028866	-2,94	K72	0,02	ABC G
TCONS_00028866	-2,97	K48	0,02	ABC G
TCONS_00028866	-4,83	PR72	0,00	ABC G
TCONS_00028866	-5,27	K24	0,00	ABC G
TCONS_00029271	4,15	K48	0,01	ABC G
TCONS_00029271	5,41	K72	0,00	ABC G
TCONS_00034839	-2,65	LG72	0,05	ABC G
TCONS_00034839	3,88	PR72	0,01	ABC G
TCONS_00034839	5,55	BA72	0,00	ABC G
TCONS_00034839	5,71	K72	0,00	ABC G
TCONS_00034840	-2,63	LG72	0,05	ABC G
TCONS_00034840	3,52	PR72	0,02	ABC G
TCONS_00034840	5,53	BA72	0,00	ABC G
TCONS_00034840	5,59	K72	0,00	ABC G
TCONS_00038660	-2,42	BA72	0,05	ABC G
TCONS_00038660	-3,24	K72	0,01	ABC G
TCONS_00038660	-3,29	K48	0,01	ABC G
TCONS_00041816	6,05	LG48	0,03	ABC G
TCONS_00044877	-2,59	K24	0,04	ABC G
TCONS_00044877	-2,95	BA72	0,02	ABC G
TCONS_00044877	-3,40	PR72	0,01	ABC G
TCONS_00044877	-4,34	K72	0,00	ABC G
TCONS_00044877	-6,18	LG48	0,00	ABC G
TCONS_00045273	-2,43	K72	0,05	ABC G
TCONS_00045278	3,12	PK72	0,01	ABC G
TCONS_00045281	3,03	K48	0,02	ABC G
TCONS_00045281	3,11	PR72	0,02	ABC G
TCONS_00045281	3,26	K24	0,01	ABC G
TCONS_00045281	3,30	PK72	0,01	ABC G
TCONS_00045281	3,39	BA72	0,01	ABC G

Transcript ID	Log2FC	HAI	P-value	Subf.	Transcript ID	Log2FC	HAI	P-value	Subf.
TCONS_00020549	-4,74	K72	0,00	ABC C	TCONS_00045281	4,03	PR24	0,01	ABC G
TCONS_00020549	3,43	LG48	0,01	ABC C	TCONS_00045282	-4,07	PR72	0,01	ABC G
TCONS_00020556	-5,21	K72	0,00	ABC C	TCONS_00045285	-3,87	PR72	0,02	ABC G
TCONS_00020556	3,77	LG48	0,00	ABC C	TCONS_00050518	2,77	K24	0,02	ABC G
TCONS_00043249	2,99	PK24	0,04	ABC C	TCONS_00050519	2,76	K24	0,02	ABC G
TCONS_00043249	3,51	PK72	0,03	ABC C	TCONS_00050530	2,77	K24	0,02	ABC G
TCONS_00043249	3,77	PK48	0,02	ABC C	TCONS_00050544	-3,60	BA72	0,00	ABC G
TCONS_00043249	3,83	H72	0,02	ABC C	TCONS_00050544	-3,98	K48	0,00	ABC G
TCONS_00043249	4,56	H48	0,01	ABC C	TCONS_00050544	-4,21	PR72	0,00	ABC G
TCONS_00043249	5,04	S72	0,01	ABC C	TCONS_00050544	-4,57	LG48	0,00	ABC G
TCONS_00043250	2,49	H72	0,04	ABC C	TCONS_00050544	-4,95	K72	0,00	ABC G
TCONS_00043250	2,61	PK72	0,04	ABC C	TCONS_00054528	-2,45	K72	0,05	ABC G
TCONS_00043250	2,83	PK24	0,02	ABC C	TCONS_00054528	-2,59	K48	0,04	ABC G
TCONS_00043250	2,98	V24	0,04	ABC C	TCONS_00054528	-4,12	LG48	0,00	ABC G
TCONS_00043250	3,17	V48	0,03	ABC C	TCONS_00054533	-2,45	K72	0,05	ABC G
TCONS_00043250	3,17	PR24	0,03	ABC C	TCONS_00054533	-2,60	K48	0,04	ABC G
TCONS_00043250	3,42	S48	0,02	ABC C	TCONS_00054533	-4,12	LG48	0,00	ABC G
TCONS_00043250	3,62	H24	0,01	ABC C	TCONS_00054535	-2,55	K48	0,04	ABC G
TCONS_00043250	3,71	H48	0,00	ABC C	TCONS_00054535	-2,71	K72	0,03	ABC G
TCONS_00043250	3,72	BA72	0,00	ABC C	TCONS_00054535	-4,14	LG48	0,00	ABC G
TCONS_00043250	4,63	PK48	0,00	ABC C	TCONS_00064050	-2,97	H72	0,04	ABC G
TCONS_00043250	4,96	S72	0,00	ABC C	TCONS_00064050	-3,24	BA72	0,03	ABC G
TCONS_00043251	2,48	BA24	0,05	ABC C	TCONS_00064050	-3,62	H48	0,02	ABC G
TCONS_00043251	2,65	PR72	0,04	ABC C	TCONS_00064050	-3,70	PK48	0,01	ABC G
TCONS_00043251	2,98	S48	0,03	ABC C	TCONS_00064050	-3,80	PR48	0,02	ABC G
TCONS_00043251	3,17	PK72	0,01	ABC C	TCONS_00064050	-4,05	PK72	0,01	ABC G
TCONS_00043251	3,19	PK24	0,01	ABC C	TCONS_00064050	-5,19	PR72	0,00	ABC G
TCONS_00043251	3,30	PR24	0,02	ABC C	TCONS_00064050	-5,34	PR24	0,01	ABC G
TCONS_00043251	3,31	V48	0,02	ABC C	TCONS_00064050	-6,68	K72	0,00	ABC G
TCONS_00043251	3,55	V24	0,01	ABC C	TCONS_00064050	-7,24	K48	0,00	ABC G
TCONS_00043251	3,56	H24	0,01	ABC C	TCONS_00064050	-7,48	K24	0,00	ABC G
TCONS_00043251	3,71	H48	0,00	ABC C	TCONS_00068827	-2,51	H72	0,04	ABC G
TCONS_00043251	3,80	BA72	0,00	ABC C	TCONS_00068827	-2,56	LG72	0,04	ABC G
TCONS_00043251	4,80	PK48	0,00	ABC C	TCONS_00068827	-2,72	PK24	0,03	ABC G
TCONS_00043251	5,03	S72	0,00	ABC C	TCONS_00068827	-3,18	K24	0,02	ABC G
TCONS_00043252	2,61	H72	0,03	ABC C	TCONS_00068827	-3,65	S48	0,01	ABC G
TCONS_00043252	2,67	BA24	0,03	ABC C	TCONS_00068827	-4,53	LG48	0,00	ABC G
TCONS_00043252	2,89	H24	0,03	ABC C	TCONS_00068827	-4,61	PK72	0,00	ABC G
TCONS_00043252	2,95	BA48	0,03	ABC C	TCONS_00068827	-6,26	K72	0,00	ABC G
TCONS_00043252	3,03	H48	0,02	ABC C	TCONS_00068828	-2,53	H72	0,04	ABC G
TCONS_00043252	3,16	BA72	0,01	ABC C	TCONS_00068828	-2,56	LG72	0,04	ABC G
TCONS_00043252	3,32	S48	0,02	ABC C	TCONS_00068828	-2,72	PK24	0,03	ABC G
TCONS_00043252	3,34	S24	0,02	ABC C	TCONS_00068828	-3,27	K24	0,01	ABC G
TCONS_00043252	3,94	PK48	0,00	ABC C	TCONS_00068828	-3,67	S48	0,01	ABC G
TCONS_00043252	4,12	PK24	0,00	ABC C	TCONS_00068828	-4,51	LG48	0,00	ABC G
TCONS_00043252	4,22	PK72	0,00	ABC C	TCONS_00068828	-4,60	PK72	0,00	ABC G
TCONS_00043252	4,38	S72	0,00	ABC C	TCONS_00068828	-6,23	K72	0,00	ABC G
TCONS_00043253	2,69	H72	0,03	ABC C	TCONS_00068831	-2,44	PK24	0,05	ABC G
TCONS_00043253	2,96	BA48	0,03	ABC C	TCONS_00068831	-2,52	LG72	0,04	ABC G
TCONS_00043253	2,96	H24	0,03	ABC C	TCONS_00068831	-2,72	H72	0,03	ABC G
TCONS_00043253	3,04	H48	0,02	ABC C	TCONS_00068831	-3,33	K24	0,01	ABC G
TCONS_00043253	3,44	S24	0,02	ABC C	TCONS_00068831	-3,86	S48	0,01	ABC G

Transcript ID	Log2FC	HAI	P-value	Subf.	Transcript ID	Log2FC	HAI	P-value	Subf.
TCONS_00043253	3,46	S48	0,01	ABC C	TCONS_00068831	-4,30	LG48	0,00	ABC G
TCONS_00043253	3,50	BA72	0,01	ABC C	TCONS_00068831	-4,35	PK72	0,00	ABC G
TCONS_00043253	3,88	PK72	0,00	ABC C	TCONS_00068831	-6,04	K72	0,00	ABC G
TCONS_00043253	3,98	PK48	0,00	ABC C	TCONS_00068834	-3,54	H72	0,02	ABC G
TCONS_00043253	4,08	PK24	0,00	ABC C	TCONS_00068834	-4,61	S48	0,01	ABC G
TCONS_00043253	4,43	S72	0,00	ABC C	TCONS_00068834	-5,00	K48	0,04	ABC G
TCONS_00043254	2,57	BA24	0,04	ABC C	TCONS_00068834	-5,09	K72	0,04	ABC G
TCONS_00043254	2,62	H72	0,03	ABC C	TCONS_00068834	-5,42	PR72	0,00	ABC G
TCONS_00043254	2,89	H24	0,03	ABC C	TCONS_00070199	-4,56	PR48	0,03	ABC G
TCONS_00043254	2,97	BA48	0,03	ABC C	TCONS_00072490	3,11	K72	0,03	ABC G
TCONS_00043254	3,05	H48	0,01	ABC C	TCONS_00072490	3,44	S48	0,02	ABC G
TCONS_00043254	3,20	BA72	0,01	ABC C	TCONS_00079419	4,48	K72	0,00	ABC G
TCONS_00043254	3,34	S24	0,02	ABC C	TCONS_00094095	-2,94	PR72	0,03	ABC G
TCONS_00043254	3,34	S48	0,02	ABC C	TCONS_00094095	2,91	H48	0,02	ABC G
TCONS_00043254	3,95	PK48	0,00	ABC C	TCONS_00094095	3,26	PR48	0,01	ABC G
TCONS_00043254	4,03	PK24	0,00	ABC C	TCONS_00094095	3,42	S24	0,02	ABC G
TCONS_00043254	4,22	PK72	0,00	ABC C	TCONS_00094095	4,35	S48	0,00	ABC G
TCONS_00043254	4,42	S72	0,00	ABC C	TCONS_00094097	-3,04	PR72	0,02	ABC G
TCONS_00043255	3,22	PK24	0,03	ABC C	TCONS_00094097	2,92	H48	0,02	ABC G
TCONS_00043255	3,28	BA72	0,03	ABC C	TCONS_00094097	3,26	PR48	0,01	ABC G
TCONS_00043255	3,40	H24	0,03	ABC C	TCONS_00094097	3,34	S24	0,02	ABC G
TCONS_00043255	3,94	PK72	0,01	ABC C	TCONS_00094097	4,34	S48	0,00	ABC G
TCONS_00043255	4,01	PK48	0,01	ABC C	TCONS_00094098	-2,99	PR72	0,02	ABC G
TCONS_00043255	4,21	S72	0,01	ABC C	TCONS_00094098	2,89	H48	0,02	ABC G
TCONS_00054310	2,41	K24	0,05	ABC C	TCONS_00094098	3,17	PR48	0,02	ABC G
TCONS_00054310	2,61	K48	0,03	ABC C	TCONS_00094098	3,62	S24	0,01	ABC G
TCONS_00054310	2,61	K72	0,03	ABC C	TCONS_00094098	4,31	S48	0,00	ABC G
TCONS_00054311	2,39	K24	0,05	ABC C	TCONS_00043434	-3,05	K72	0,05	ABC I
TCONS_00054311	2,47	K72	0,04	ABC C	TCONS_00066524	-2,77	K72	0,03	ABC I
					TCONS_00066524	-2,92	K48	0,02	ABC I

Subf.: Subfamily.